AD-A035 701 AIRESEARCH MFG CO OF ARIZONA PHOENIX F/G 21/5
A FLUIDIC FUEL AND AIR BLEED LOAD CONTROL SYSTEM FOR GAS TURBIN--ETC(U)
DEC 76 R S MCCARTY, H R GAMBLE DAAG53-76-C-0012
UNCLASSIFIED 76-411516 NL

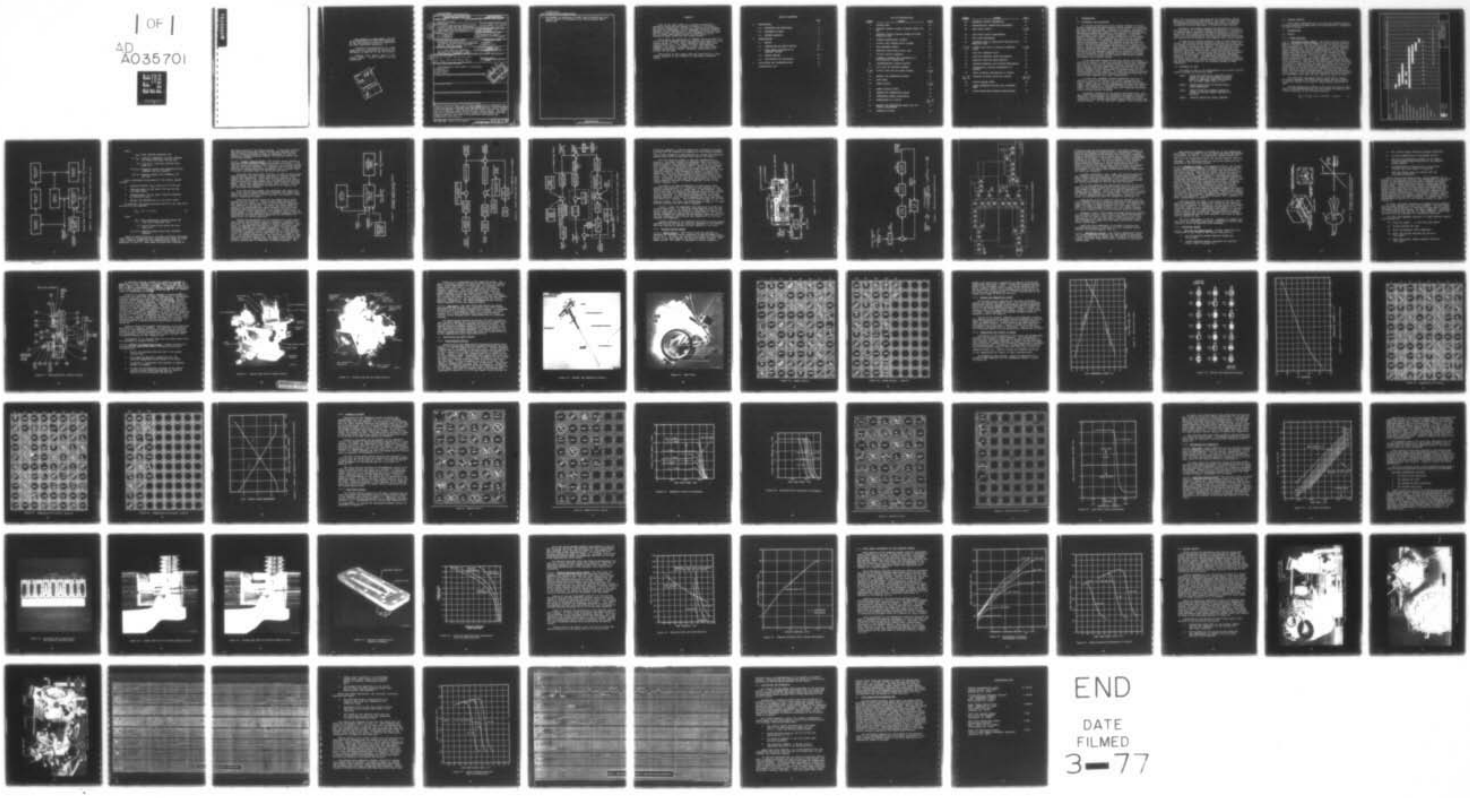

END
DATE FILMED
3-77

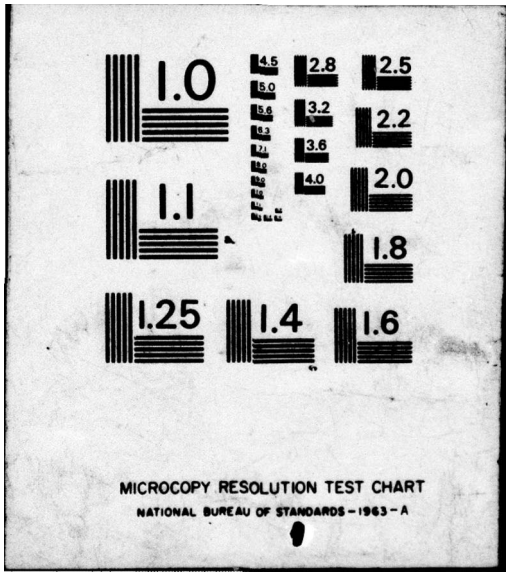
1.0
1.1
1.25
1.4
1.6
1.8
2.0
2.2
2.5
2.8
3.2
3.6
4.0
4.5
5.0
5.6
6.3
7.1
8.0
9.0
10
11
12
13
MICROCOPY RESOLUTION TEST CHART
NATIONAL BUREAU OF STANDARDS - 1963 - A

The findings in this report are not to be construed as an official Department of the Army position unless so designated by other authorized documents.

Citation of manufacturers' or trade names does not constitute an official indorsement or approval of the use thereof.

Destroy this report when it is no longer needed. Do not return it to the originator.

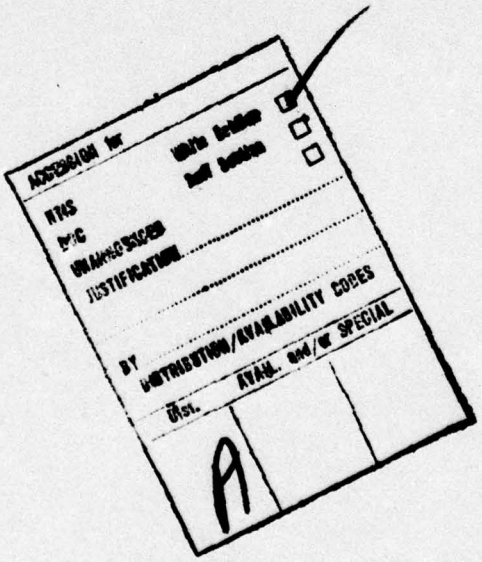

Unclassified

SECURITY CLASSIFICATION OF THIS PAGE (When Data Entered)

| REPORT DOCUMENTATION PAGE | READ INSTRUCTIONS BEFORE COMPLETING FORM |
|---|---|
| 1. REPORT NUMBER: DAAG53-76-C-0012 | 2. GOVT ACCESSION NO. |
| 3. RECIPIENT'S CATALOG NUMBER | |
| 4. TITLE (and Subtitle): A FLUIDIC FUEL AND AIR BLEED LOAD CONTROL SYSTEM FOR GAS TURBINE ENGINES. (See other side for subtitle) | 5. TYPE OF REPORT & PERIOD COVERED: Final Report for Period 8-25-75 thru 8-25-76 |
| | 6. PERFORMING ORG. REPORT NUMBER: 76-411516 |
| 7. AUTHOR(s): R. S. McCarty, H. R. Gamble | 8. CONTRACT OR GRANT NUMBER(s): DAAG53-76-C-0012 NEW |
| 9. PERFORMING ORGANIZATION NAME AND ADDRESS: AiResearch Manufacturing Co. of Ariz. A Division of The Garrett Corporation 402 So. 36th St., P. O. Box 5217 Phoenix, Arizona 85010 | 10. PROGRAM ELEMENT, PROJECT, TASK AREA & WORK UNIT NUMBERS: Item 0002 Sequence A002 |
| 11. CONTROLLING OFFICE NAME AND ADDRESS: U. S. Army Mobility Equipment Research and Development Center Fort Belvoir, Virginia 22060 | 12. REPORT DATE: 15 December 1976 |
| | 13. NUMBER OF PAGES: 75 |
| 14. MONITORING AGENCY NAME & ADDRESS (if different from Controlling Office): Final rept. 25 Aug 75 - 25 Aug 76 | 15. SECURITY CLASS. (of this report): Unclassified |
| | 15a. DECLASSIFICATION/DOWNGRADING SCHEDULE |
| 16. DISTRIBUTION STATEMENT (of this Report): Distribution of this report is unlimited. 12 76p. | |
| 17. DISTRIBUTION STATEMENT (of the abstract entered in Block 20, if different from Report) | |
| 18. SUPPLEMENTARY NOTES | |
| 19. KEY WORDS (Continue on reverse side if necessary and identify by block number) | |

DDC RECEIVED FEB 16 1977 C

20. ABSTRACT (Continue on reverse side if necessary and identify by block number)

This is the final report of a program conducted by AiResearch and funded by the U.S. Army Mobility Equipment Research and Development Center to develop a fluidic fuel and air bleed load control system for the AiResearch Model GTCP85-180 gas turbine engine. The basic functions provided by the control system include engine starting, speed governing, and bleed load extraction and exhaust gas temperature limiting.

DD FORM 1 JAN 73 1473 EDITION OF 1 NOV 65 IS OBSOLETE

Unclassified 404796

SECURITY CLASSIFICATION OF THIS PAGE (When Data Entered)



LB

4. Development of AiResearch Fluidic Fuel and Bleed Air Load Control System for AiResearch Gas Turbine Engine Model GTCP85-180.

## PREFACE

This is the final report on a program conducted by AiResearch Manufacturing Company of Arizona, a Division of The Garrett Corporation, for the U.S. Army Mobility Equipment Research and Development Center (USAMERDC) to design, develop, fabricate, test, and deliver to the government a fluidic fuel and air bleed load control system for application on an AiResearch Model GTCP85-180 gas turbine engine.

The program was authorized by USAMERDC Contract DAAG53-76-C-0012 and was conducted during the period from August 25, 1975, through August 25, 1976, under AiResearch Master Work Order 3209-214757-01-0100. Mr. Robert N. Ware, Code STSFB-EP, USAMERDC, Fort Belvoir, Virginia, and Mr. John Goto, Harry Diamond Laboratories, Adelphi, Maryland, administered the program for the Army.

Publication of this report does not constitute U.S. Army (MERDC) approval of the findings or conclusions presented herein.

TABLE OF CONTENTS

## LIST OF ILLUSTRATIONS

C

# 1. INTRODUCTION

## 1.1 BACKGROUND AND OBJECTIVES

As a major manufacturer of gas turbine engines and accessories, AiResearch has maintained an active interest in fluidics for more than eleven years. Research in fluidics, initiated with the intent of applying fluidic control and sensing concepts to AiResearch-manufactured products, has resulted in development of all necessary basic fluidic circuit components, as well as special sensors for control of such parameters as shaft speed, pressure, pressure ratio, temperature, acceleration, angular rate, and position. In addition, AiResearch has developed special photochemical etching and bonding techniques that are used to manufacture completely integrated fluidic control circuits. Fluidic control systems are presently in production for several aerospace applications. These include a speed and torque control system for the thrust reverser on the General Electric CF6 engine on the McDonnell Douglas DC-10 airplane, a ram air pressure regulator on the Lockheed S-3A airplane, and a speed control for the air motor on the Concorde SST thrust reverser and engine nozzle control system.

It has long been recognized that the ability of fluidic circuits to operate in hostile environments makes this technology well suited to fuel control applications on gas turbine engines. Utilizing the available compressor discharge pressure as a control parameter and functional compressor flow as the operating fluid, integral control systems may be designed which do not require external power supplies. In addition, studies pertaining to reliability and cost have revealed considerable advantage for fluidics when compared with other technologies.

In early 1974, USAMERDC awarded AiResearch a contract to develop a fluidic fuel control for a small recuperated gas turbine engine used to provide standby or portable electrical power. Based upon the engine requirements for speed and exhaust temperature regulation, a breadboard fluidic control was fabricated. This control drew heavily upon the technology developed during previous control programs.

Successful completion of the program described above, and many other related sensor and transducer development programs at AiResearch, has confirmed the suitability of applying fluidic technology to the control requirements associated with small gas turbine engines. For the most part, however, these programs have

dealt with one-of-a-kind applications with subsequent limited exposure to conditions encountered in the field. In addition, the breadboard configuration of these units has not provided information directly applicable to production-type hardware.

Therefore, the present program was formulated to lead to the fabrication of a fluidic control system which can be applied to engines under a variety of operating conditions. Field evaluation data from these units can then be obtained which will result in a new generation of controls with improved reliability and reduced cost of ownership when compared with current systems.

To realize the greatest possible range of field exposure, a fluidic fuel control system designed to operate with a gas turbine engine utilized by all three military services was selected, the AiResearch Series 85 gas turbine. In Navy and Air Force applications, this engine is used to provide electrical and pneumatic power for aircraft main engine starting and support while on the ground. The engine is used by the Army for generation of electrical power for standby and portable emergency operation in the field. Although these applications require different engine models, the fuel control functions are similar and direct exchange is possible through recalibration procedures. The specific unit chosen for the proposed program is Model GTCP85-180.

## 1.2 STATEMENT OF WORK

The scope of work in the development of the fluidic control system included the following tasks.

TASK A DESIGN AND FABRICATE A PROTOTYPE CONTROL SYSTEM TO MEET THE PERFORMANCE REQUIREMENTS IN AIRESEARCH MODEL SPECIFICATION NO. SC-5990B, DATED JUNE 27, 1973

TASK B CONDUCT BENCH TESTS TO CONFIRM STEADY-STATE PERFORMANCE

TASK C CONDUCT TESTS WITH CONTROL SYSTEM ON ENGINE TO CONFIRM DYNAMIC RESPONSE AND ACCURACY

TASK D FINALIZE DESIGN AND UPDATE DRAWINGS

## 1.3 PROGRAM SCHEDULE

A bar chart representation of the program schedule showing the more important program steps and their periods of completion is given in Figure 1.

# 2. INVESTIGATION

## 2.1 DESIGN

### 2.1.1 Design Analysis

2.1.1.1 Existing Control System - The control system currently used on the subject engine consists of seven discrete items as shown in Figure 2. The load valve is used to limit bleed airflow extraction from the engine compressor to prevent excessive exhaust temperature. The fuel control regulates fuel flow for engine starting, proportional speed governing, and exhaust temperature-limiting during starting. The thermostat senses exhaust temperature and serves as an input to both the fuel control and load valve. All three items are powered by air pressure extracted from the engine compressor. The regulator (Part 108032-3) is required in the system to establish the gain of the thermostat. The check valve and solenoid (Parts 968390-1 and 692546-1, respectively) are used to inhibit the input of the thermostat to the fuel control after engine starting. This is necessitated by the fact that the thermostat is a single, set-point device and cannot be used as an input to both the load valve and fuel control simultaneously. A 95-percent-speed electrical signal to the load valve and solenoid is used to transfer the thermostat input from the fuel control to the load valve.

The electrical fine-speed control (Part 305136) senses alternator frequency and electrically resets the fuel control to provide precise (±1/4 percent) speed control regardless of load.

Through analysis and testing of the existing control components, it was determined that the gas turbine is presently controlled according to the following equation:

$$P_{FA} = 13\ P_{CD} + 60 - 1.68\ T_5e - 1.50\ Ne \qquad (1)$$

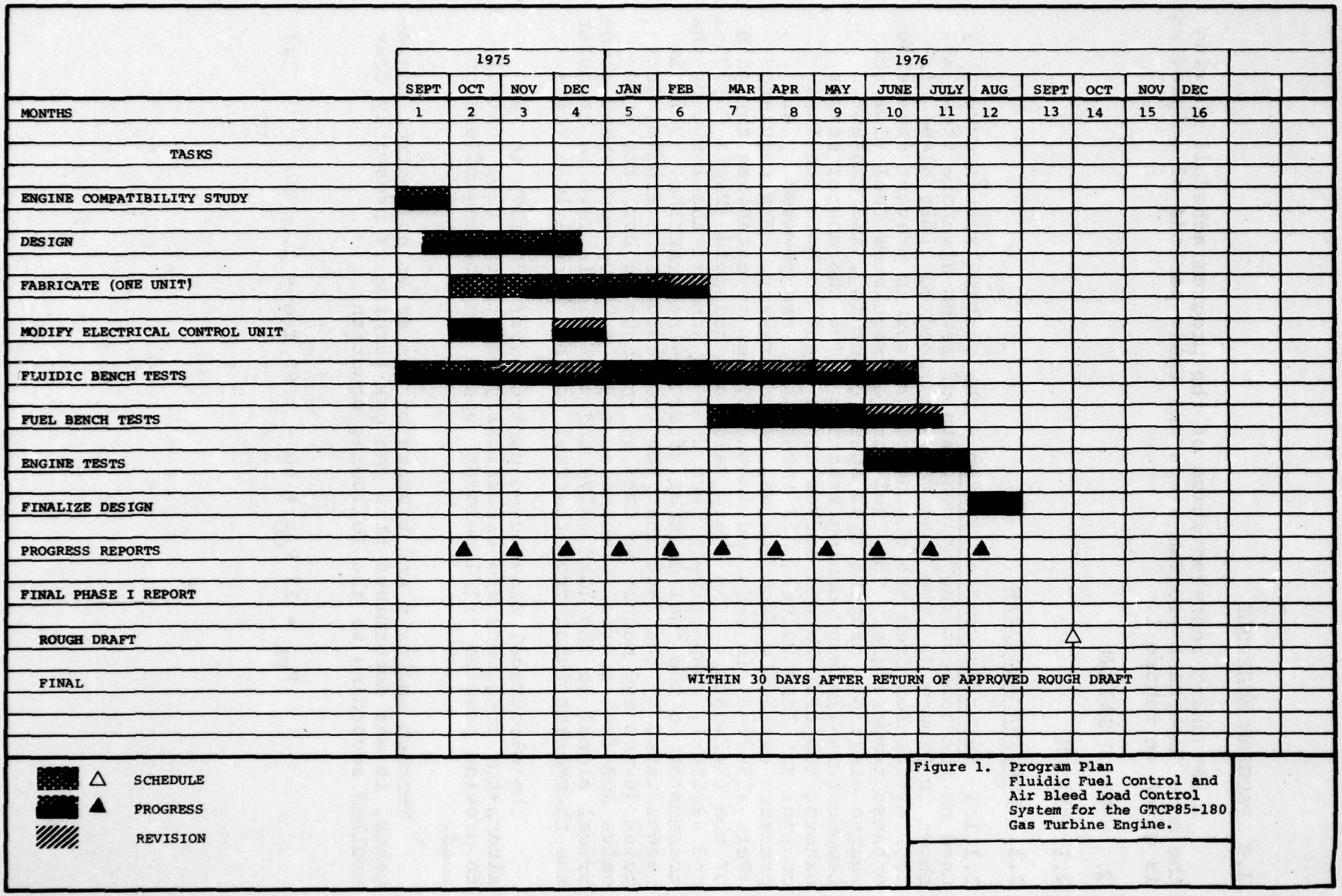


Figure 1. Program Plan
Fluidic Fuel Control and
Air Bleed Load Control
System for the GTCP85-180
Gas Turbine Engine.

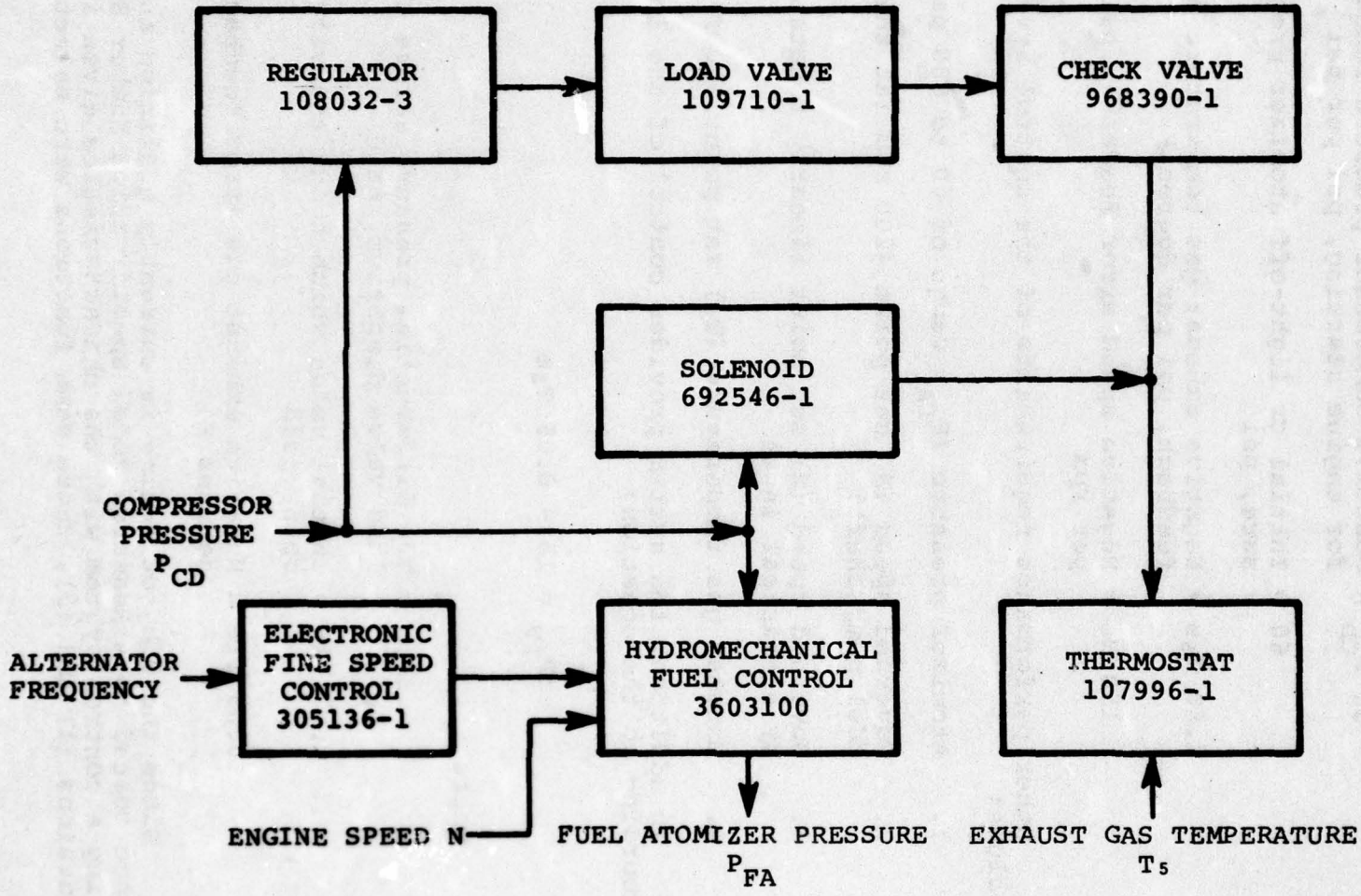


**Figure 2. Existing Control System on Model GTCP85-180 APU.**

where

$P_{FA}$ = Fuel atomizer pressure, psi

13 $P_{CD}$ = Positive compressor pressure feedback for engine starting, psi per psi

60 = Initial or light-off atomizer pressure, psi

1.68 $T_5e$ = Negative exhaust gas temperature error feedback, psi per degree F

150 Ne = Negative speed error feedback, psi per rpm

Other performance requirements of the control system include:

1. Atomizer pressure ($P_{FA}$) range of 60 to 600 psi
2. Governed speed (N) set point 4200 rpm (at the fuel pump shaft)
3. Governed speed (N) set point linearly resetable by electrical input
4. Exhaust gas temperature ($T_5$) set point 1200F

In addition, the system provides control of the load valve according to the equation:

$$\Delta P_{LV} = 15 - 0.05\ T_5e \qquad (2)$$

where

$\Delta P_{LV}$ = The differential pressure across the load valve diaphragm, psid

15 = Initial value which holds the valve open, psid

0.05 $T_5e$ = Negative exhaust gas error feedback, degrees F

Since the subject engine is currently qualified and acceptance tested to AiResearch Model Specification Number SC-5990B using a control system with the characteristics given in Equations (1) and (2), these same functions were selected as

the design goals for the fluidic system. It was also realized that the gain terms might have to be adjusted somewhat as a result of engine testing in order to compensate for the differences in dynamic response between the existing control and the fluidic control.

2.1.1.2 Fluidic Control System - The fluidic control system is composed of four discrete components as shown in Figure 3. The fuel and bleed load control (Part 710518-1), as its name implies, performs two basic functions. It regulates fuel flow for engine starting and proportional speed governing, and, at speeds above 95 percent, provides inputs to the bleed load valve.

The bleed load valve (Part 109772-1) is used to limit bleed load extraction from the engine compressor to prevent excessive exhaust gas temperature. This valve is very similar to the normal valve used on the engine with the exception that several solenoid parts have been deleted and a fluidic circuit has been added. The fluidic temperature sensor (Part 710552-1) monitors engine exhaust gas temperature and serves as an input to the fuel and bleed load control.

As in the existing system, the electronic fine speed control (Part 305136) senses alternator frequency and electrically resets the fuel control to provide precise (±1/4 percent) speed control regardless of speed.

These various control functions are summarized in block diagram form in Figure 4. Figure 5 shows these functions in more detail and reveals the almost entirely fluidic mechanization employed in the control. As shown, the engine speed is sensed by an interrupted-jet, pulse generator with the output frequency amplified and rectified by a series of flueric (no moving parts) fluidic amplifiers. The pressure level output of these stages is then compared with a pneumatic pressure reference representing the desired engine speed and the difference (or speed error) is further amplified.

Exhaust gas temperature ($T_5$) is detected by a sonic oscillator flueric sensor which produces a pneumatic frequency proportional (in the operating range) to exhaust temperature. This signal is amplified and rectified by a series of flueric amplifiers and compared with a pneumatic pressure reference which represents the maximum allowable temperature. If the maximum is exceeded, an error signal is generated which, after amplification, is transmitted to the load valve and to a summing junction. The signal transmitted to the load valve is used to close the valve and reduce bleed load. The signal transmitted to the summing junction is combined with the speed error signal and a pressure proportional to compressor discharge pressure. The

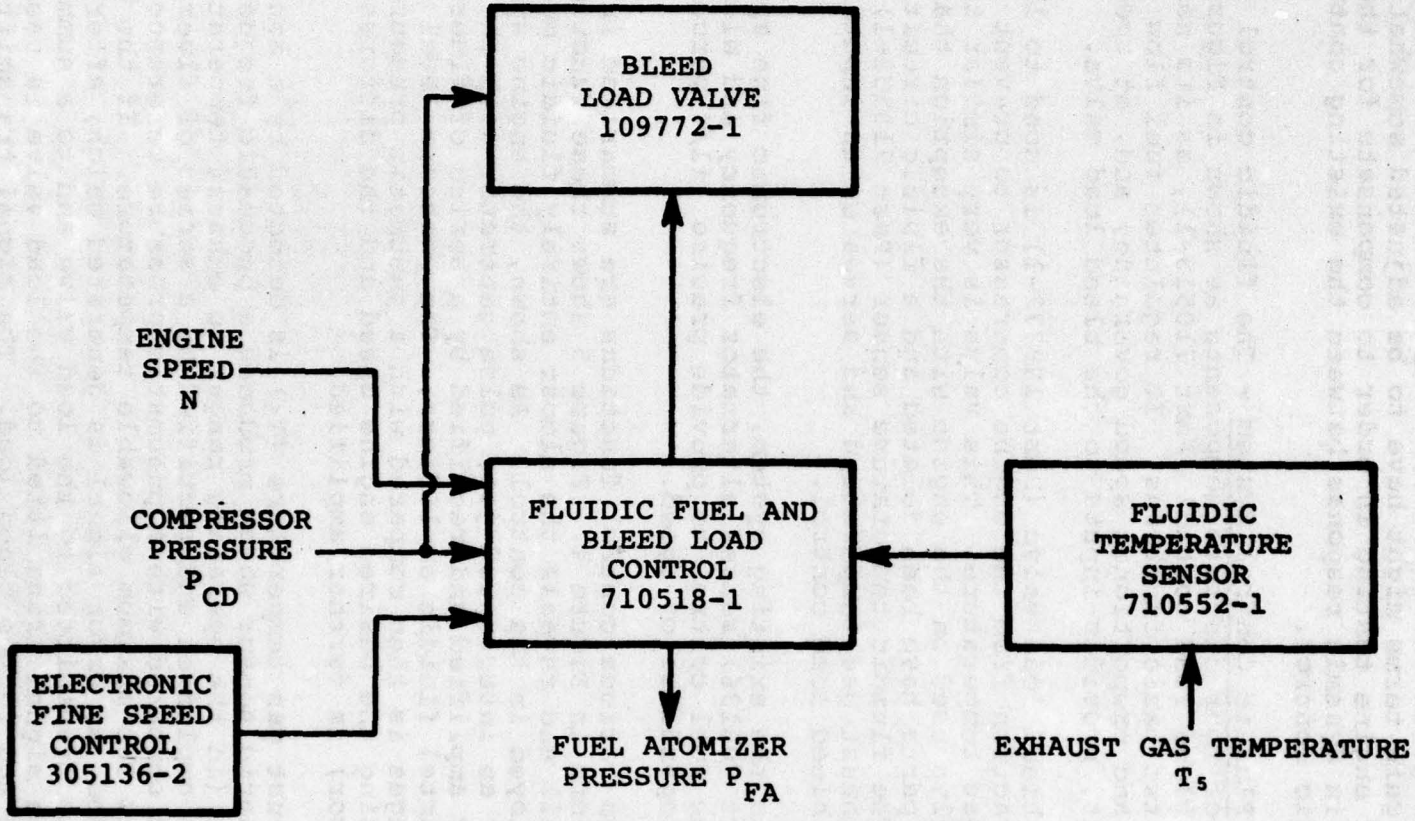


Figure 3. Proposed Fluidic Control System for Model GTCP85-180 APU.

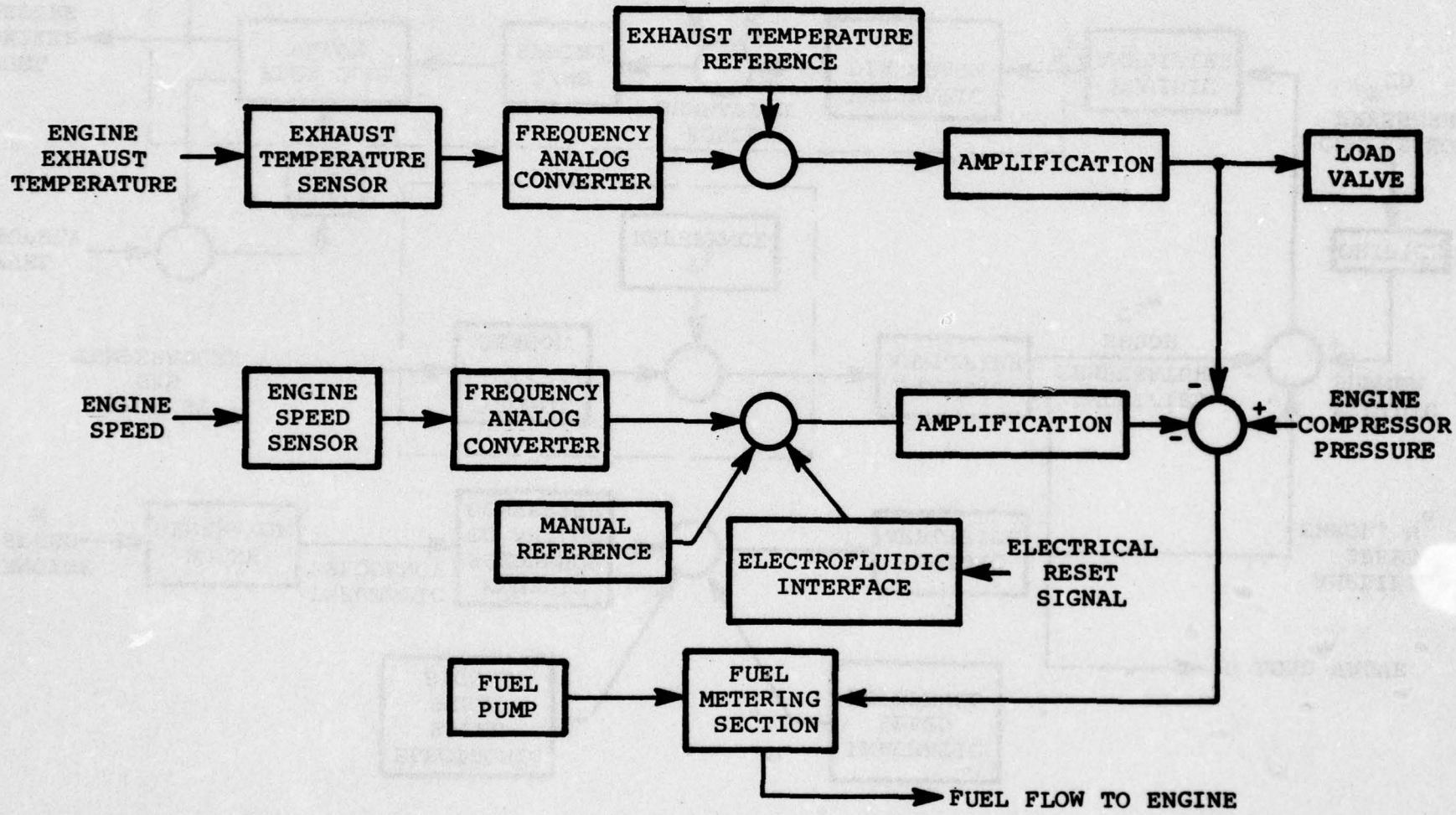


Figure 4. Control System Block Diagram.

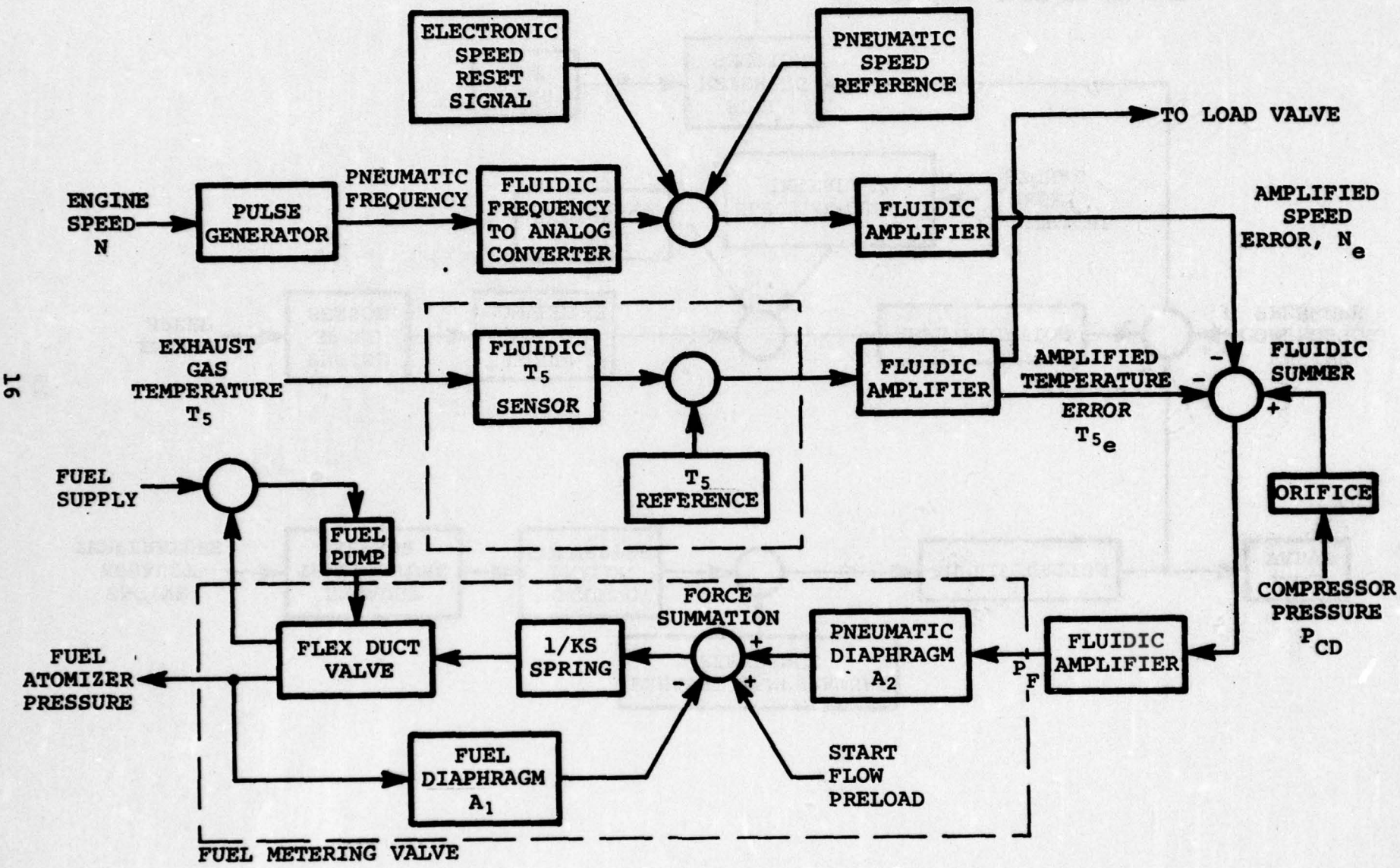


Figure 5. Fluidic Fuel Control Block Diagram.

resulting summation is further amplified to produce the signal $P_F$ which will be referred to hereafter as the fluidic pressure. This fluidic pressure is then applied to a unique fuel metering system which serves to modulate fuel flow to the engine.

The fuel metering system is depicted schematically in Figure 6. As shown, fluidic air pressure, from the circuits described above, acts through a diaphragm, lever, and pivot to move or deflect a flexible-duct valve. As the duct is brought into alignment with its nozzle port, a greater percentage of fuel pump discharge pressure is recovered, thereby raising fuel atomizer pressure. This pressure is sensed by a small fuel diaphragm, thus providing a feedback force to rebalance the lever. Fuel flow not recovered by the flex-duct valve is collected in the vent area of the valve and returned to fuel pump inlet. Adjustment of the start flow screw sets the initial nozzle pressure required at engine light-off (60 psi in the control Equation (1)).

To provide for some adjustability of the engine start schedule (see Equation (1)), a ratio of fuel atomizer to compressor pressures of 13.5, rather than 13, was selected. This ratio could then be reduced to the desired value during calibration by orificing the compressor pressure supply to the last fluidic amplifier. It was further estimated that the lowest pressure recovery which could be expected from this last amplifier would be 50 percent. The minimum required gain of the fuel metering system, therefore, was established as $\frac{13.5}{0.5}$, or 27.0 psi atomizer pressure per psi fluidic pressure.

Figure 7 shows the diaphragm areas selected to yield this metering valve gain. It should be noted that the high (10,000 psi per inch) gain of the flex-duct valve makes the system virtually independent of spring rate and lever ratio. A 0.5-inch nominal diameter was selected as the smallest practical size for the fuel diaphragm, which choice then resulted in a 2.66-inch diameter air diaphragm.

Dynamic analysis of the complete fuel metering valve system revealed that an orifice of 0.020-inch diameter in the feedback path was required to provide critical damping of the valve.

### 2.1.2 Fluidic Circuit Design

2.1.2.1 Speed Circuit - The fluidic circuitry employed to generate the required control equations is shown schematically in Figure 8. As shown, the circuit is divided into three groups which, in the final system, are discrete bonded "stacks". The speed circuit ("N" stack) is designed to convert pneumatic

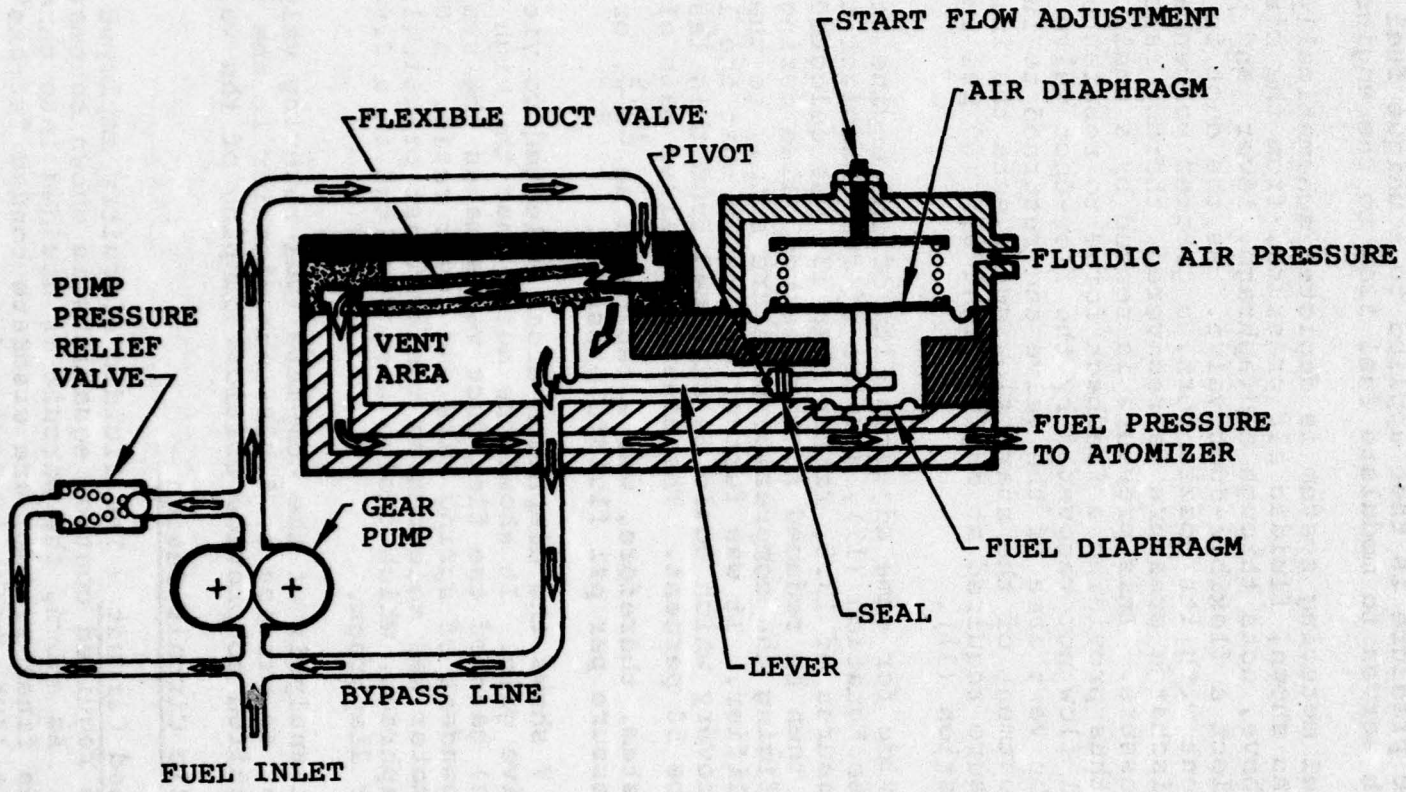


Figure 6. Fuel Metering System.

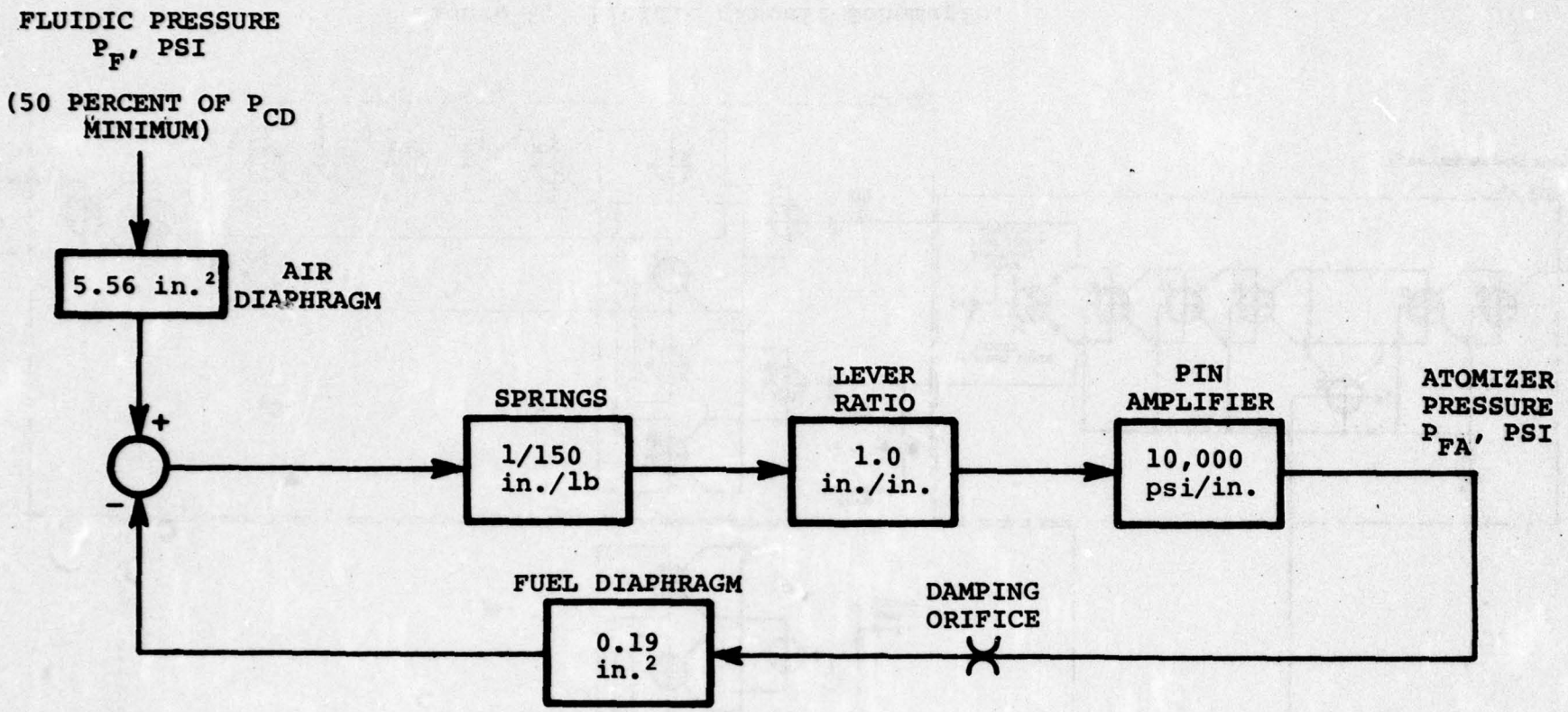


$$\text{METERING VALVE GAIN} = \frac{\Delta P_{FA}}{\Delta P_F} = \frac{\frac{(5.56)(1.0)(10{,}000)}{150}}{1 + \frac{(1.0)(10{,}000)(0.19)}{150}} = \frac{5.56}{0.015 + 0.19} = 27.1 \frac{\text{psi}}{\text{psi}}$$

Figure 7. Metering Valve Steady-State Gain.

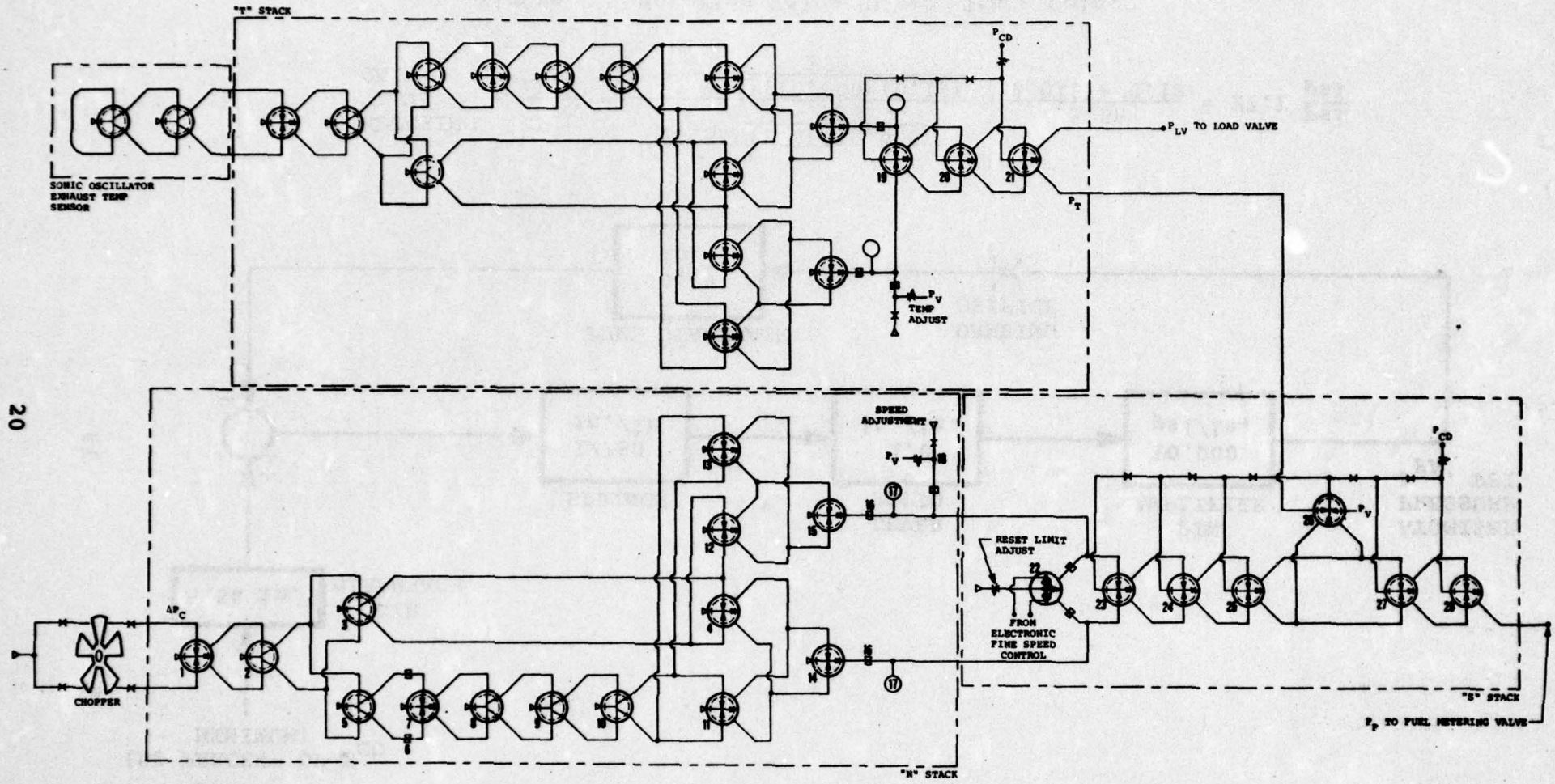


Figure 8. Fluidic Circuit Schematic.

pulsations from the gear-pump-mounted, five-bladed "chopper" to an analog differential pressure which is proportional to speed. Early in the program it was decided that the fluidic circuits would be operative at as low a speed (and, therefore, compressor pressure) as possible. Therefore, regulated supply pressure was selected as 3.0 psig and the circuit exhaust or vent pressure was selected as ambient. It was realized that using such a gauge differential-pressure, supply system would result in shifts in circuit gain and set point with altitude and temperature variations for the normal frequency to analog circuit. Accordingly, a new circuit was devised which can be compensated for these two variables.

As shown, amplifiers 1 and 2 shape the pulse derived from the "chopper" and feed two paths, the undelayed and delayed paths, which begin with amplifiers 3 and 5, respectively. The delayed path 5 through 11 consists of a series of proportional and digital amplifiers as well as capillary resistors.

Due to the transport time associated with each of the elements in both paths, a phase shift in the output of amplifier 11 with respect to amplifier 4 will occur which increases with chopper input frequency. Since the output of amplifiers 11 and 4 are summed, the relative "on" versus "off" time of the rectifier, 14, will be proportional to input frequency. Ripple on this signal is attenuated by means of resistor 16 and volume 17.

Experimental data has revealed that the transport time of these elements vary with changes in temperature and supply pressure (altitude) in unique and dissimilar ways. By adjusting the number and types of these elements, the total delay time of path 5 to 11 with respect to path 3 to 4 will remain constant at a given frequency over the environmental range of interest.

Elements 12 and 13 also detect the phase difference between the two paths; however, their outputs are summed with reverse sign to that of 4 and 11 such that rectifier 15 is "off" when rectifier 14 is "on" and vice versa. This arrangement allows for a differential output from the speed circuit with consequently higher gain.

Speed set point adjustment is provided by biasing the filtered output level of rectifier 15 with a pressure signal derived from supply pressure (see 18).

2.1.2.2 Temperature Circuit - The fluidic temperature circuit ("T" stack) operates in exactly the same manner as the speed circuit described above, except that its input is derived from a sonic oscillator temperature sensor installed in the engine exhaust pipe.

Amplification (elements 19 through 21) of the temperature error signal is provided in the "T" stack from which two signals are derived, $P_{LV}$ and $P_T$. $P_{LV}$ decreases, thereby closing the load valve for temperatures above the desired maximum, while $P_T$ increases. The resulting action of the latter signal will be discussed in the following section.

2.1.2.3 Summation Circuit - The summation circuit ("S" stack), as its name implies, performs a summation of the speed and temperature error signals as well as inputs from the electronic fine speed control, amplifies the result, and drives the metering valve diaphragm. The device used to convert electrical signals from the fine speed control is the AiResearch-patented electrofluidic transducer, element 22. This device consists of a permanent magnet surrounding a wire-wound bobbin which is supported from the magnet by a cruciform flex pivot. Extending from the bobbin is a small diameter pin, the opposite end of which is inserted into the interaction region of a fluidic amplifier. When the windings of the coil are energized, a torque is produced which deflects the bobbin against the spring rate of the flex pivot and the pin moves laterally with respect to the power jet of the fluidic amplifier. This action deflects the power jet and produces a pressure differential in the output ports of the amplifier. The electrofluidic (E/F) transducer is shown schematically in Figure 9.

Referring again to Figure 8, the output of the E/F transducer is summed with the speed error signal and the result is amplified by elements 23 through 25. At this point the temperature error signal, $P_T$, is introduced through amplifier 26. It should be noted that the temperature error signal is a "single-sided" input to the "S" stack because its function is that of limiting rather than controlling. Provided that the maximum exhaust temperature has not been exceeded, the output of amplifier 26 remains at null.

The final amplifiers, 27 and 28, increase the overall control gains to the proper levels and, in addition, provide power staging to drive the metering valve diaphragm.

2.1.3 Mechanical Design

2.1.3.1 Fuel and Air Bleed Control - Primary mechanical considerations in the design of the control were that it:

1. Fit the existing gearbox mounting flange and drive shaft.

2. Provide adequate gearbox clearance for mounting bolts, lines, fittings, etc.

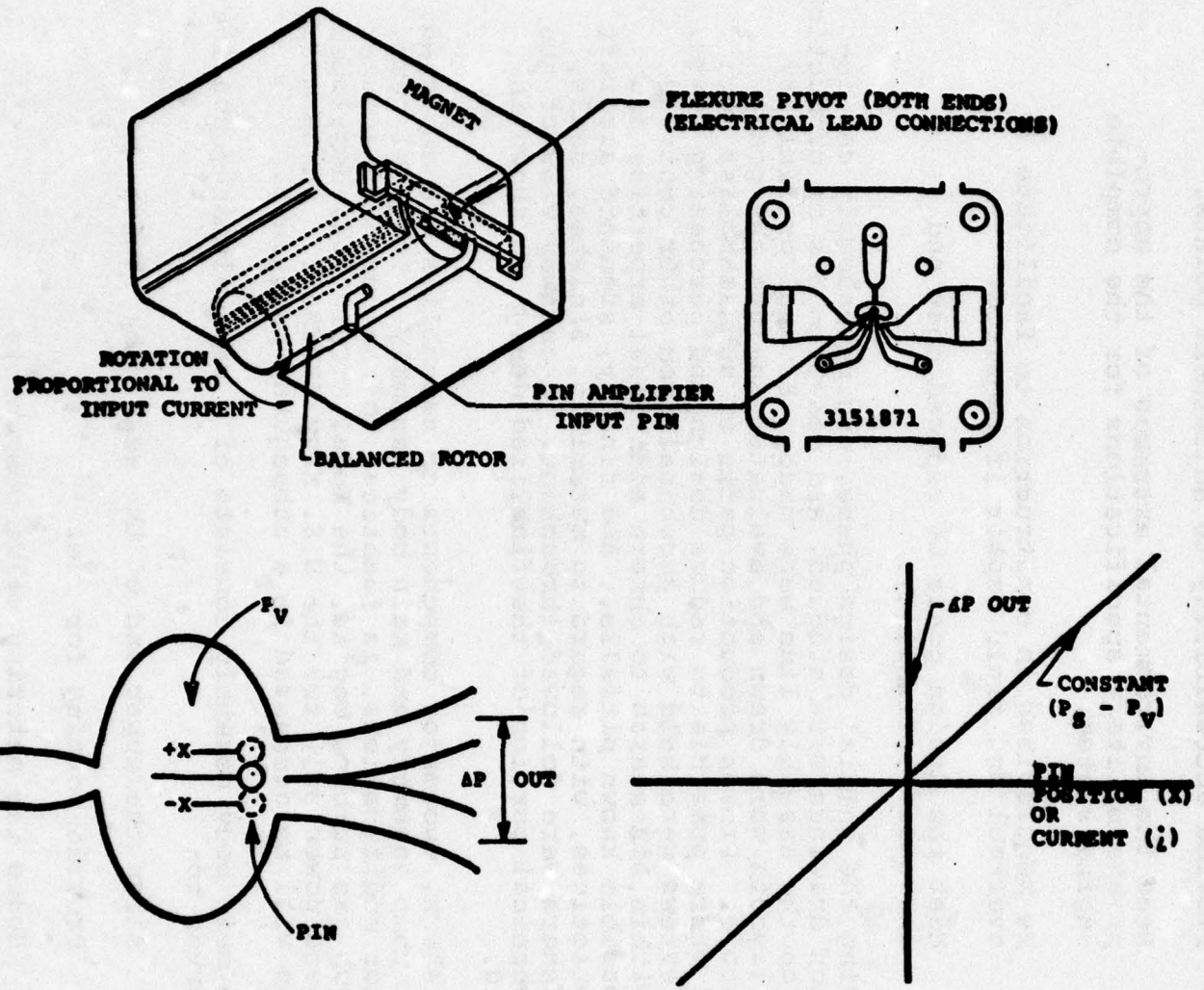


Figure 9. Schematic Diagram and Performance of Electrofluidic Transducer.

3. Not violate engine external envelope dimensions.

4. Provide accessibility to adjustment points.

5. Meet the environmental extremes of the appropriate military specifications for the complete engine system.

6. Be modularized in construction to facilitate overhaul and field repair if required.

7. Meet the design goals of reduced cost and increased reliability.

During the initial design phase, engine assembly and installation drawings were studied, and measurements of production engines on the assembly line were made. Several preliminary control layouts were drawn and evaluated against the goals stated above. Proven production parts or subassemblies were selected where possible to reduce design and purchasing costs. Design reviews were held with personnel from other controls groups within AiResearch to obtain additional expertise and avoid possible known pitfalls. And finally, standard aircraft design practices, with regard to materials, finishes, seals, and fasteners were followed throughout. A cutaway view of the hydromechanical portion of the finalized design is shown in Figure 10.

As shown, two major components or assemblies are employed, the fuel pump assembly and main body assembly. The fuel pump, with minor modifications, is identical to that used on another AiResearch gas turbine engine, the Model GTCP100-54, developed as a ground power unit for the U.S. Navy (BUWEPS). These modifications will be discussed in a subsequent paragraph.

The main body assembly consists of a cast aluminum housing which serves to:

(a) Align the upper end of the gear pump shafts

(b) Provide porting for fuel

(c) House the metering valve components

(d) Mount the fluidic manifold and circuits (not shown)

(e) Mount the fluidic supply pressure regulator (not shown)

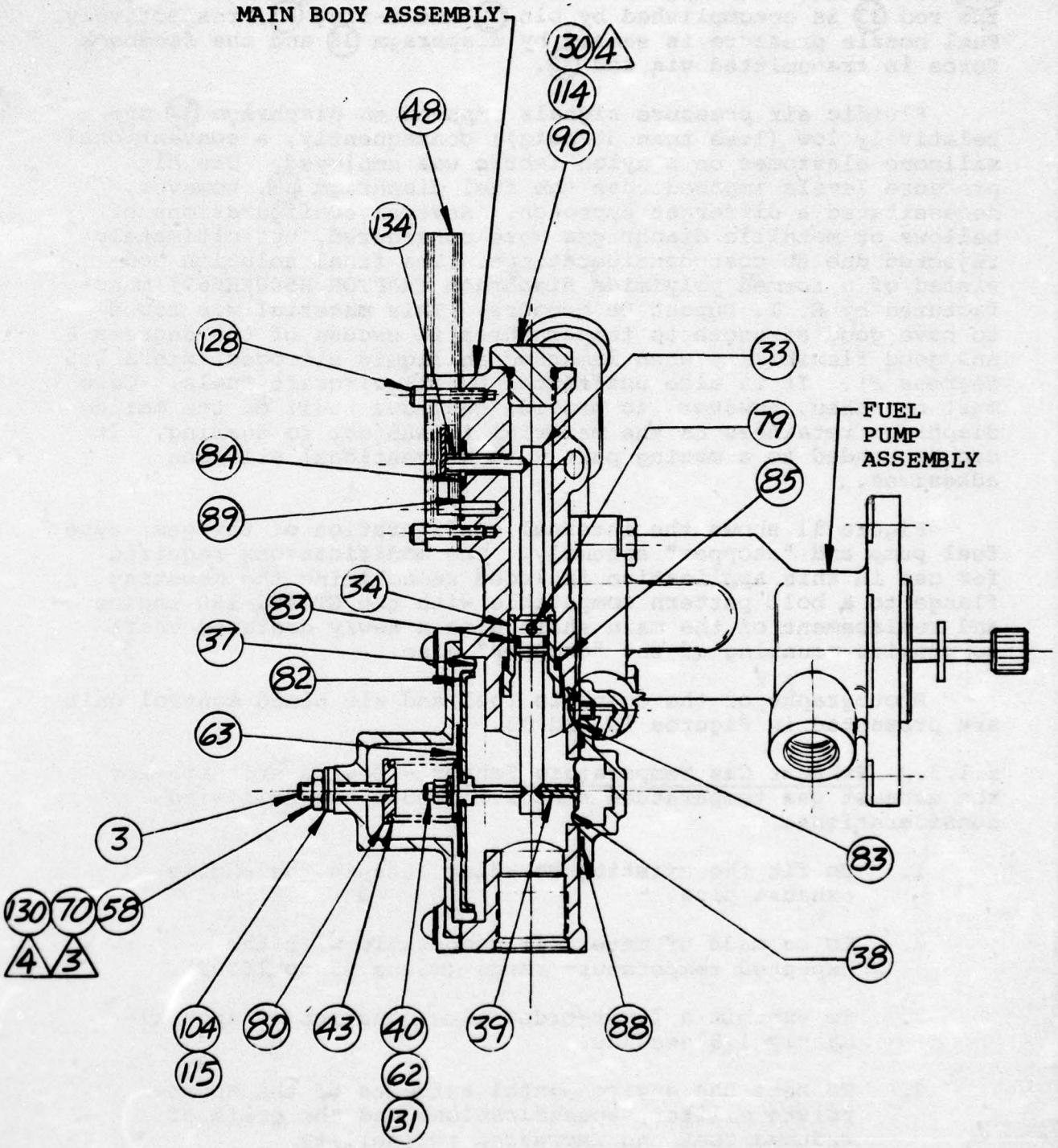


Figure 10. Hydromechanical Cutaway Drawing.

As described earlier, fluidic air pressure is sensed by diaphragm 37 which transmits a force through rods (40), (33), and (134) to deflect the flex-duct valve (48). Pivoting and sealing of the rod (33) is accomplished by pin (79) and O-ring (83), respectively. Fuel nozzle pressure is sensed by diaphragm (38) and the feedback force is transmitted via rod (39).

Fluidic air pressure signals imposed on diaphragm (37) are relatively low (less than 30 psig); consequently, a conventional silicone elastomer on a nylon fabric was employed. The high pressure levels imposed upon the fuel diaphragm (38), however, necessitated a different approach. Several configurations of bellows or metallic diaphragms were considered, but ultimately rejected due to cost considerations. The final solution consisted of a formed polyimide diaphragm (KAPTON H500XH667) manufactured by E. I. Dupont De Nemours. This material was found to have good strength to temperatures in excess of 600 degrees F and good flexibility when immersed in liquid nitrogen (minus 325 degrees F). It is also unaffected by all aircraft fuels. Care must be taken, however, to provide generous radii on the mating diaphragm retainers as the material is subject to tearing. It can be bonded to a mating part with conventional silicone adhesives.

Figure 11 shows the internal configuration of the gear-type fuel pump and "chopper" assembly. The modifications required for use in this application included remachining the mounting flange to a bolt pattern compatible with the GTCP85-180 engine and replacement of the main shaft with a newly designed shaft to provide mounting of the "chopper" disc.

Photographs of the complete fuel and air bleed control unit are presented in Figures 12 and 13.

2.1.3.2 Exhaust Gas Temperature Sensor - Design criteria for the exhaust gas temperature sensor included the following considerations:

1. To fit the existing mounting boss in the engine exhaust pipe.

2. To be made of materials compatible with the expected temperature range (minus 65 to 1500F).

3. To exhibit a first-order time constant of approximately 1.5 seconds.

4. To meet the environmental extremes of the appropriate military specifications and the goals of reduced cost and increased reliability.

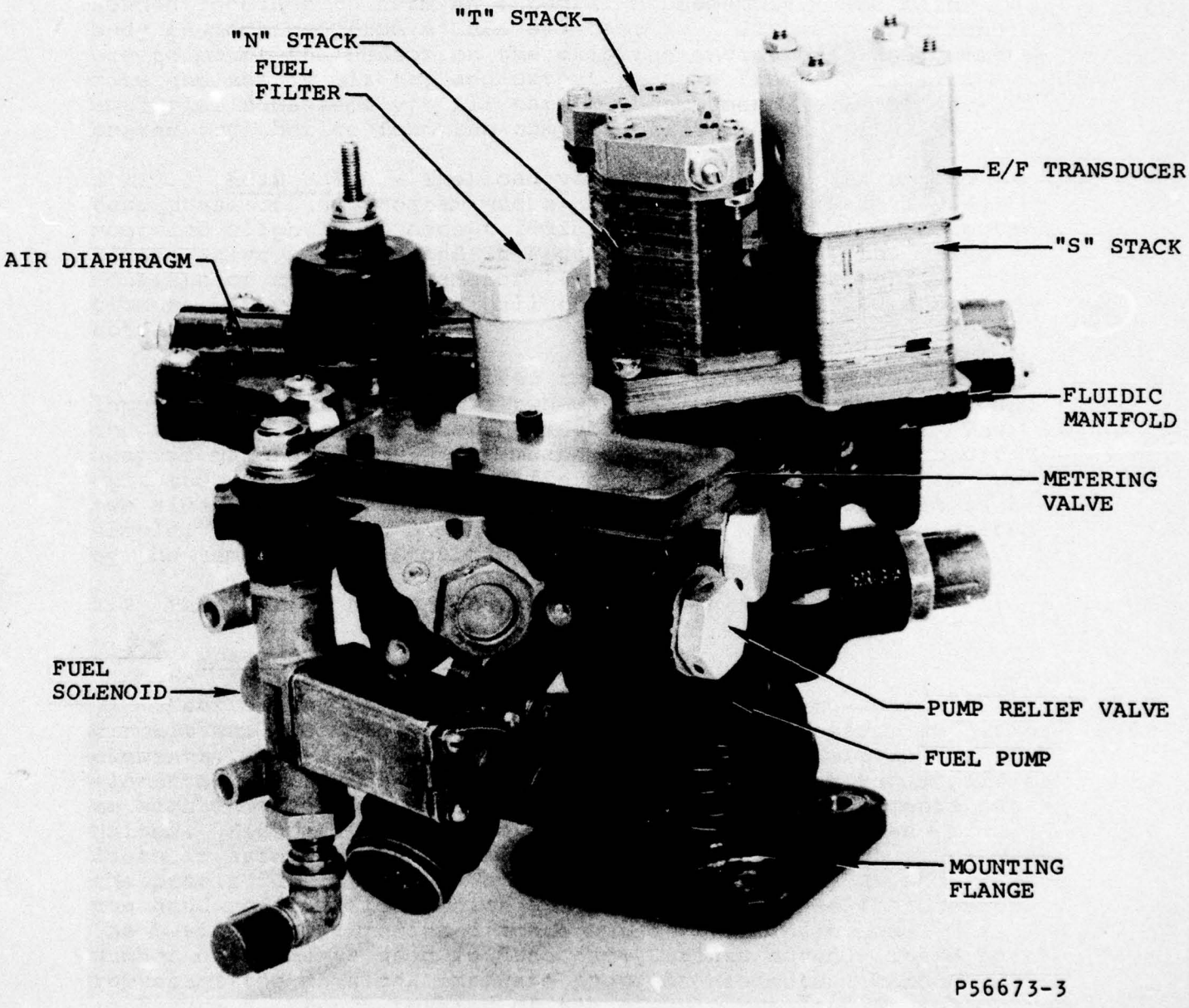


**Figure 12. Fluidic Fuel and Air Bleed Control.**

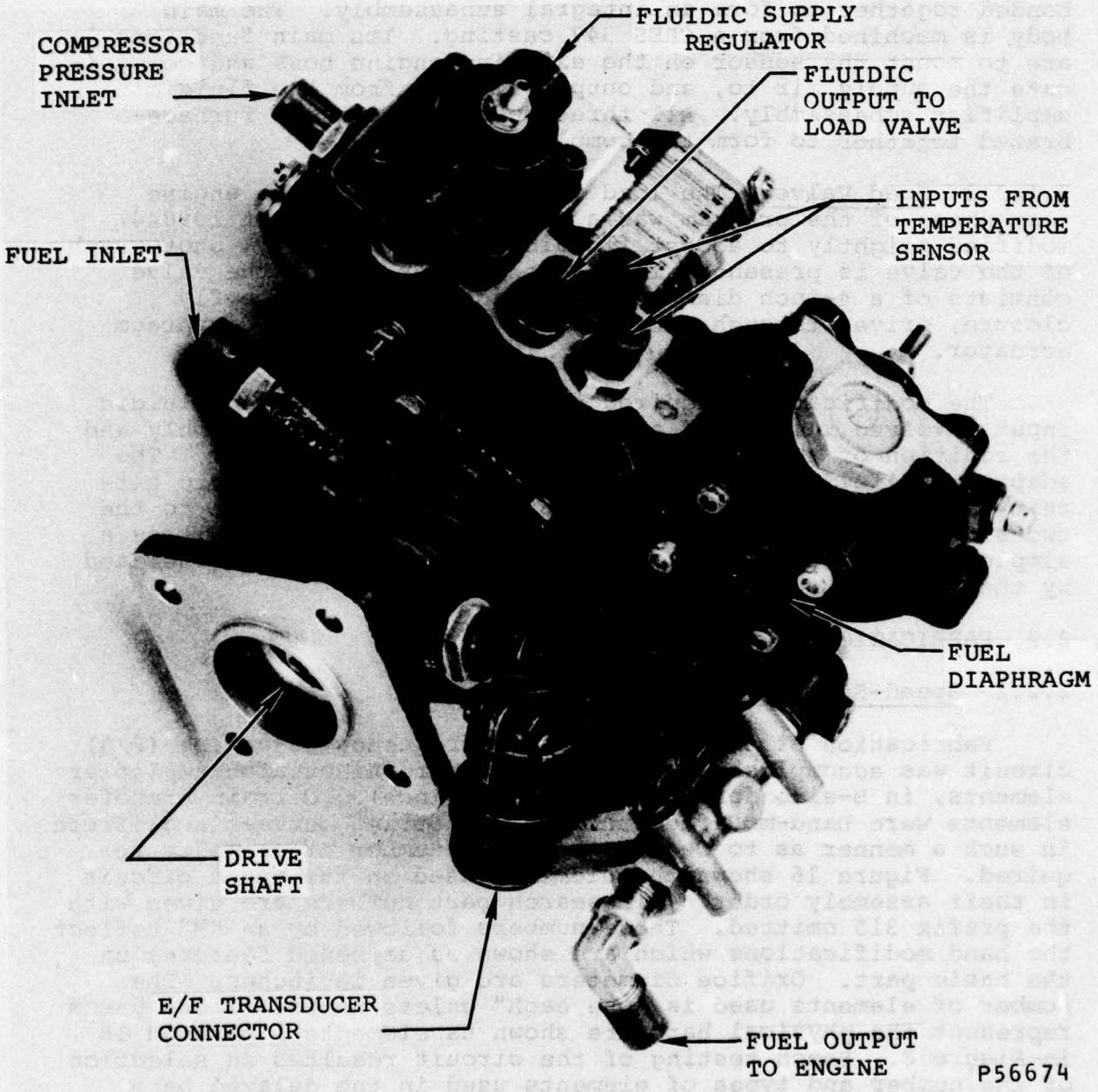


**Figure 13. Fluidic Fuel and Air Bleed Control.**

Figure 14 is a photograph of the completed sensor. As shown, the sensor consists of three primary parts, the sensing tube, fluidic amplifiers, and main body. The sensing tube is formed from 0.125-inch O.D., 0.010-inch wall thickness, Hasteloy X material. The fluidic amplifiers are circular elements, chemically milled from CRES 347 sheet stock and bonded together to form an integral subassembly. The main body is machined from a CRES 347 casting. Its main functions are to mount the sensor on the existing engine boss and communicate the supply air to, and output signals from the fluidic amplifier subassembly. All three subcomponents are furnace-brazed together to form the complete sensor.

2.1.3.3 Load Valve - The load valve used during the engine test phase of the program was a production unit (Part 109644) modified slightly to accept fluidic input signals. A photograph of the valve is presented in Figure 15. As shown, the valve consists of a 4-inch diameter flow section with butterfly closure, driven through a bell crank mechanism by a diaphragm actuator.

The modification required to convert the valve to fluidic input involved removal of a two-way solenoid valve assembly and the addition of an adaptor manifold and fluidic circuit. The adaptor manifold provides a means of mounting the fluidic circuit and ports the fluidic differential output pressure to the two sides of the actuator diaphragm. The fluidic circuit is a simple, 3-stage gain block which amplifies the signal generated by the temperature circuit described earlier.

## 2.2 FABRICATION AND BENCH TESTING

### 2.2.1 Speed-Sensing Circuit

Fabrication of the speed sensing frequency-to-analog (F/A) circuit was accomplished utilizing standard AiResearch amplifier elements, in B-size format (0.84 x 0.84 inch). Certain transfer elements were hand-modified to provide porting between amplifiers in such a manner as to reduce the total number of elements required. Figure 16 shows the elements used in the speed circuit in their assembly order. AiResearch part numbers are given with the prefix 315 omitted. These numbers followed by an "M" reflect the hand modifications which are shown as darkened features on the basic part. Orifice diameters are given in inches. The number of elements used is "one each" unless noted. These parts represent the physical hardware shown as elements 1 through 18 in Figure 8. Bench testing of the circuit resulted in selection of the number and types of elements used in the delayed path (discussed in Section 2.1.2.1 of this report) which yielded the

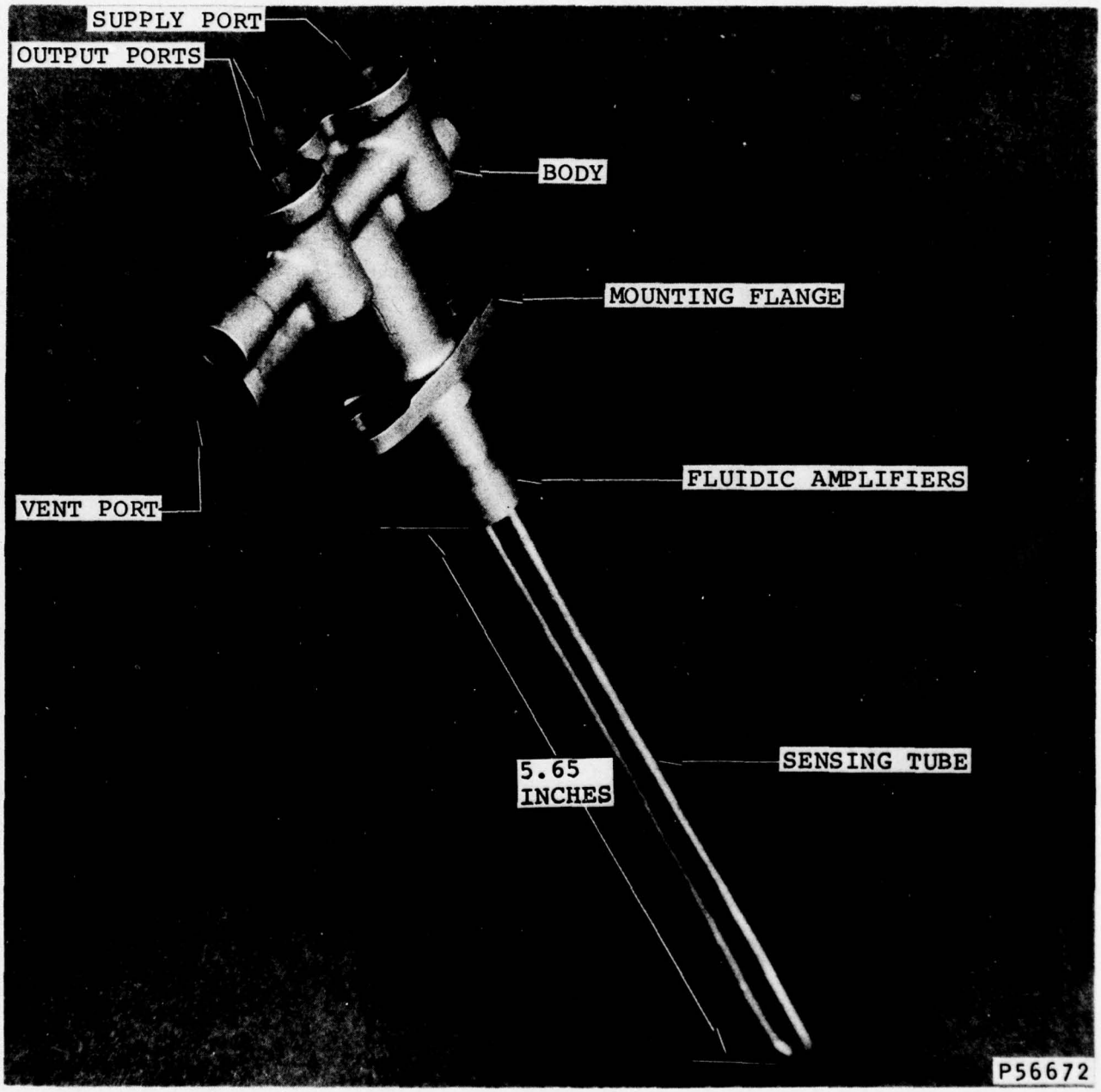


Figure 14. Exhaust Gas Temperature Sensor.

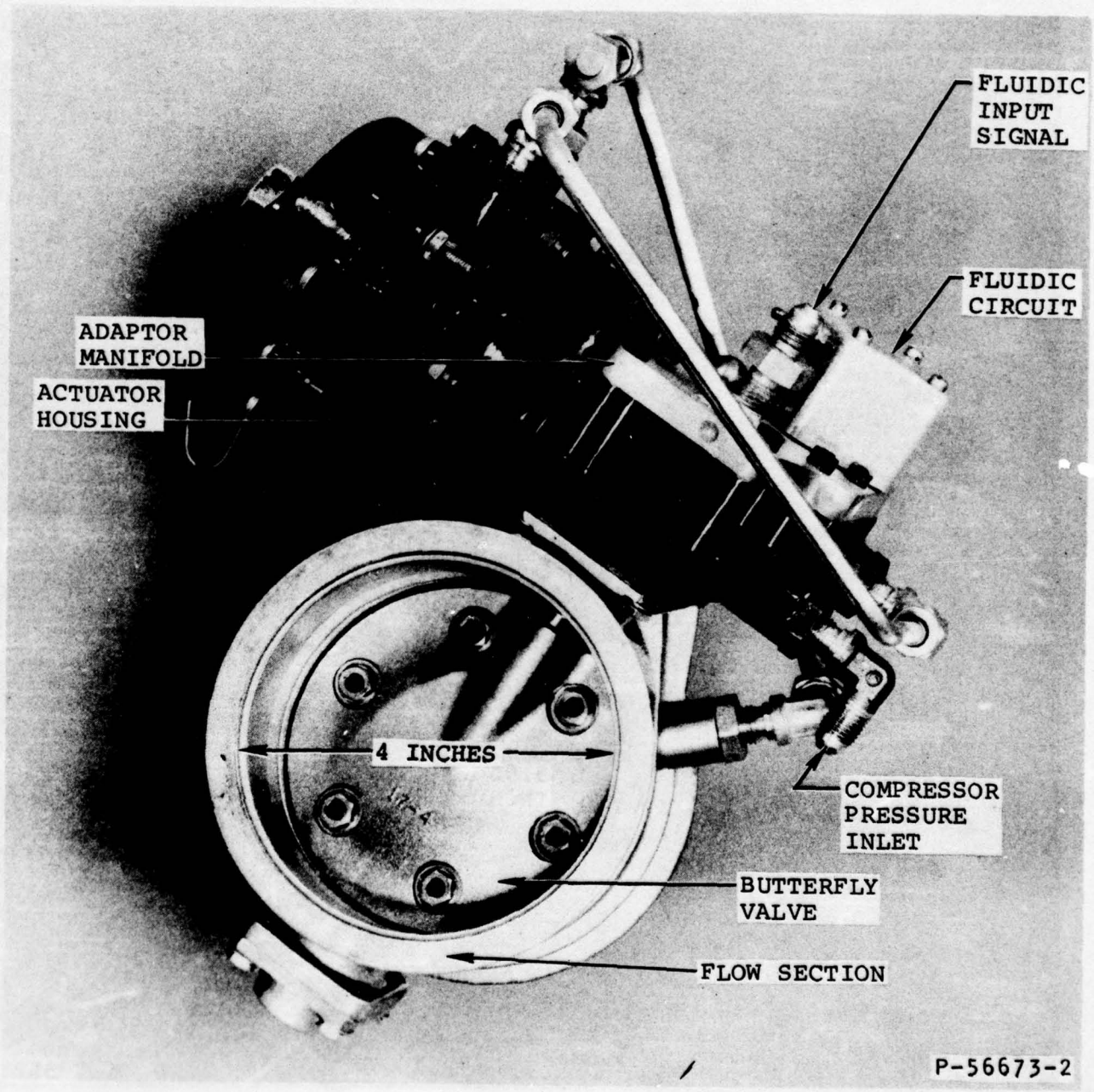


**Figure 15. Load Valve.**

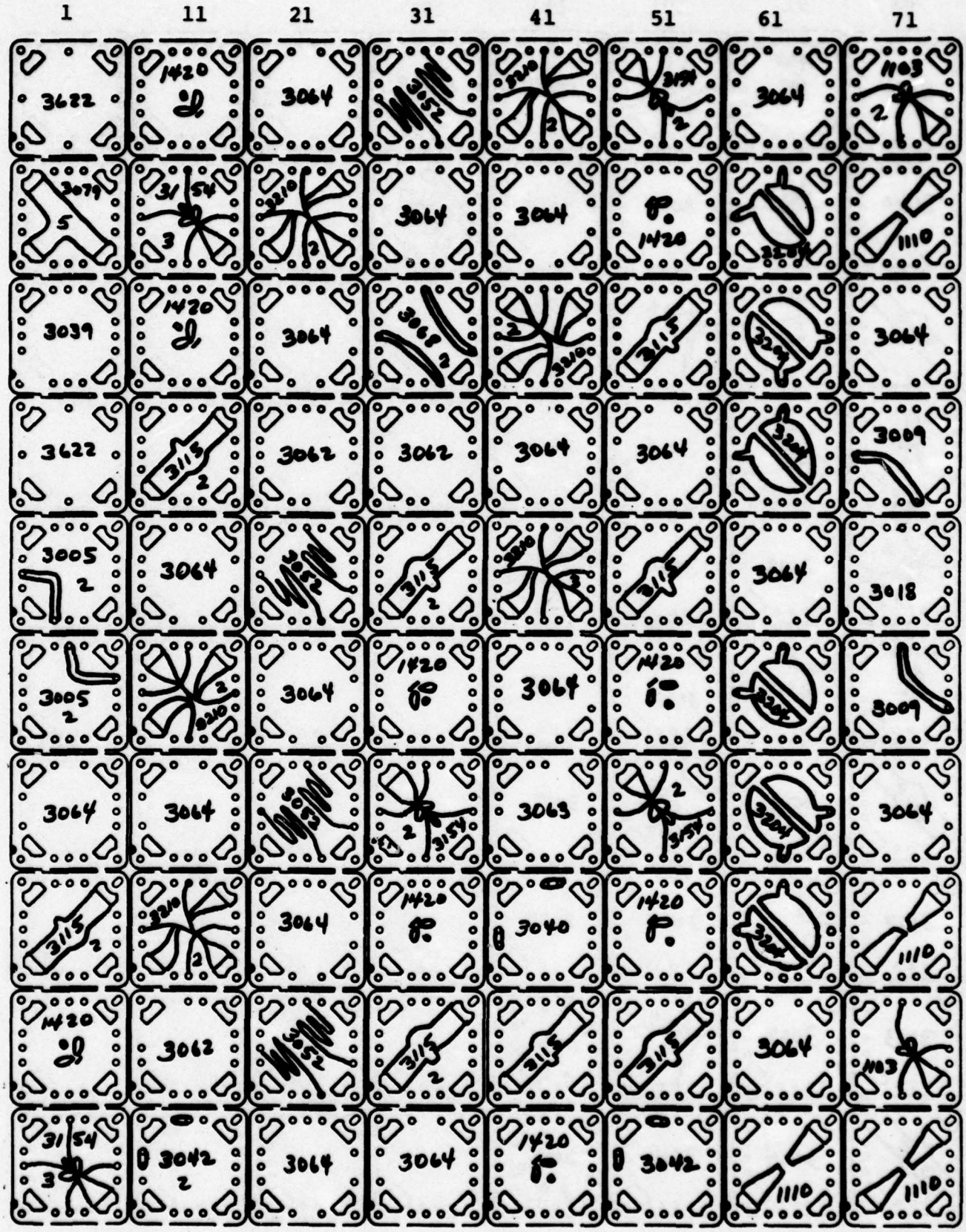


Figure 16. Speed Circuit.

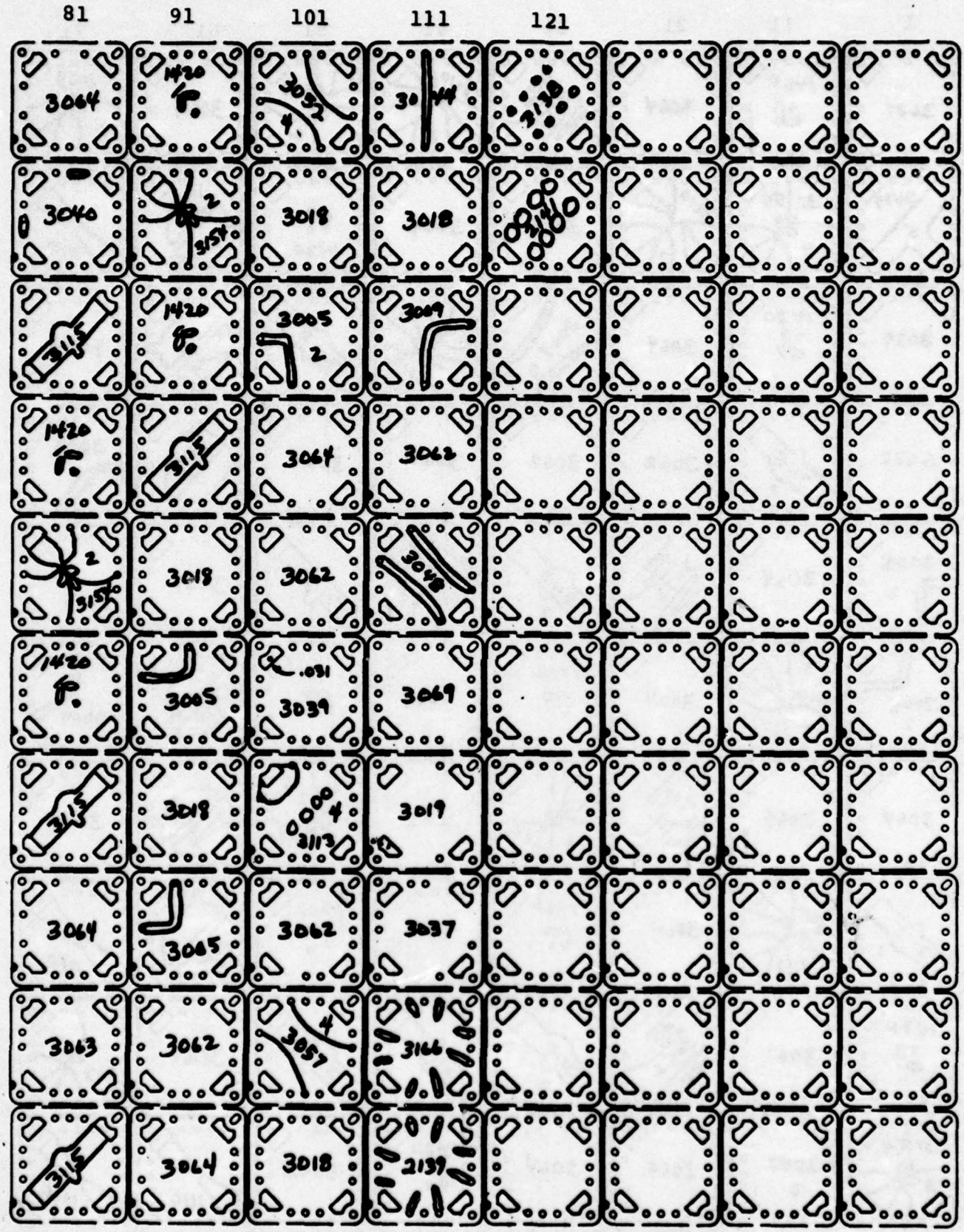


Figure 16. Speed Circuit. (Cont'd)

highest gain while being insensitive to ambient altitude and temperature variations. Figure 17 shows the finalized performance of the F/A speed circuit. The curves represent the two output pressure signals from elements 14 and 15 of Figure 8. The gain of the circuit is the arithmetical difference of the two curves and is approximately $3.1 \times 10^{-4}$ psig per rpm at the design point speed of 4200 rpm (350 Hz).

### 2.2.2 Exhaust Gas Temperature Sensor

The fluidic circuit required for the sonic oscillator, exhaust gas temperature sensor used in the current program was fabricated from the one-half-inch diameter laminates designed during the previous USAMERDC Program (Contract No. DAAK02-74-C-0175) for the GTPR36-61A engine control. Figure 18 shows the elements used in the temperature sensor circuit in their assembly order. These represent the physical hardware shown as elements 29 and 30 of Figure 8.

Testing of the circuit resulted in the selection of amplifier aspect ratios which produced reliable oscillations over the range of temperatures to be sensed and at the supply pressure level discussed earlier. Proper function was also required at altitudes up to 11,000 feet. Figure 19 shows the resulting performance characteristics of the sensor. Gain of the sensor is 0.18 Hz per degree F at the design point temperature of 1200F.

### 2.2.3 Temperature F/A Circuit (T Stack)

Fabrication of the temperature F/A circuit was accomplished utilizing the B-format fluidic elements. As discussed previously, this circuit is identical in concept to the speed circuit; however, the input frequency is higher (700-800 Hz rather than 350-360 Hz) resulting in a different combination of elements in the delayed path. In addition, a three-stage gain block is used which provides output to the load valve, $P_{LV}$, and to the summation stack, $P_T$. Figure 20 shows the elements contained in the temperature F/A circuit in their stacking order.

Performance of this circuit (output of amplifier 21 in Figure 8) when combined with the temperature sensor is shown in Figure 21.

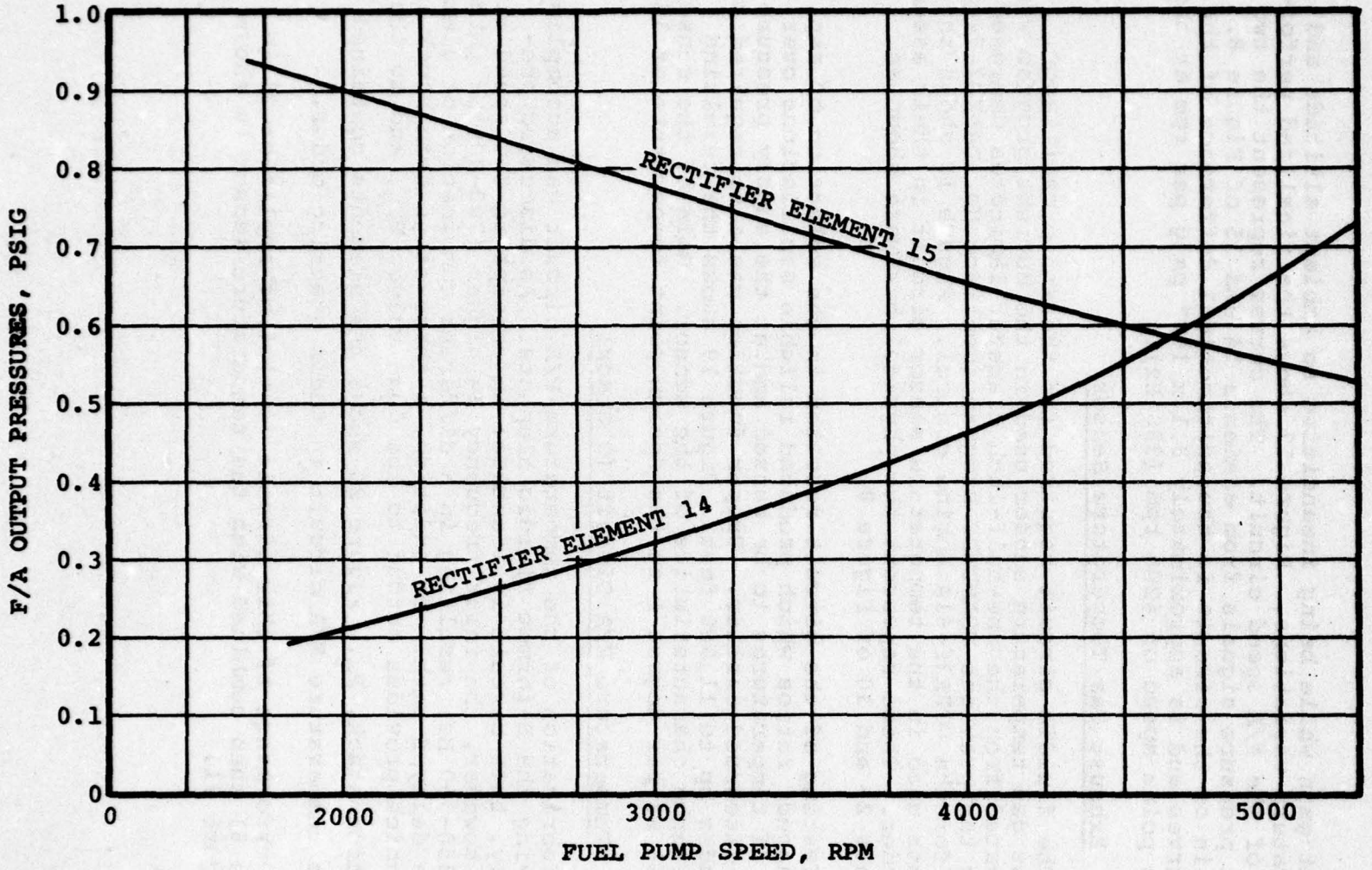


Figure 17. Speed Circuit Output.

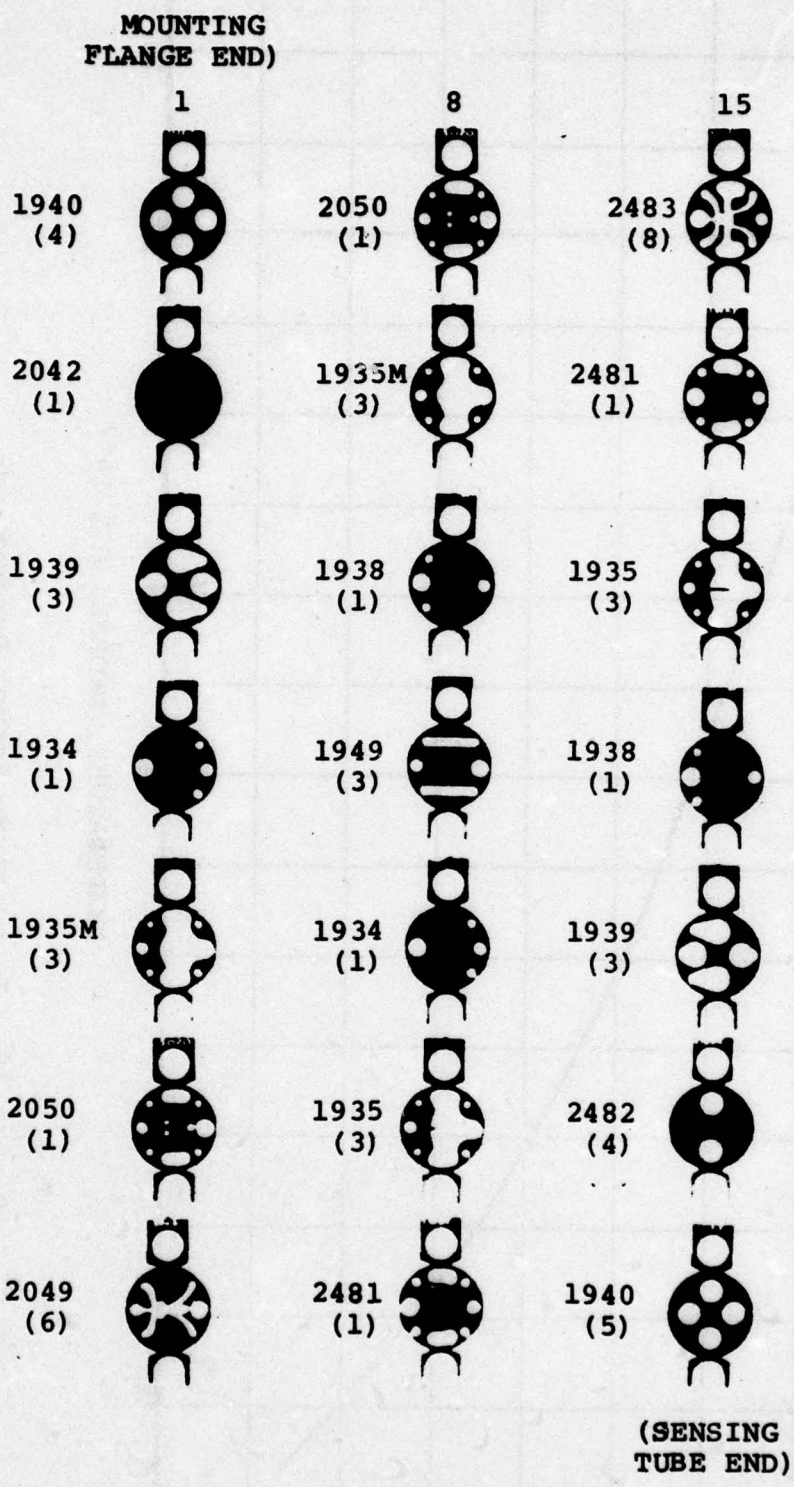


Figure 18. Exhaust Gas Temperature Sensor.

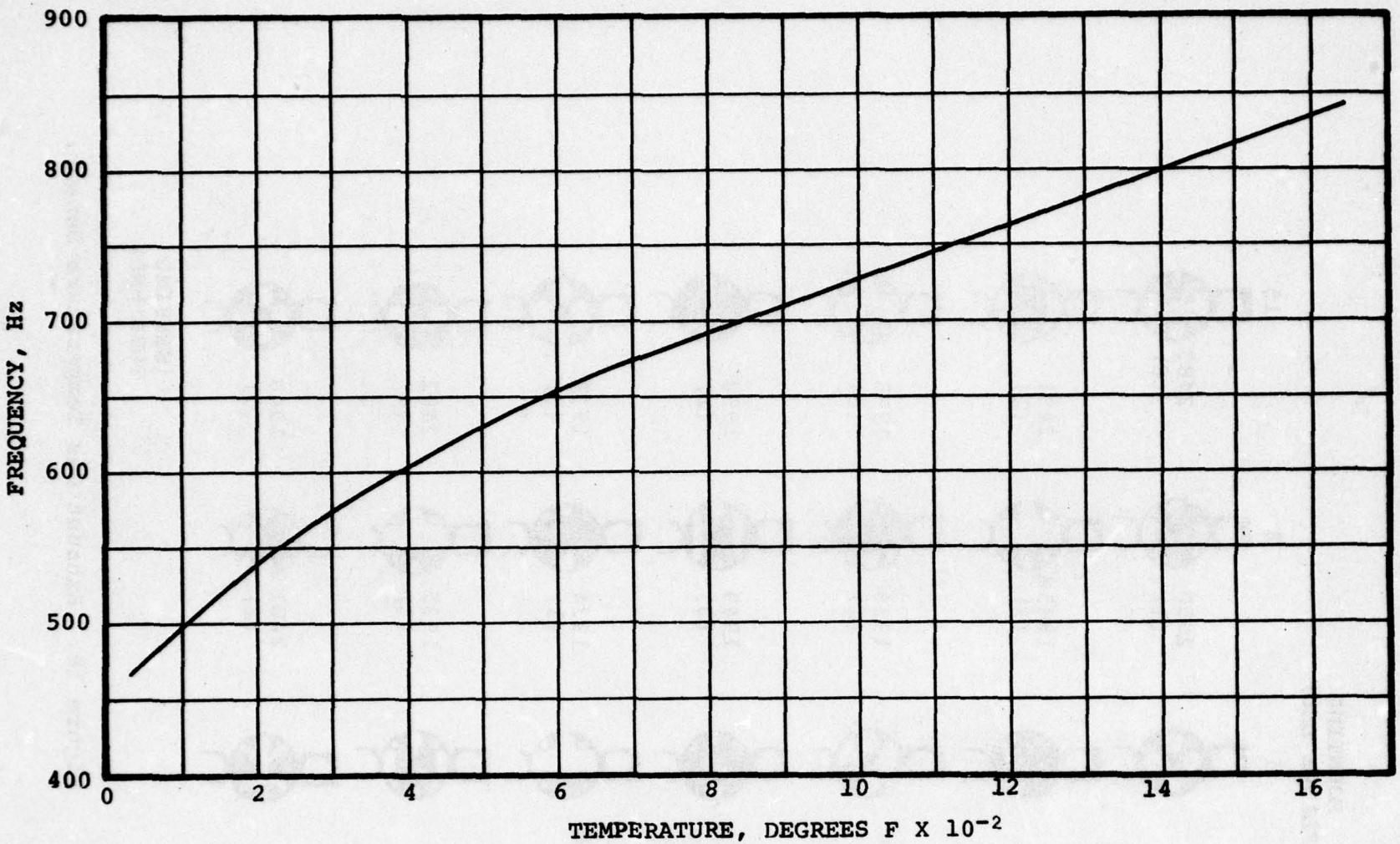


Figure 19. Temperature Sensor Performance.

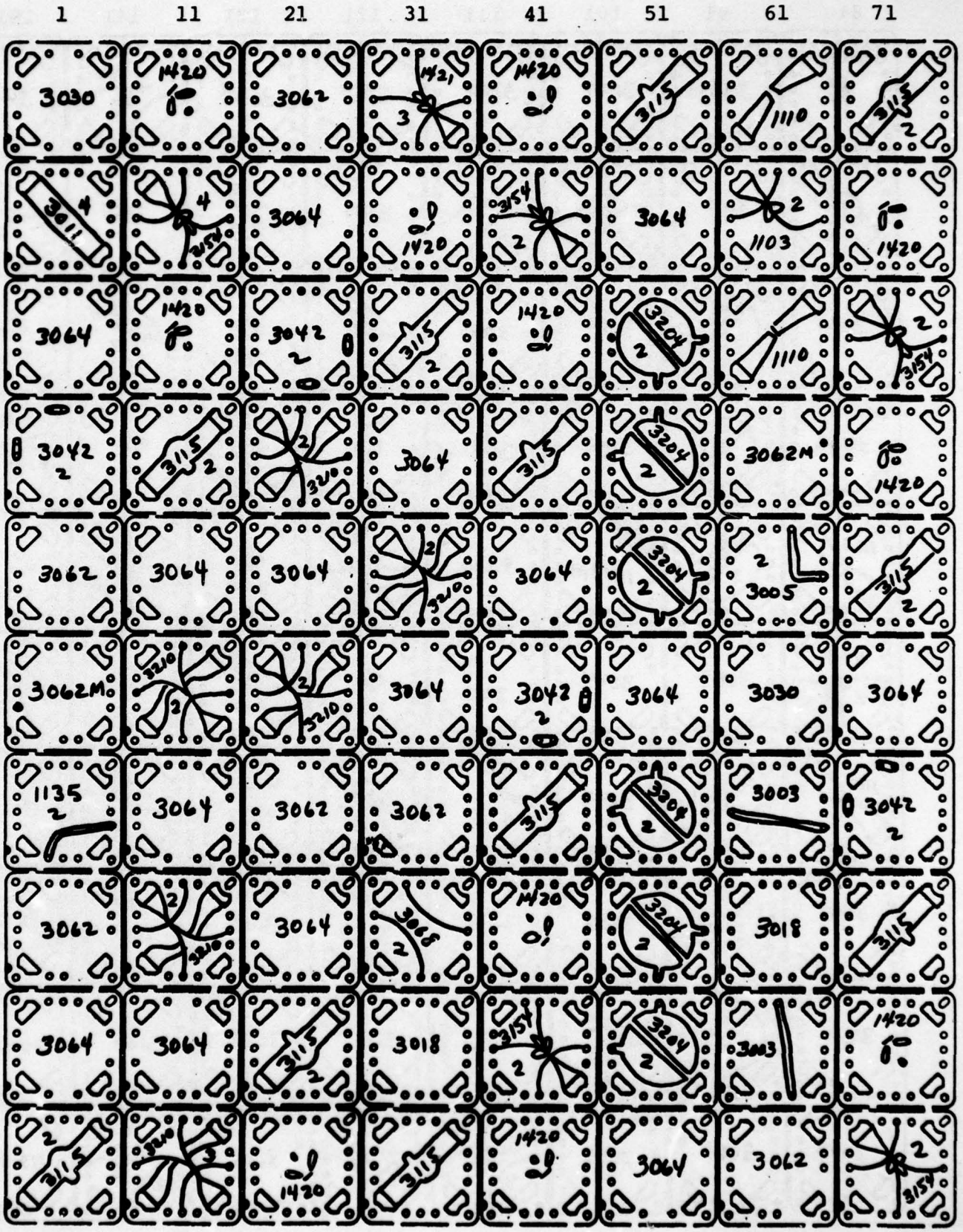


Figure 20. Temperature F/A Circuit.

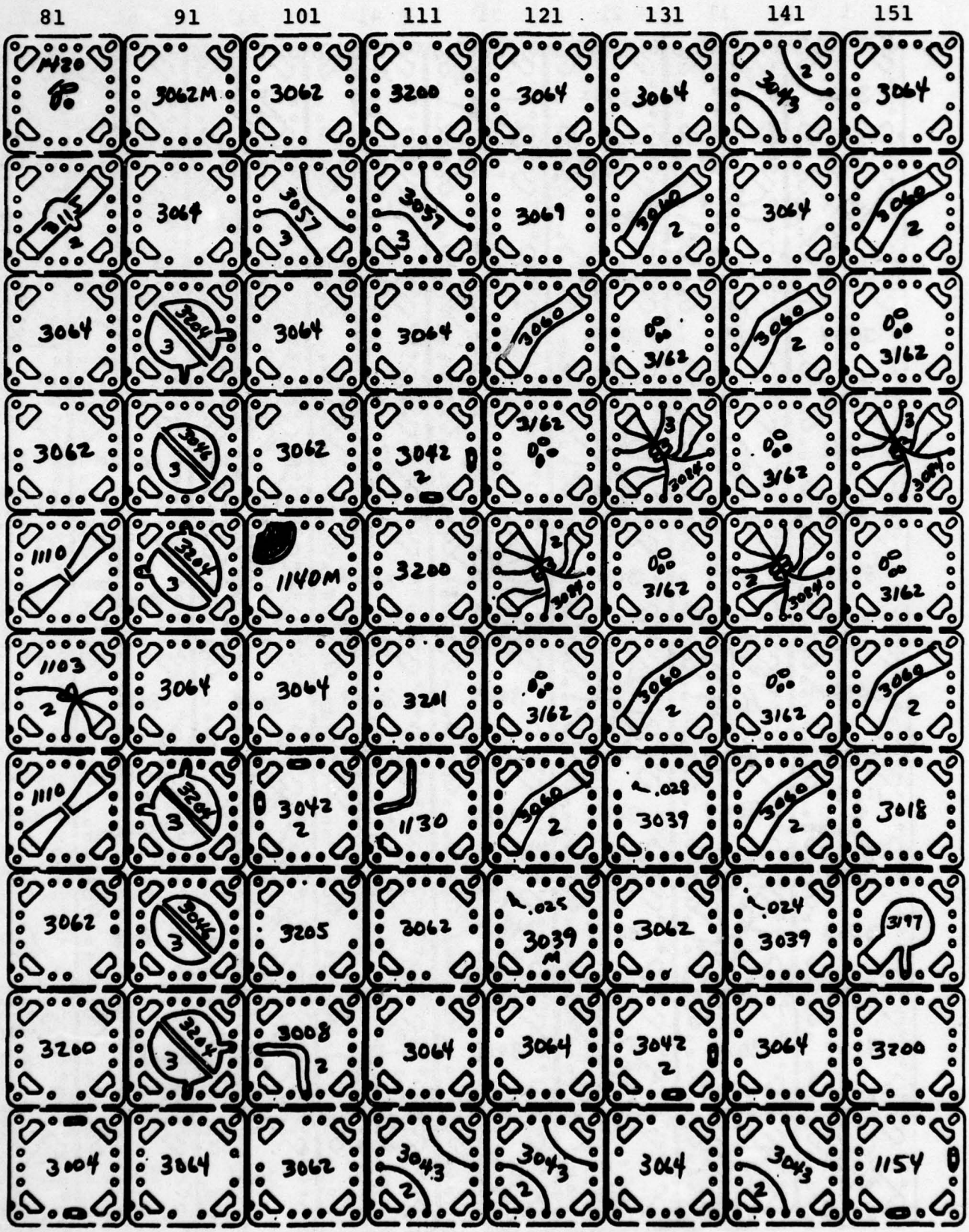


Figure 20. Temperature F/A Circuit. (Cont'd)

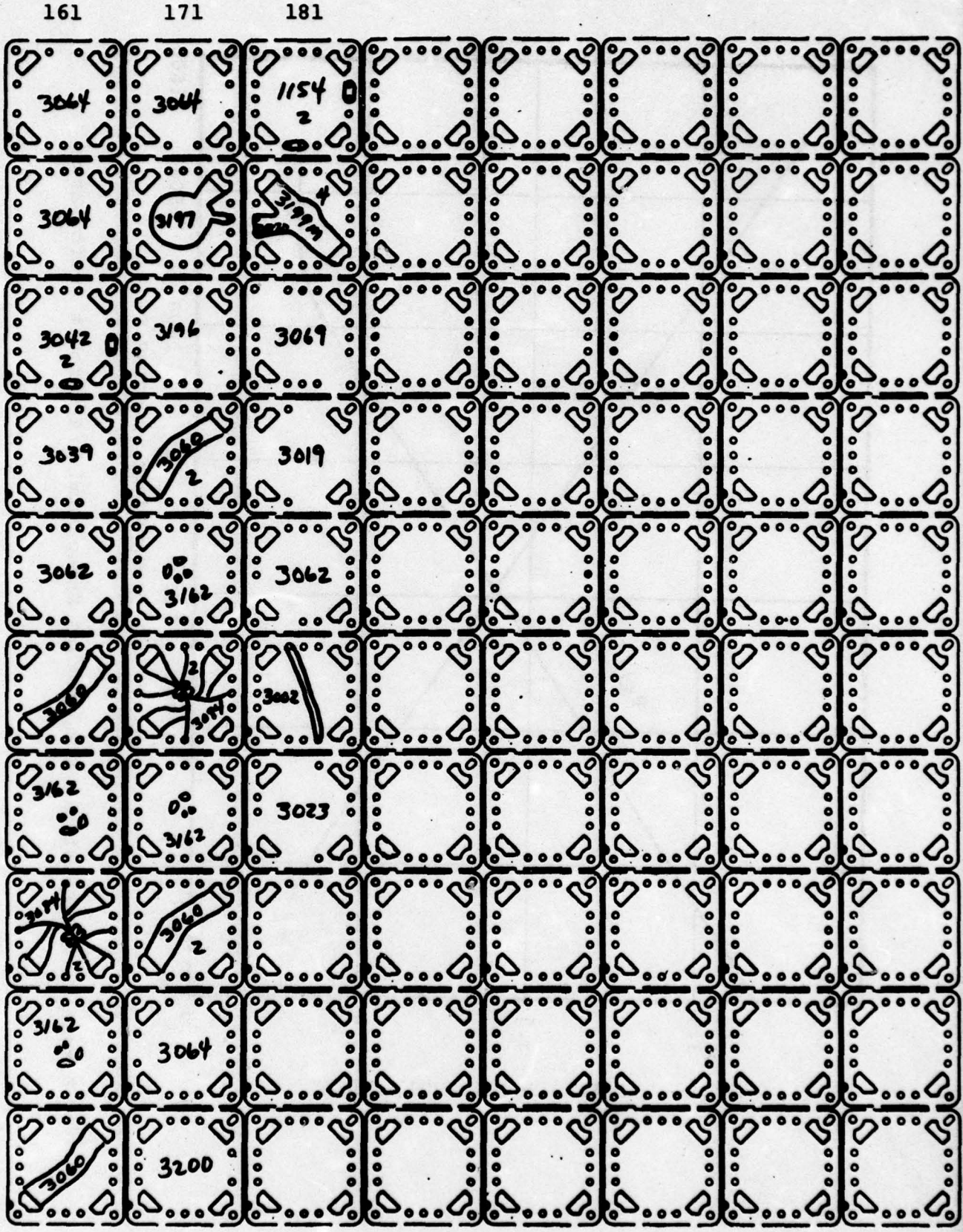


Figure 20. Temperature F/A Circuit. (Cont'd)

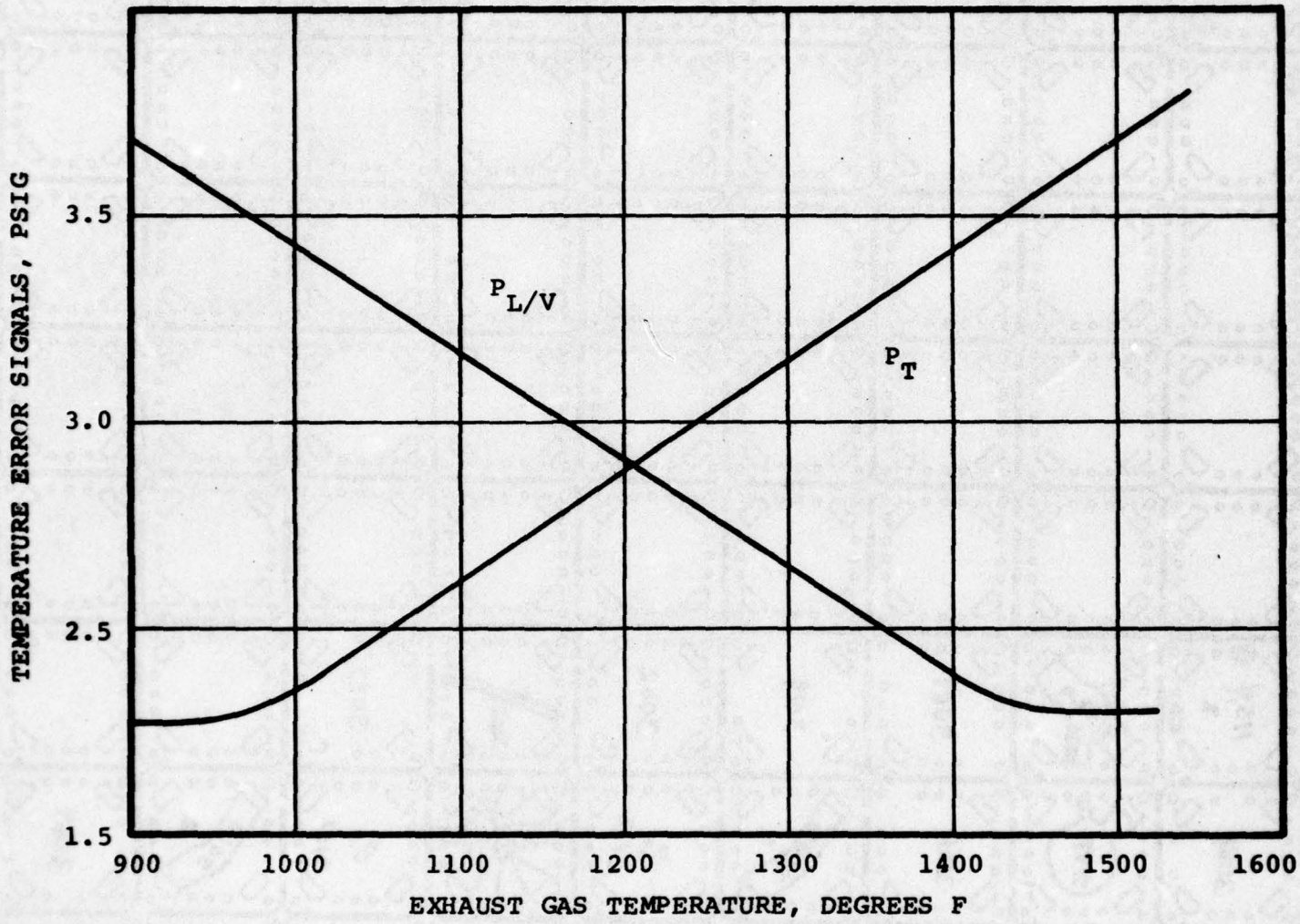


Figure 21. Exhaust Gas Temperature Sensor and F/A Circuit Performance.

### 2.2.4 Summation Circuit

Fabrication of the summation circuit (S stack) was accomplished using the C-format (1.3 x 1.3 inch) elements. This was done for two reasons: (1) The ports in this laminate size are large, thereby providing low pressure drop for the output or driver stage; and (2) the electrofluidic transducer could be mounted directly on top of a stack of these plan dimensions. The elements employed are shown in Figure 22. It should be noted that the final output amplifier, element 5013M, has one output leg cutaway to vent. This modification was made in order to allow the other active leg, which drives the metering valve, to be driven to as near vent pressure as possible.

Figure 23 illustrates the performance of the summation circuit with respect to speed and exhaust temperature ($T_5$) error signals. As shown, the temperature signal does provide a limiting function with a gain of 0.059 psi per degree F. Assuming a metering valve gain of 27 psi per psi, the overall fuel atomizer pressure to temperature gain of the control is 1.59 per degree F (0.059 x 27) which compares well with the design goal of 1.68 $T_{5e}$ given in Equation (1) of Section 2.1.1.1.

The gain of the speed control function was observed to be 0.052 psi per rpm which yields an overall fuel atomizer pressure to speed gain of 1.4 psi per rpm (0.052 x 27) which is also in close agreement with the design goal of 1.5 Ne given in Equation (1).

The other function provided by the summation circuit is to reset the speed control set point as a function of electrical current input from the fine speed control unit. As previously noted, this function is accomplished using an electrofluidic (E/F) transducer mounted on the summation stack. Figure 24 depicts the performance of this device and its effect upon the speed set point. As shown, positive current input of up to 100 milliamps raises the set point, while negative inputs lower the set point. Precise linearity of this function is not required since the device receives its signal from an integrator in the fine speed control unit.

### 2.2.5 Load Valve Circuit

The fluidic circuit mounted on and used to actuate the air bleed load valve was fabricated using C-format fluidic elements in the assembly order given in Figure 25. Supply air for the circuit is filtered but unregulated air at compressor discharge pressure ($P_{CD}$). Performance of the circuit when combined with the temperature ($T_5$) sensor and frequency-to-analog circuit is presented in Figure 26.

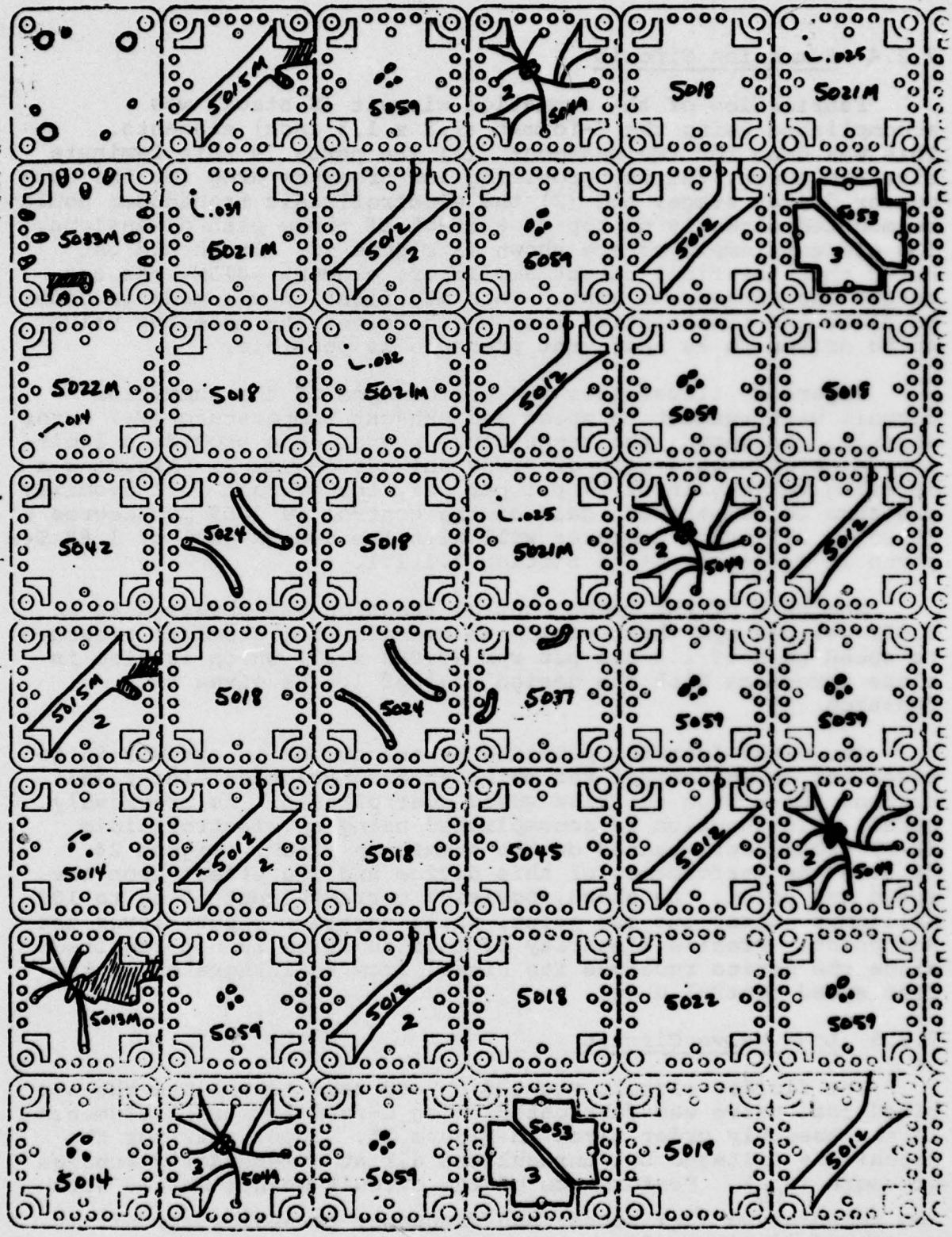


Figure 22. Summation Circuit.

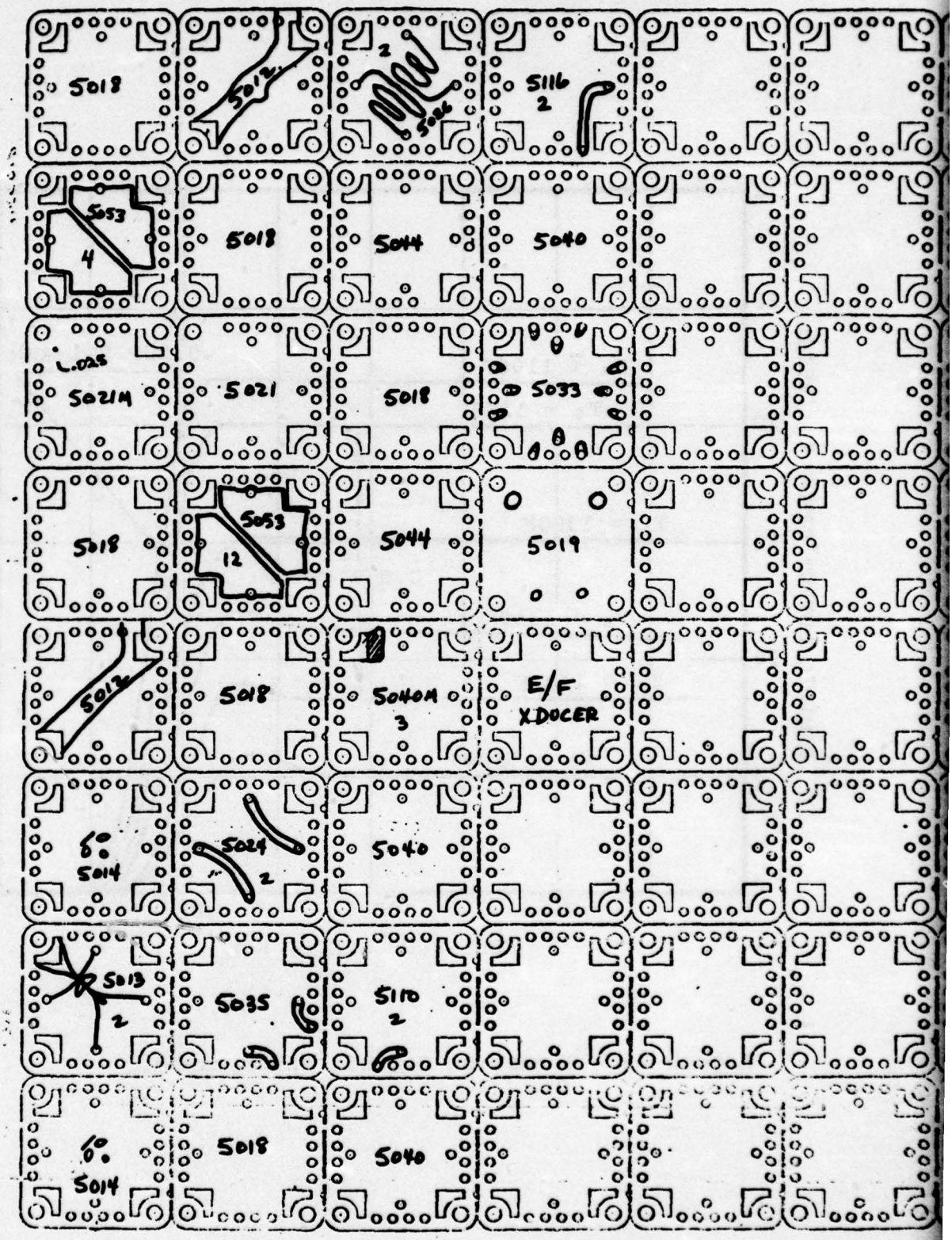


Figure 22. Summation Circuit. (Cont'd)

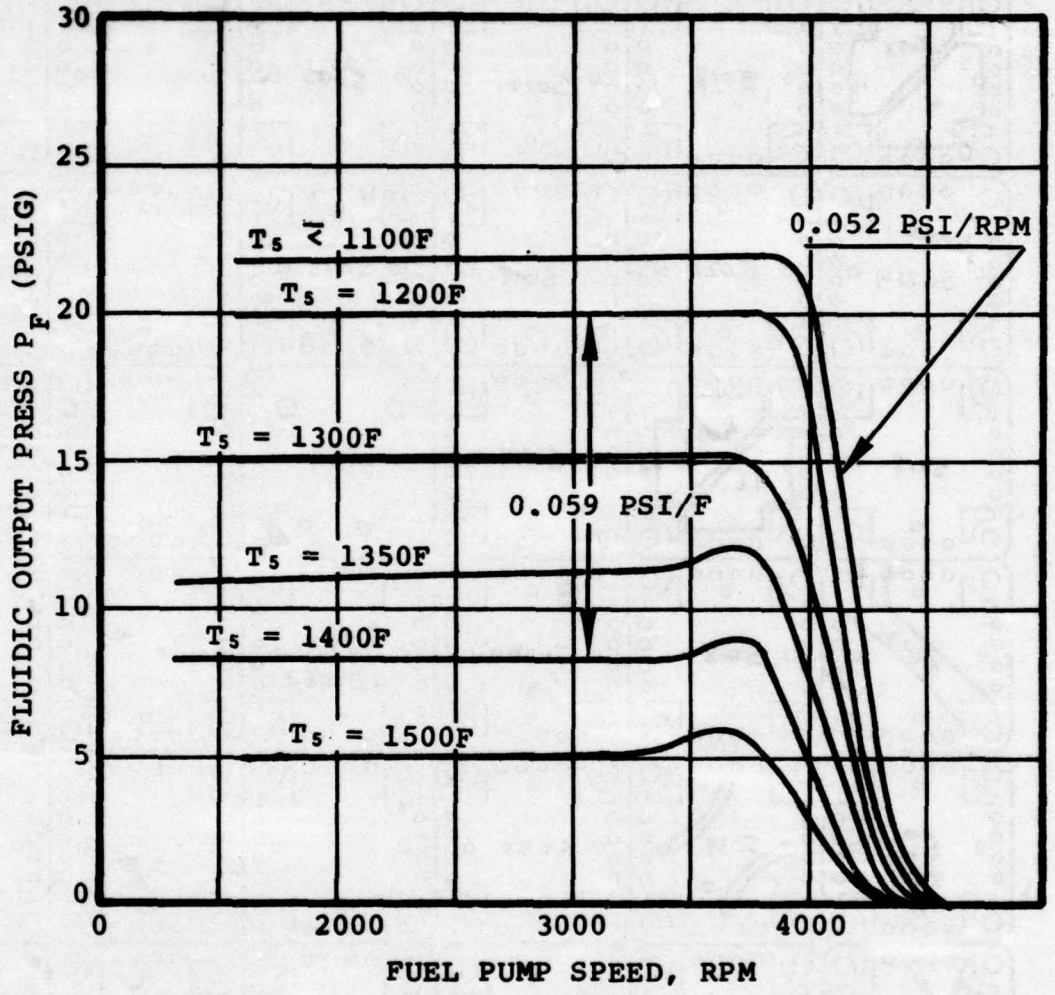


**Figure 23. Summation Circuit Performance.**

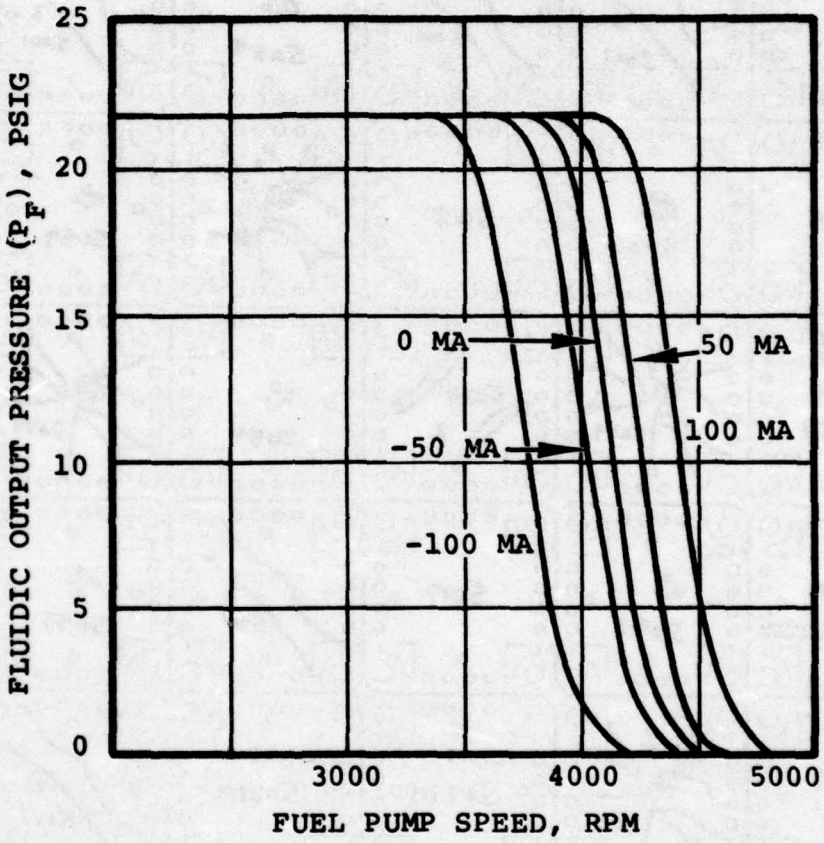


Figure 24. Electrofluidic Transducer Performance.

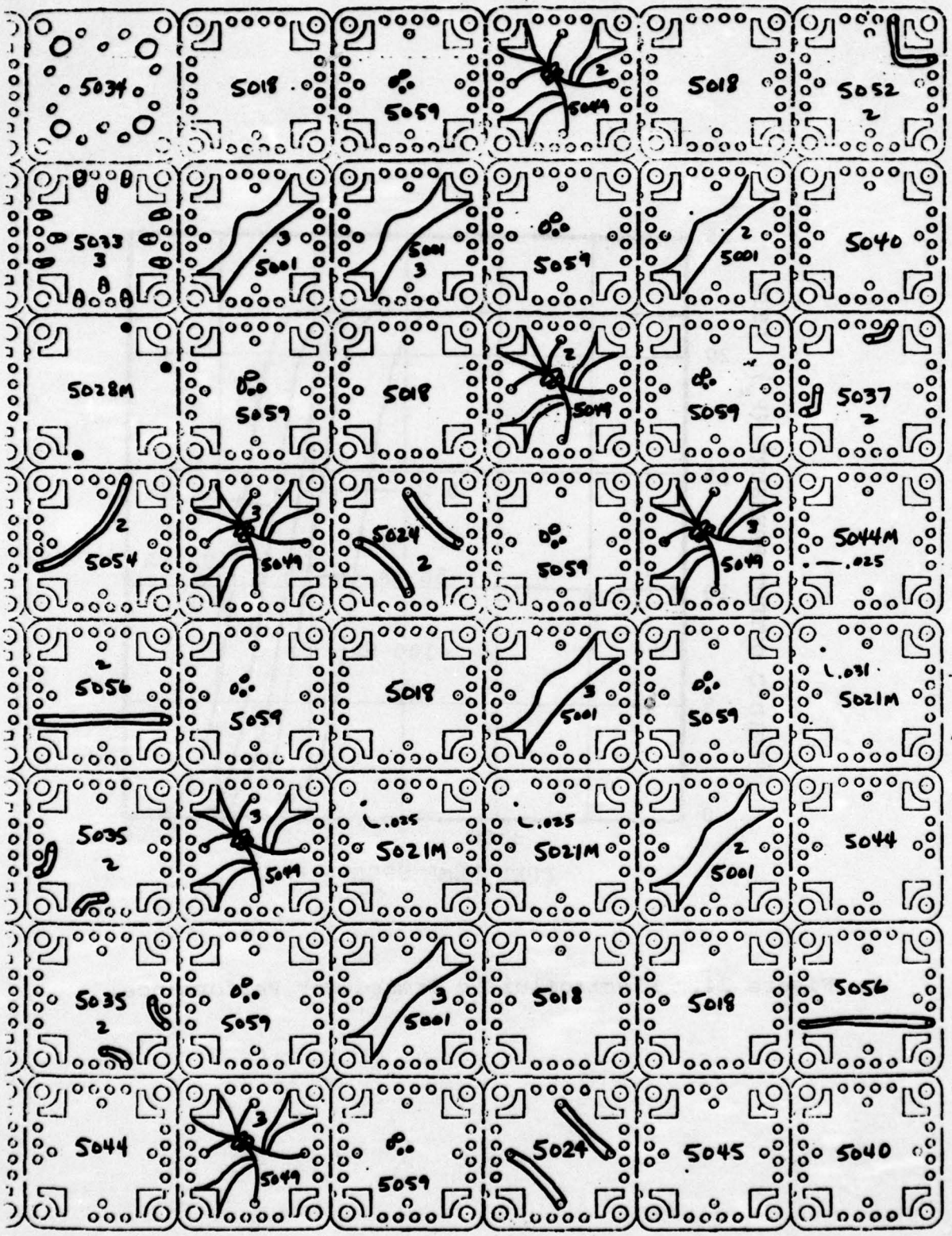


Figure 25. Load Valve Circuit.

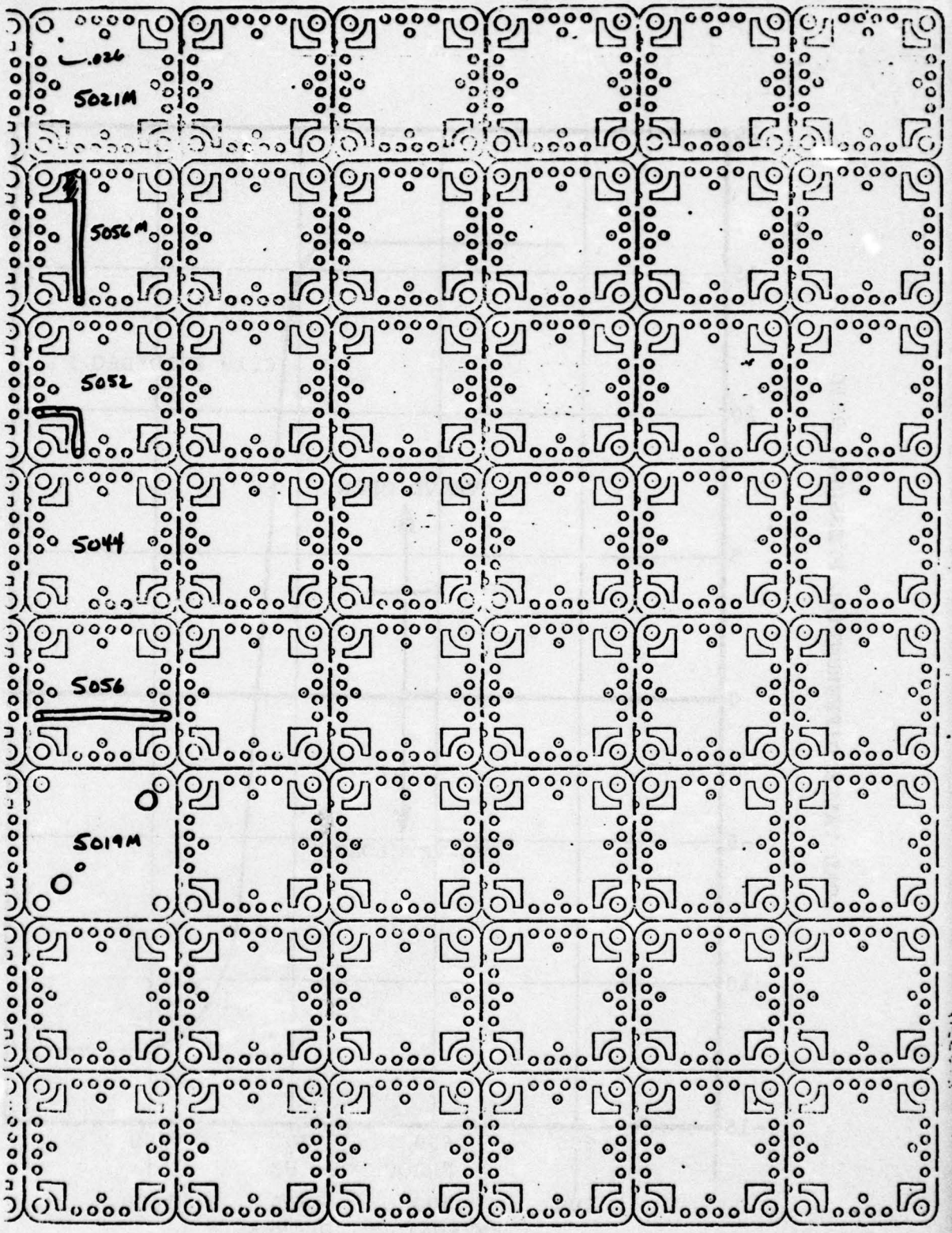


Figure 25. Load Valve Circuit. (Cont'd)

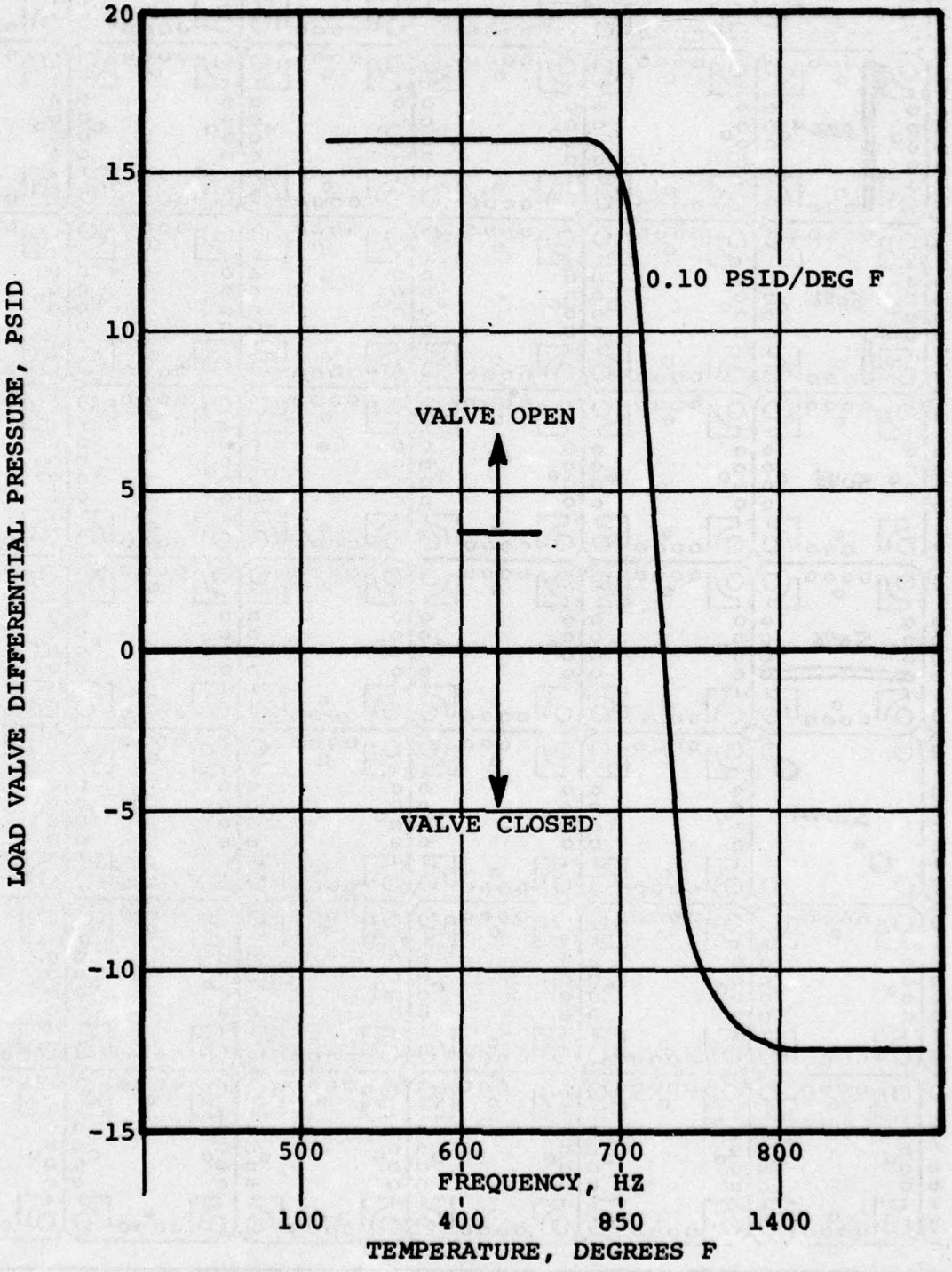


Figure 26. Load Valve Circuit Performance.

As shown, the overall gain of the system was 0.10 psig per deg F which was twice the nominal design gain of 0.05 psid per deg F given in Equation (2) of Section 2.1.1.1. Although gain reduction could have been easily accomplished, it was decided to attempt the first engine run at this setting. It was considered possible that the faster response of the fluidic temperature sensor (when compared with the thermostat system) would allow higher gains to be utilized while maintaining the necessary system stability. If true, this higher gain would result in a more accurate overall control of exhaust gas temperature.

The existing bleed load valve contains a spring whose preload holds the valve closed. A diaphragm differential pressure of 4.0 psid is required to initiate valve opening as shown in Figure 26.

### 2.2.6 Hydromechanical Components

2.2.6.1 Fuel Pump - Early predictions of the flex-duct metering valve performance indicated that its flow and pressure recovery would be approximately 72 and 85 percent, respectively, at the design point condition. In order to meet the engine maximum flow condition of 460 pounds per hour at 600 psi atomizer pressure, the fuel pump must be capable of producing 639 pounds per hour (460/0.72) at 706 psig (600/0.85) backpressure.

The pump, which is a production device with minor modifications as discussed previously, was assembled and bench tested. The resulting pump performance is shown in Figure 27. As shown, the pump capacity is well in excess of the originally estimated requirement. However, as will be discussed in the next section of this report, the additional capacity exhibited by the pump ultimately became a requirement of the system.

2.2.6.2 Flex-Duct Metering Valve - The flex-duct valve is essentially a converging-diverging nozzle which is divided at the throat by a small gap. The converging secton, or nozzle, is fixed in place and is supplied with fuel directly from the fuel pump. The diverging section, or diffuser, is flexible and is deflected by means of the diaphragm and linkage system. Output of the diffuser is ported to the engine fuel atomizer. When the diffuser is aligned with the nozzle, all of the pump discharge flow, with the exception of leakage at the gap, is directed to the engine. When the two are not in alignment, the fuel not received by the diffuser is collected and returned to the pump inlet.

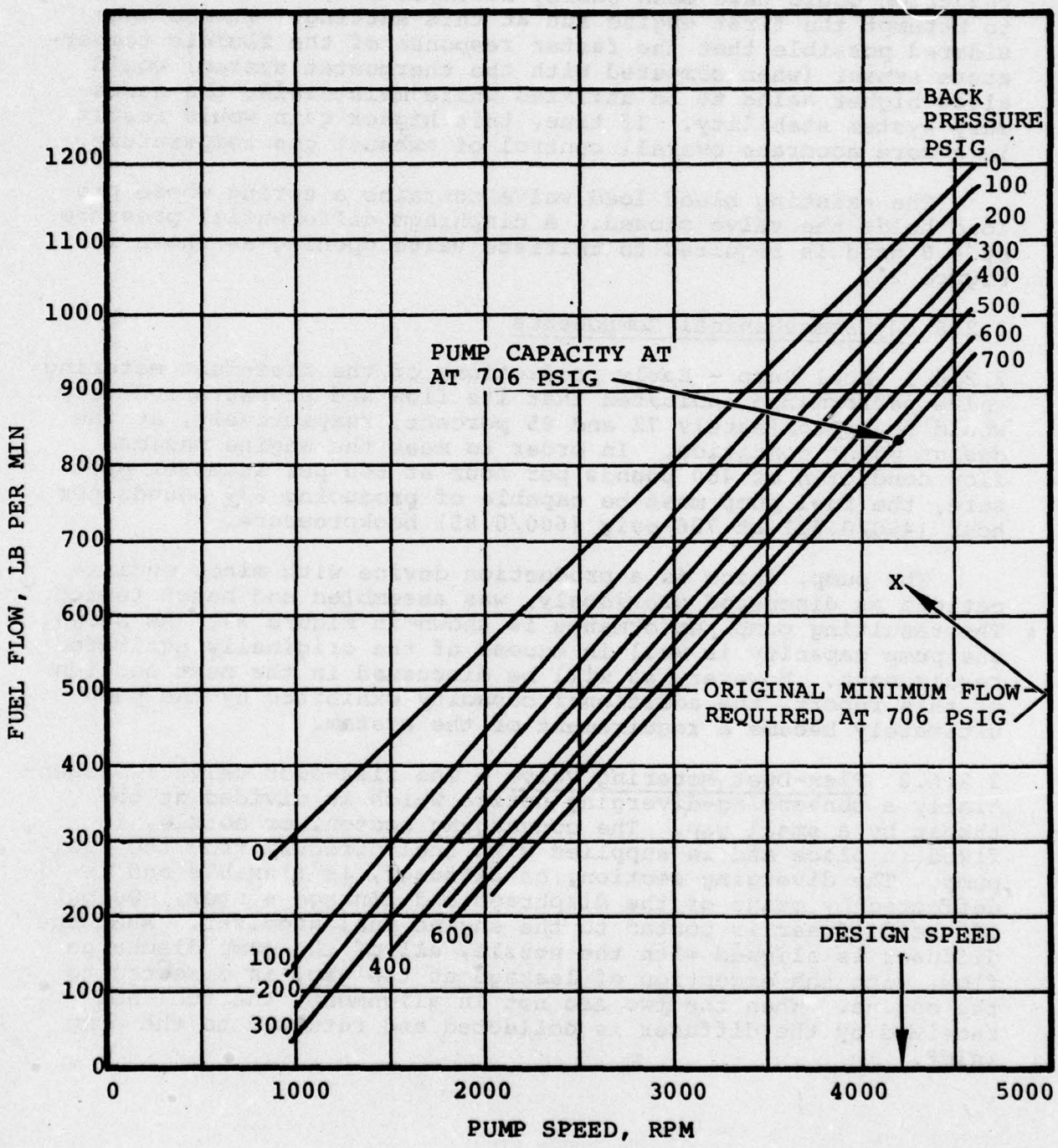


Figure 27. Fuel Pump Performance.

Fabrication of the valve was accomplished by photochemically producing a series of laminates, stacking them in the correct order and bonding them. Figure 28 shows some of the individual laminates used on the valve construction. Elements 4, 5, and 6 form the nozzle assembly, while elements 1, 2, and 3 form the flexible diffuser. Flow capacity of the valve may be altered by varying the number of elements 2 and 5, thereby changing the flow channel height. For this application, a height of 0.030 inch was used. Channel width at the nozzle throat was fixed at 0.150 inch. Figure 29 shows a cutaway view of the valve in a partially aligned position. Figure 30 depicts the valve in the fully aligned position.

All laminates used in the valve were fabricated from 400 series stainless steel which, when bonded, provided a yield strength well in excess of the maximum stress at the base of the diffuser when fully deflected.

Bench testing of the valve resulted in two modifications to the initial design which improved performance. The first involved lengthening the diffuser elements to reduce the nozzle/diffuser tip clearance when fully aligned, and thus reduce the leakage at the gap. The second modification was the addition of a sealing flap to one side of the diffuser to further seal the leakage gap when fully aligned. Figure 31 depicts the latter modification.

During the analysis phase, certain assumptions were made in order to size the flex-duct valve and predict its performance.

The major assumptions included:

- The nozzle flow coefficient
- The leakage gap width
- The leakage gap flow coefficient
- The diffuser efficiency

Design of both the nozzle and diffuser were made in accordance with established principles for two-dimensional flow of incompressible fluids. Initial performance tests of the valve, however, fell considerably short of the design objectives. Figure 32 shows a comparison of the test results for the fully aligned position. The major cause of this discrepancy was considered to be excessive leakage flow at the nozzle/diffuser gap interface. The modifications described above resulted in the improved performance shown (center curve) in Figure 32. An improvement of approximately 9 percent was obtained in the operating range.

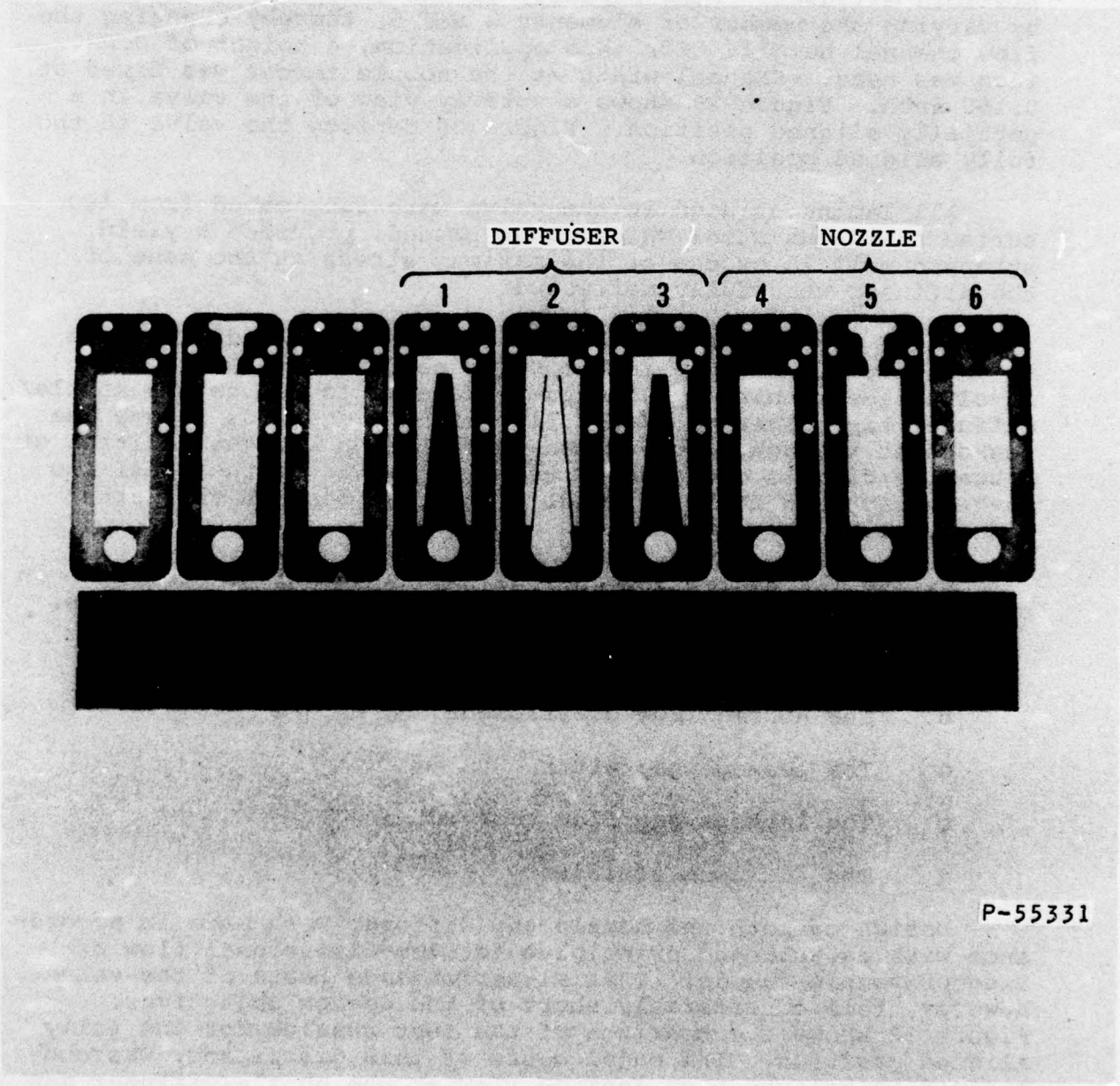


Figure 28. Laminates Used in Fabricating the Flex-Duct Metering Valve.

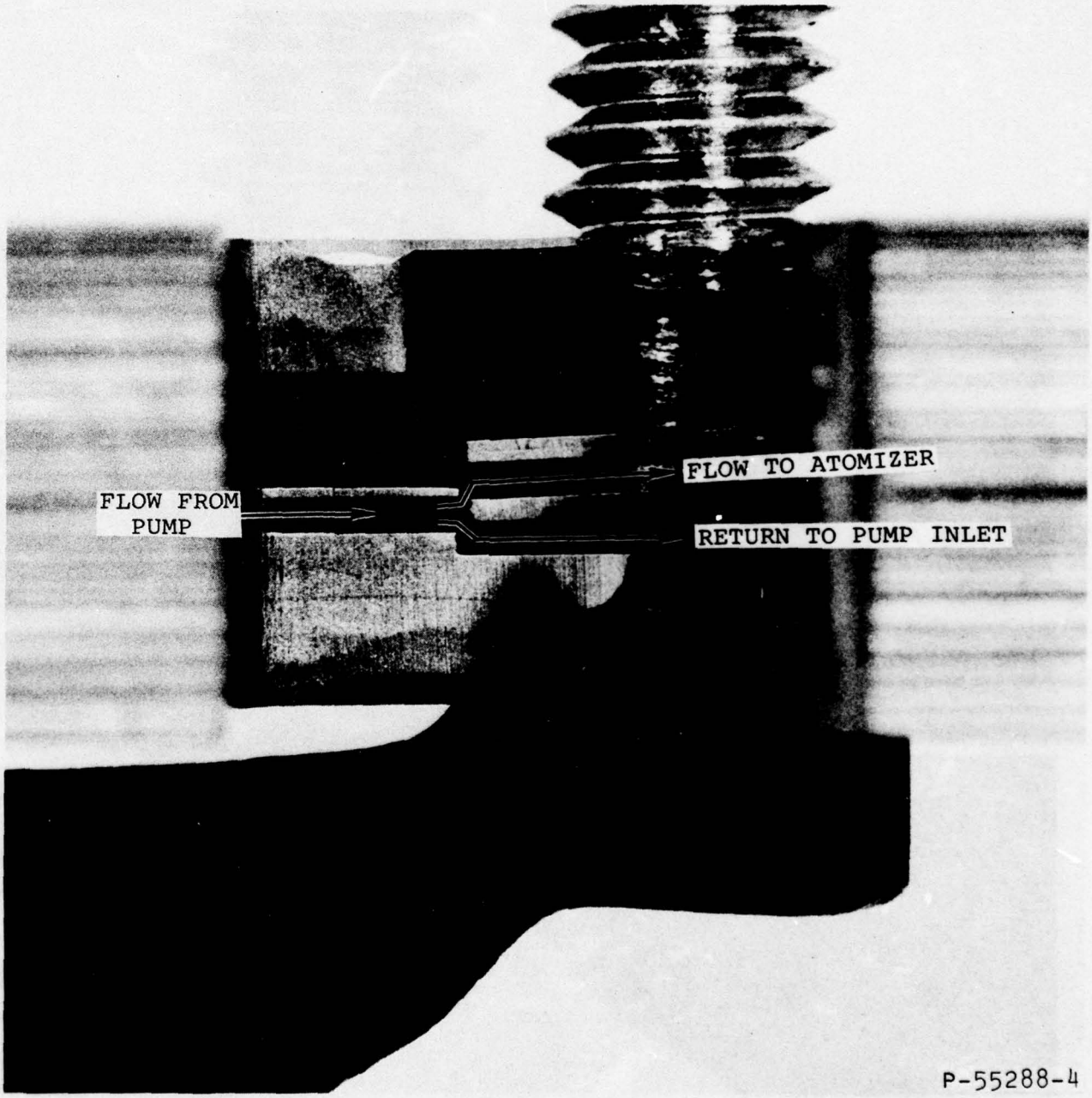


**Figure 29. Cutaway Side View of Flex-Duct Metering Valve.**

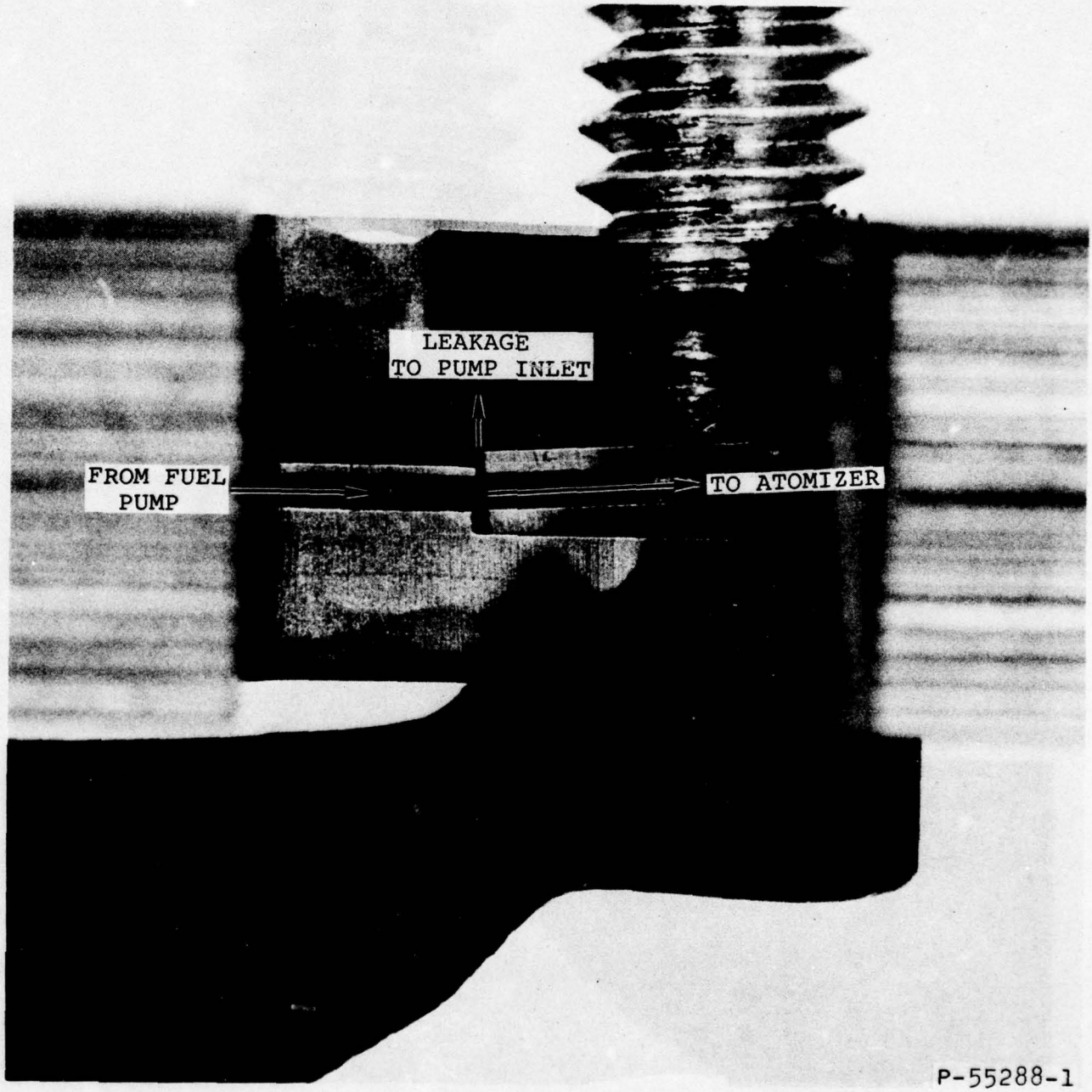


**Figure 30. Cutaway Side View of Flex-Duct Metering Valve.**

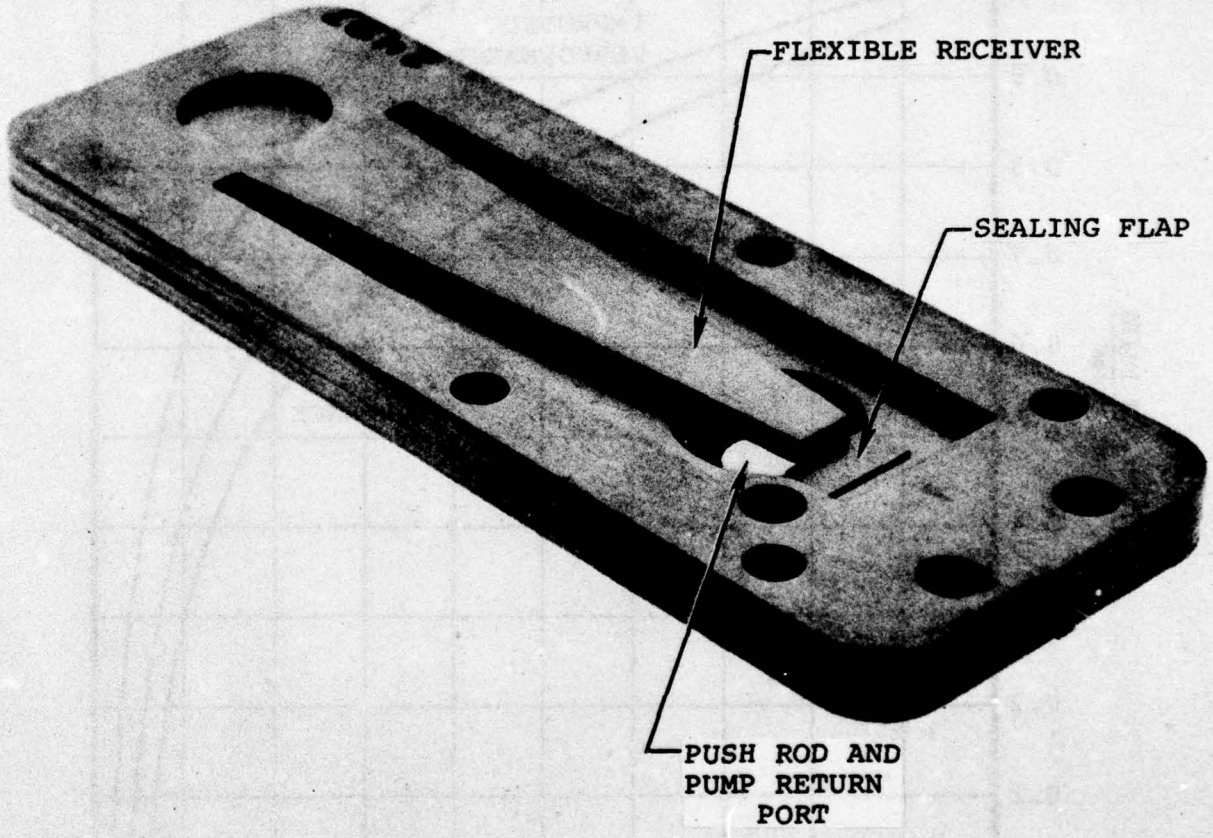


Figure 31. Flex-Duct Metering Valve (Receiver Assembly).

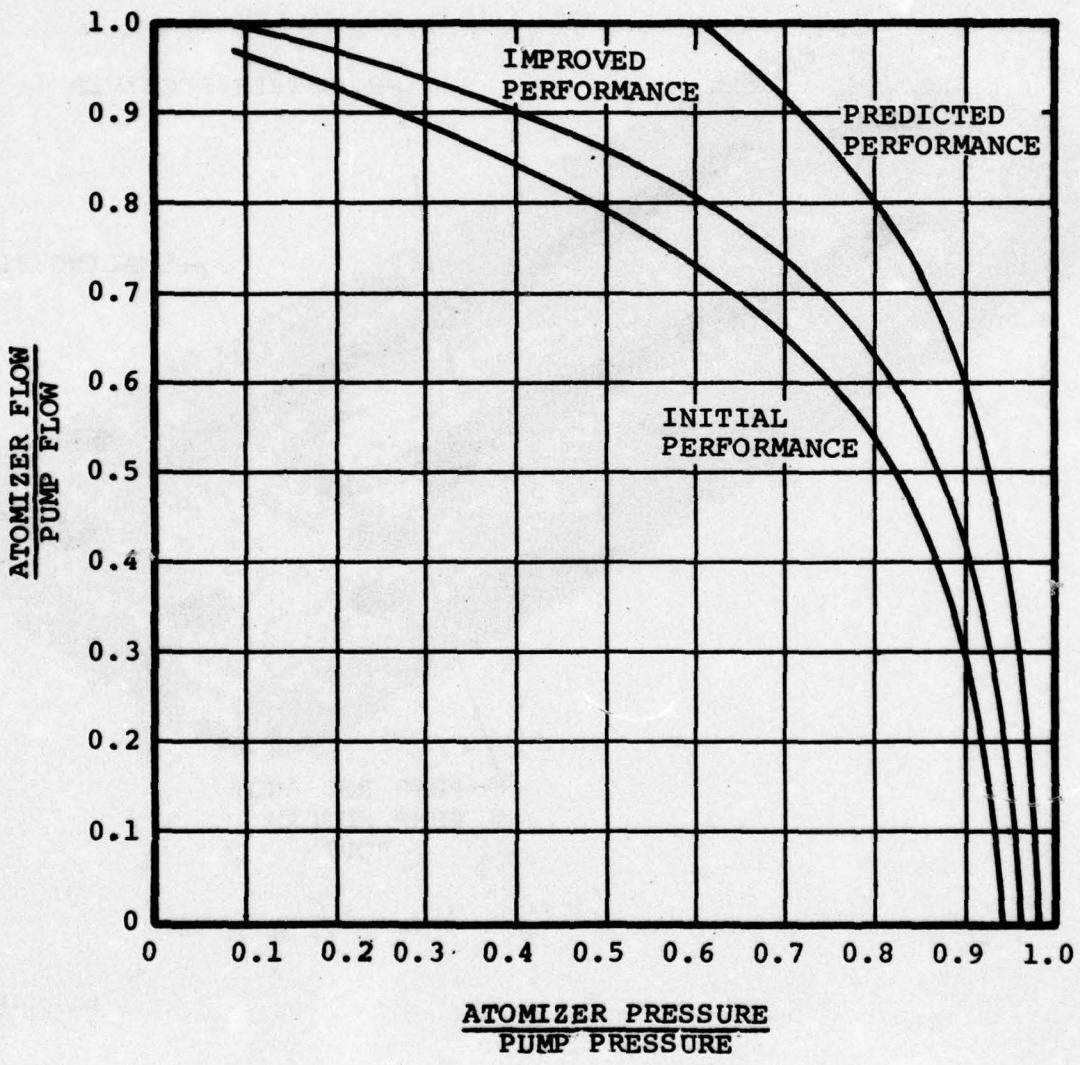


Figure 32. Flex-Duct Metering Valve Performance (Fully Aligned Position).

Using the engine maximum atomizer requirements of 600 psi and 460 pounds per hour, the metering valve input requirements were computed, using the data of Figure 32, and compared with the fuel pump output characteristics. The results of this matching process are given in Figure 33. As shown, the circled intersection points reveal the operating condition of the combined pump/metering valve system.

The improved flex-duct valve was found to backpressure the pump only 40 psi (700-660) higher than predicted. This was not considered excessive with regard to pump life; therefore, no additional modifications to the flex-duct valve design were considered.

2.2.6.3 Complete Metering Valve System - The fuel pump, diaphragms, pivot/linkage mechanism, and flex-duct valve were assembled and tested on the fuel test stand using MIL-F-7024B, Type II, calibrating fluid. Initial tests revealed that the overall gain (atomizer pressure to fluidic pressure) of the metering system was considerably lower than required. The observed value was 19 to 1 while the required gain was 27 to 1. It was determined that the effective area of the Kapton diaphragm used to sense atomizer pressure was excessive. In other words, it was flexing nearer its outer radius rather than at the center of its convolute. To remedy the problem a smaller diaphragm retainer was machined and new diaphragms were fabricated.

Testing of the new diaphragms revealed that the correct effective area had been obtained; however, several diaphragms failed by tearing at atomizer pressures of from 600 to 650 psig (600 psig is the maximum required by the engine). This problem was solved by doubling the diaphragm thickness to 0.010 inch. No diaphragm failures were experienced with this configuration, although atomizer pressures of up to 800 psi were sustained.

Figure 34 depicts the performance of the complete metering valve system. As shown, some nonlinearity was observed which was attributed to the increased diaphragm thickness. When combined with the inverse nonlinearity of the fuel atomizer, this metering valve characteristic does not pose a problem. Hysteresis of the metering valve system is extremely low as shown by the small difference between the increasing and decreasing curves.

Overall gain of the valve is 26.5 psi per psi which compares favorably with the design goal of 27.1 psi per psi.

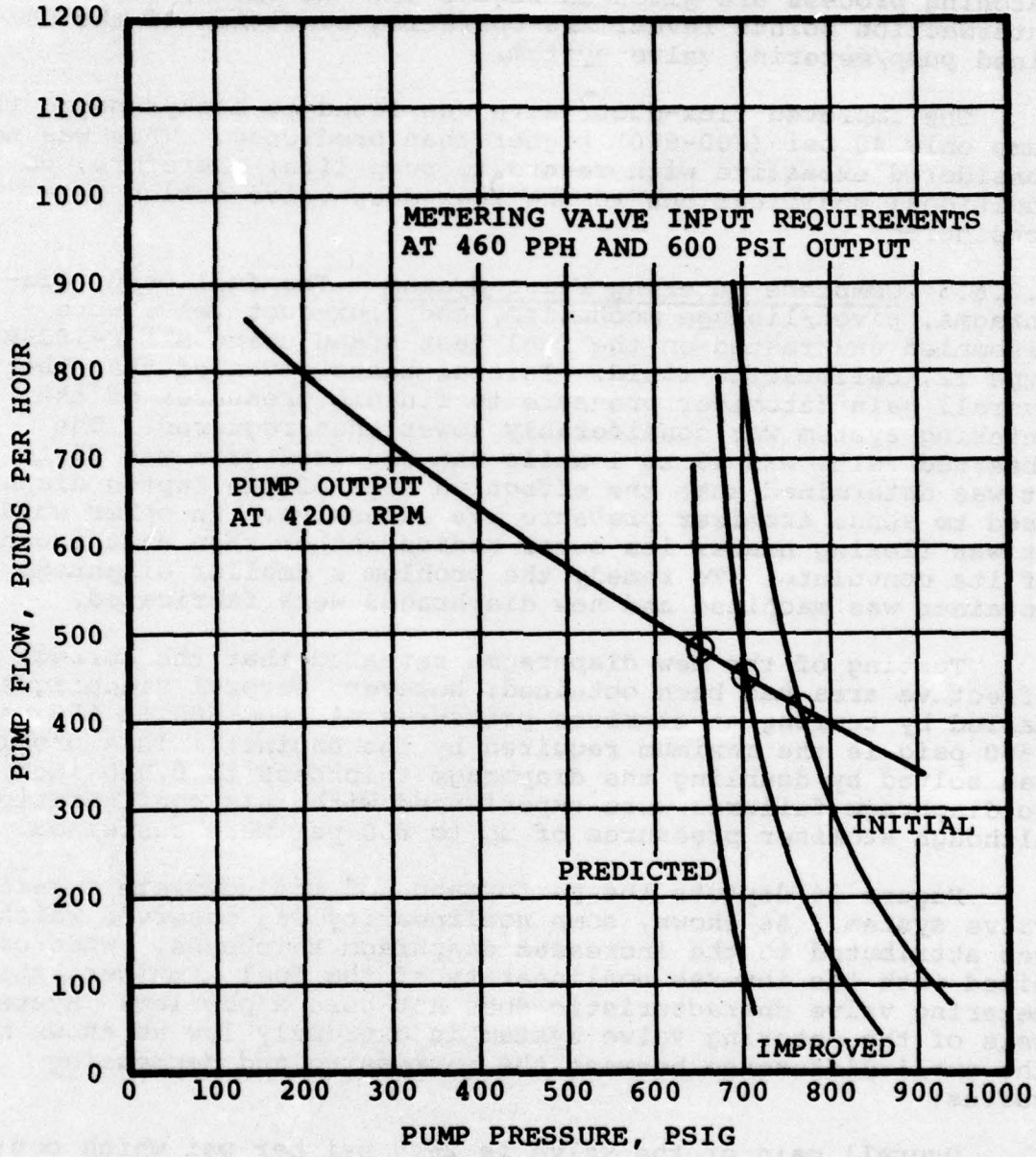


Figure 33. Metering Valve and Pump Matching.

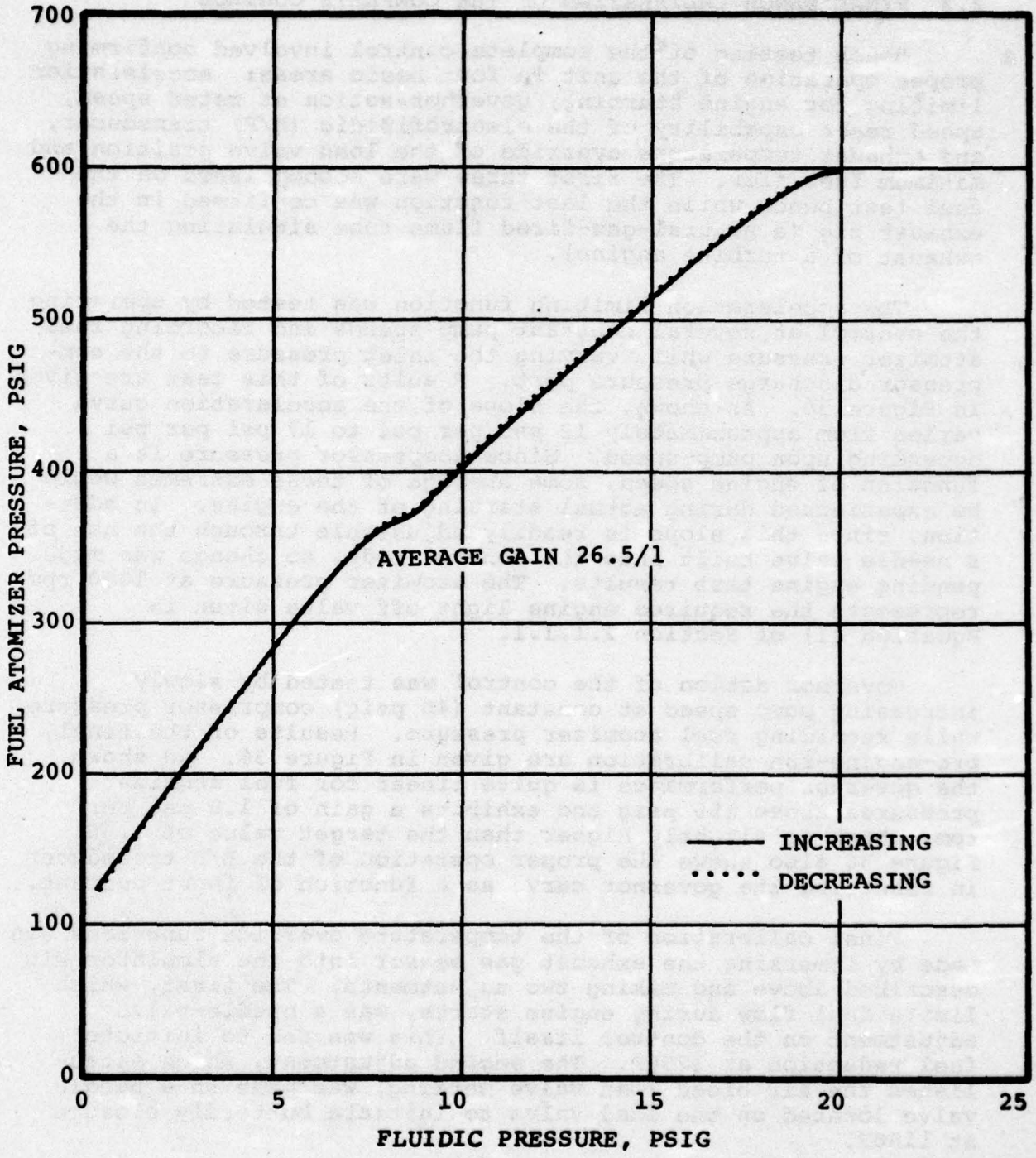


Figure 34. Complete Metering Valve System Performance.

## 2.3 FINAL BENCH CALIBRATION OF THE COMPLETE CONTROL

Bench testing of the complete control involved confirming proper operation of the unit in four basic areas: acceleration limiting for engine starting, governor action at rated speed, speed reset capability of the electrofluidic (E/F) transducer, and exhaust temperature override of the load valve position and maximum fuel flow. The first three were accomplished on the fuel test bench while the last function was confirmed in the exhaust rig (a natural-gas-fired flame tube simulating the exhaust of a turbine engine).

The acceleration limiting function was tested by operating the control at several constant pump speeds and recording fuel atomizer pressure while varying the inlet pressure to the compressor discharge pressure port. Results of this test are given in Figure 35. As shown, the slope of the acceleration curve varies from approximately 12 psi per psi to 17 psi per psi depending upon pump speed. Since compressor pressure is a function of engine speed, some average of these extremes would be experienced during actual starting of the engine. In addition, since this slope is readily adjustable through the use of a needle valve built into the control body, no change was made pending engine test results. The atomizer pressure at 1000 rpm represents the required engine light-off value given in Equation (1) of Section 2.1.1.1.

Governor action of the control was tested by slowly increasing pump speed at constant (40 psig) compressor pressure while recording fuel atomizer pressure. Results of the final, pre-engine-run calibration are given in Figure 36. As shown, the governor performance is quite linear for fuel atomizer pressures above 150 psig and exhibits a gain of 1.8 psi per rpm, which is slightly higher than the target value of 1.50. Figure 36 also shows the proper operation of the E/F transducer in resetting the governor curve as a function of input current.

Final calibration of the temperature override functions was made by immersing the exhaust gas sensor into the simulator rig described above and making two adjustments. The first, which limits fuel flow during engine starts, was a needle-valve adjustment on the control itself. This was set to initiate fuel reduction at 1250F. The second adjustment, which establishes the air bleed load valve setting, was made on a needle valve located on the load valve to initiate butterfly closure at 1150F.

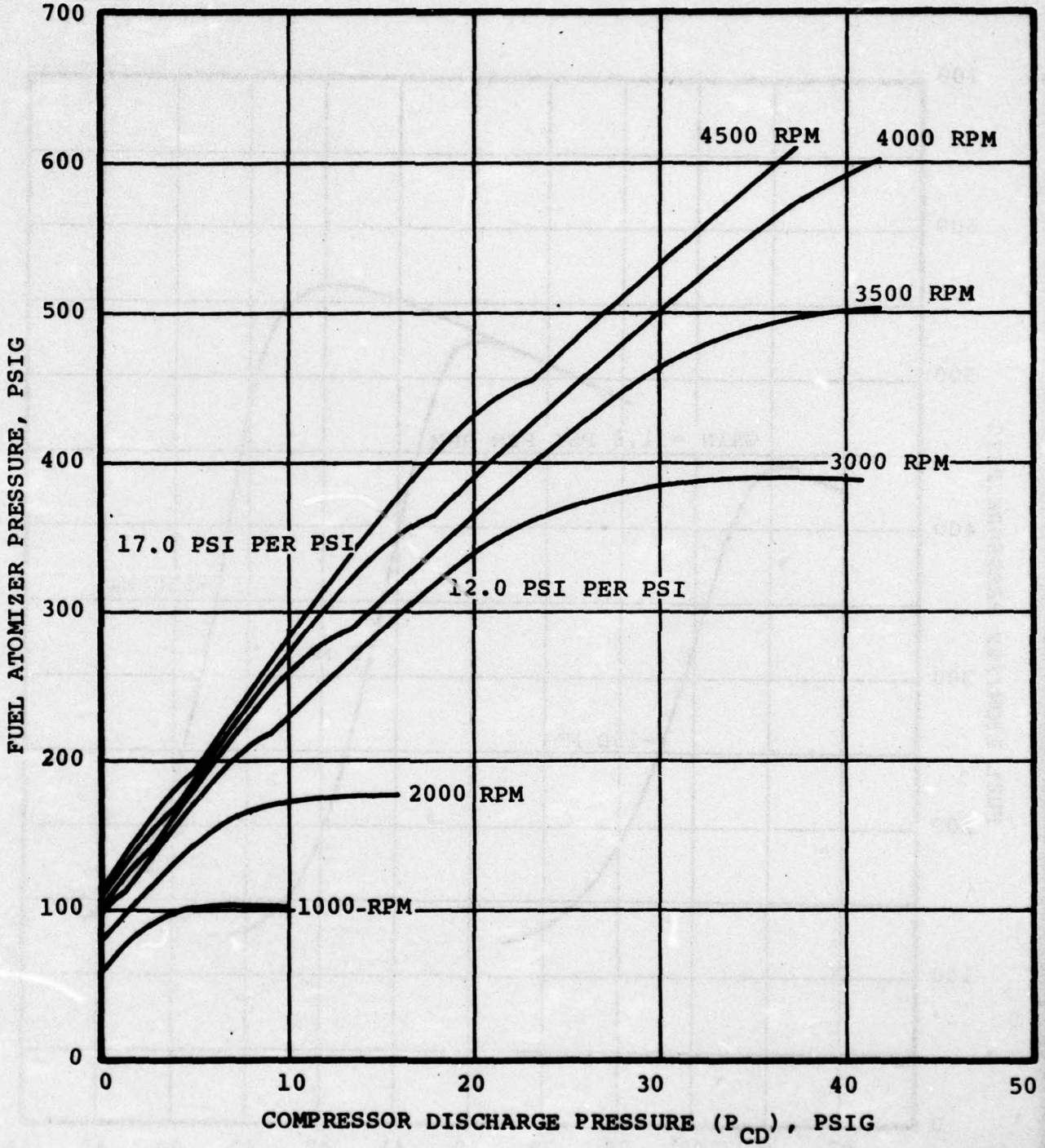


Figure 35. Acceleration Limiting Performance of Control.

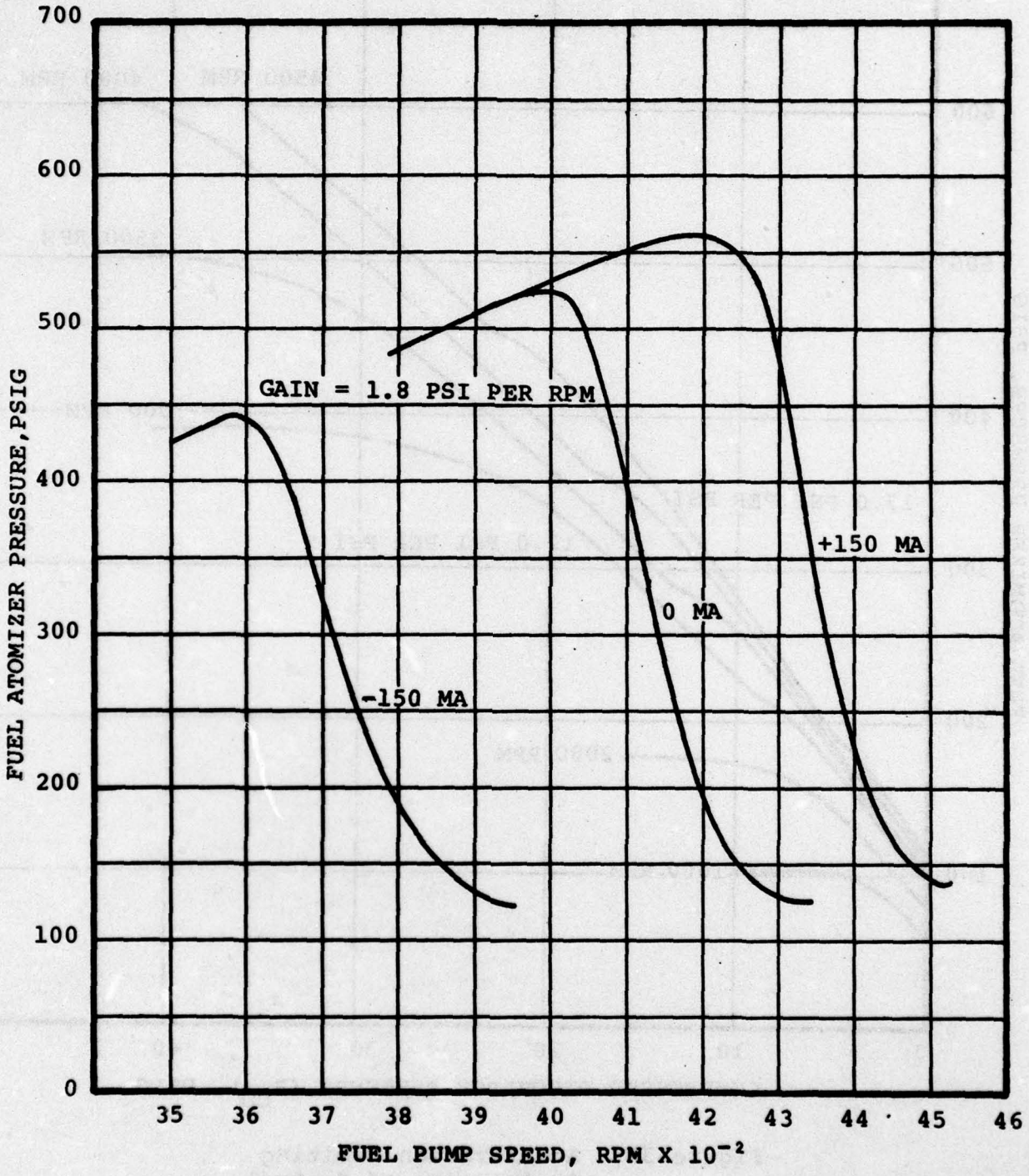


Figure 36. Speed Governing Performance of Control.

## 2.4 ENGINE TESTING

Engine testing of the fluidic fuel and air bleed load control system was conducted in the AiResearch laboratory during the period from July 19 through July 28, 1976. The engine used in the testing was an AiResearch Model GTCP85-180 gas turbine engine, Serial Number P-982C, bailed from the U.S. Air Force Logistics Command, San Antonio, Texas. Figures 37, 38, and 39 show several views of the engine including the location of the three major components of the fluidic control system as well as other engine features. Prior to testing, a 400-cycle alternator was mounted on the large circular drive pad on the forward end of the engine.

Initial attempts to start the engine resulted in a "hung" condition at approximately 35 percent speed. This difficulty was traced to excessive pressure drop through the lines and air filter used to supply compressor discharge pressure to the control. The lines were replaced with the next larger size, and an air filter of larger capacity and lower flow resistance was installed. Several additional start attempts were required during which the start flow and temperature override settings were adjusted. Following these adjustments, successful starts were made as shown in the left-hand portion of Figure 40. Exhaust gas temperature was limited to a maximum of 1250F, as shown by the high response thermocouple trace and start times were of normal duration, 26 to 30 seconds.

When the electronic fine-speed control (integrator) was energized, the system was found to be unstable. Reduction of the integrator gain resulted in marginally stable operation; however, the control would not maintain speed at 100 percent (400 Hz alternator frequency) with load addition. The center portion of Figure 40 illustrates this speed "droop" with bleed load addition. In addition, excessive (greater than 2 percent) speed overshoots were experienced with sudden bleed load removals as shown in the right-hand portion of Figure 40.

Evaluation of the results of these first engine tests resulted in the following conclusions.

1. Proportional speed gain of the fluidic control was too low, especially at the no-load (low fuel flow) condition.

2. Flow capacity of the output fluidic amplifier was insufficient to rapidly drive the large metering valve diaphragm.

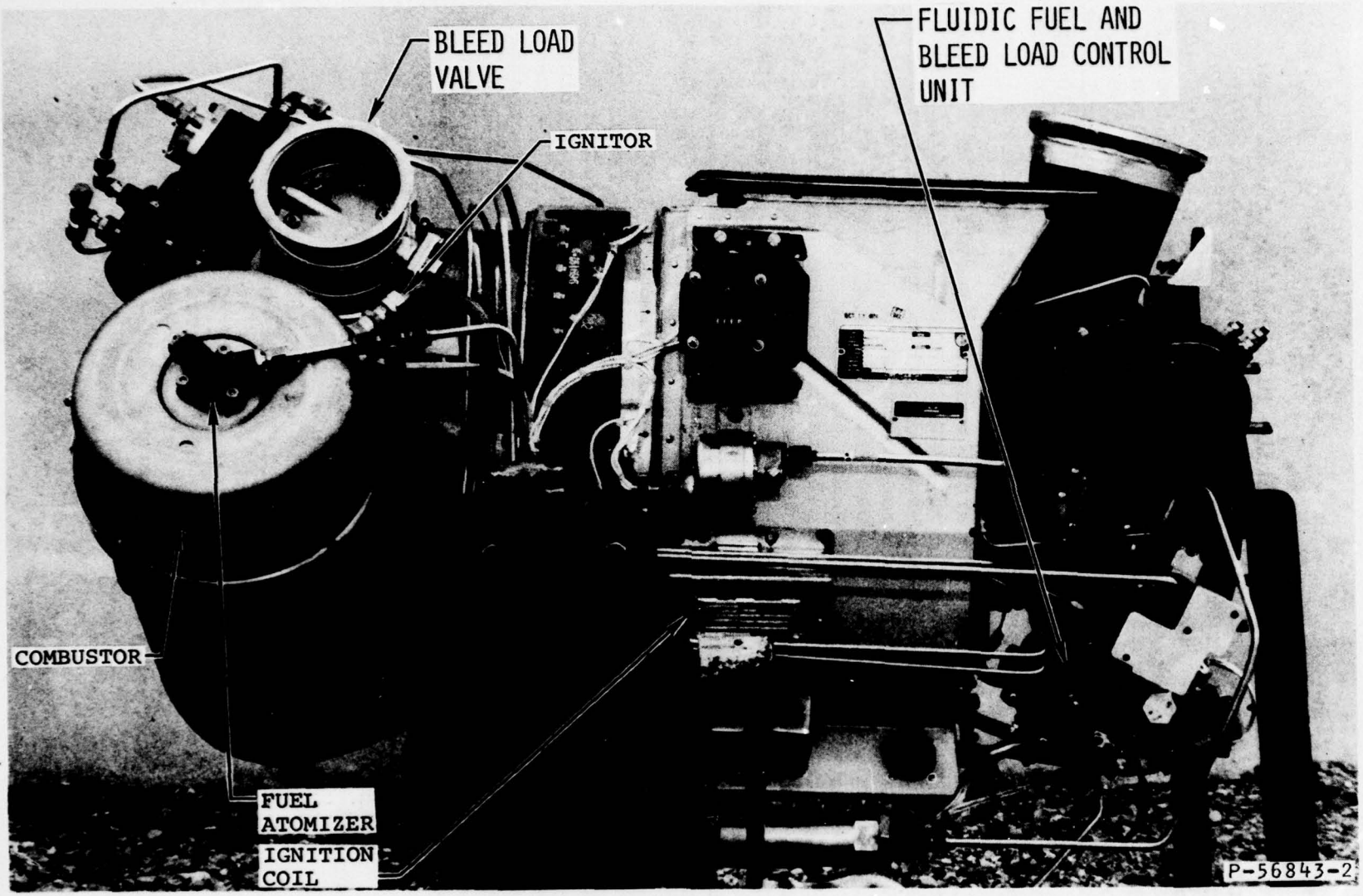


Figure 37. Controls on Model GTCP85-180 Engine.

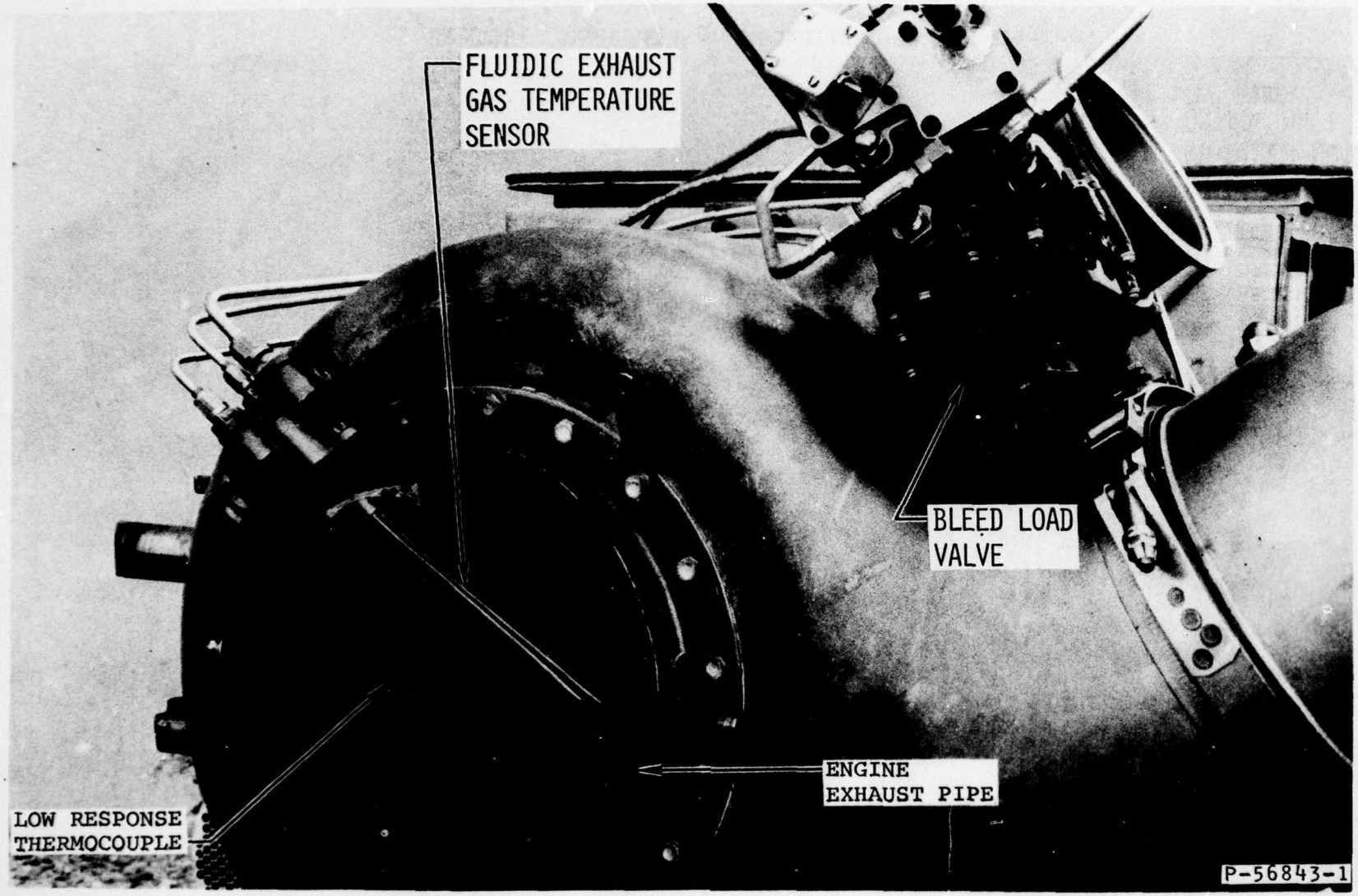


Figure 38. Controls on Model GTCP85-180 Engine.

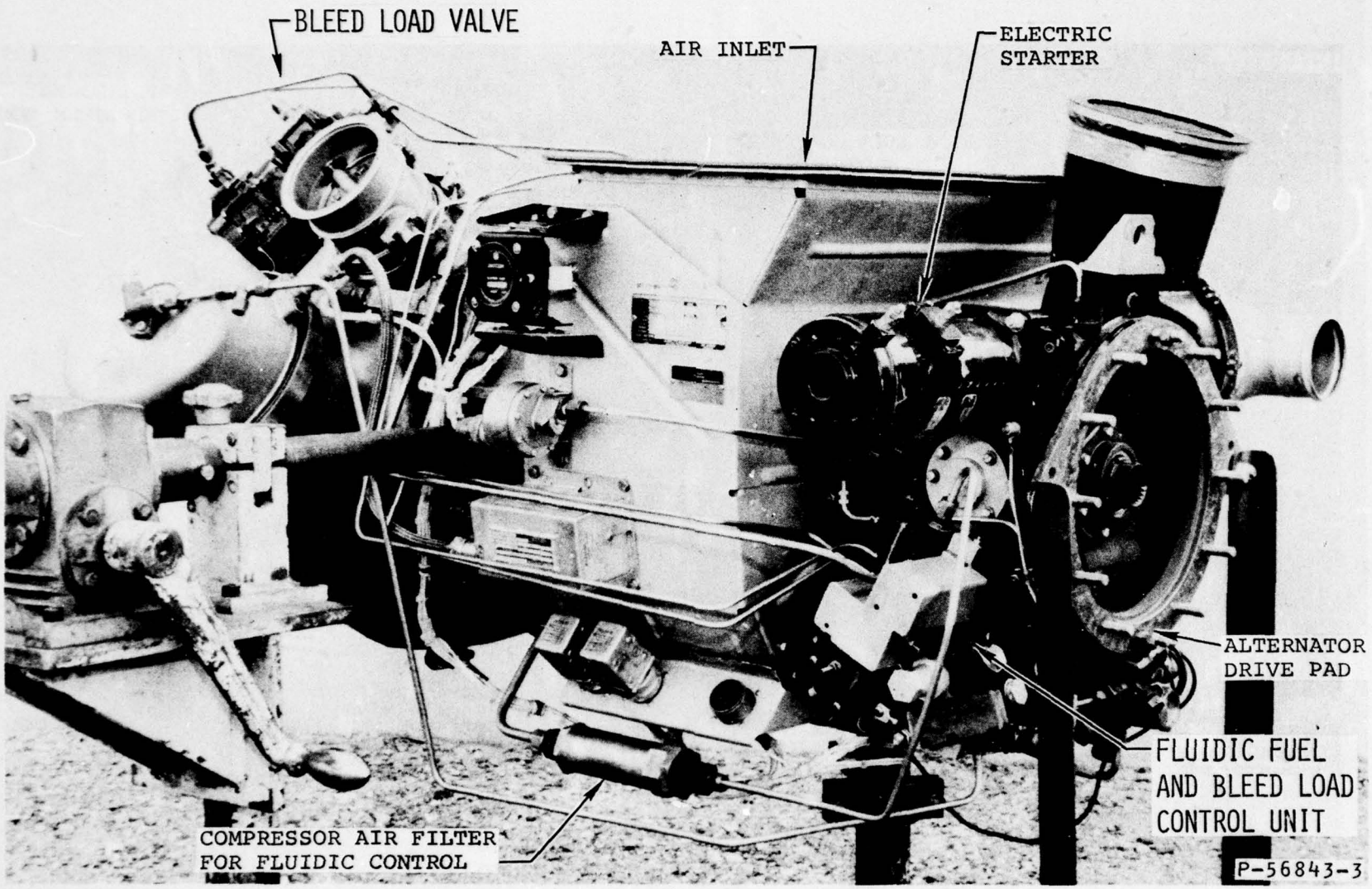


Figure 39. Controls on Model GTCP85-180 Engine.

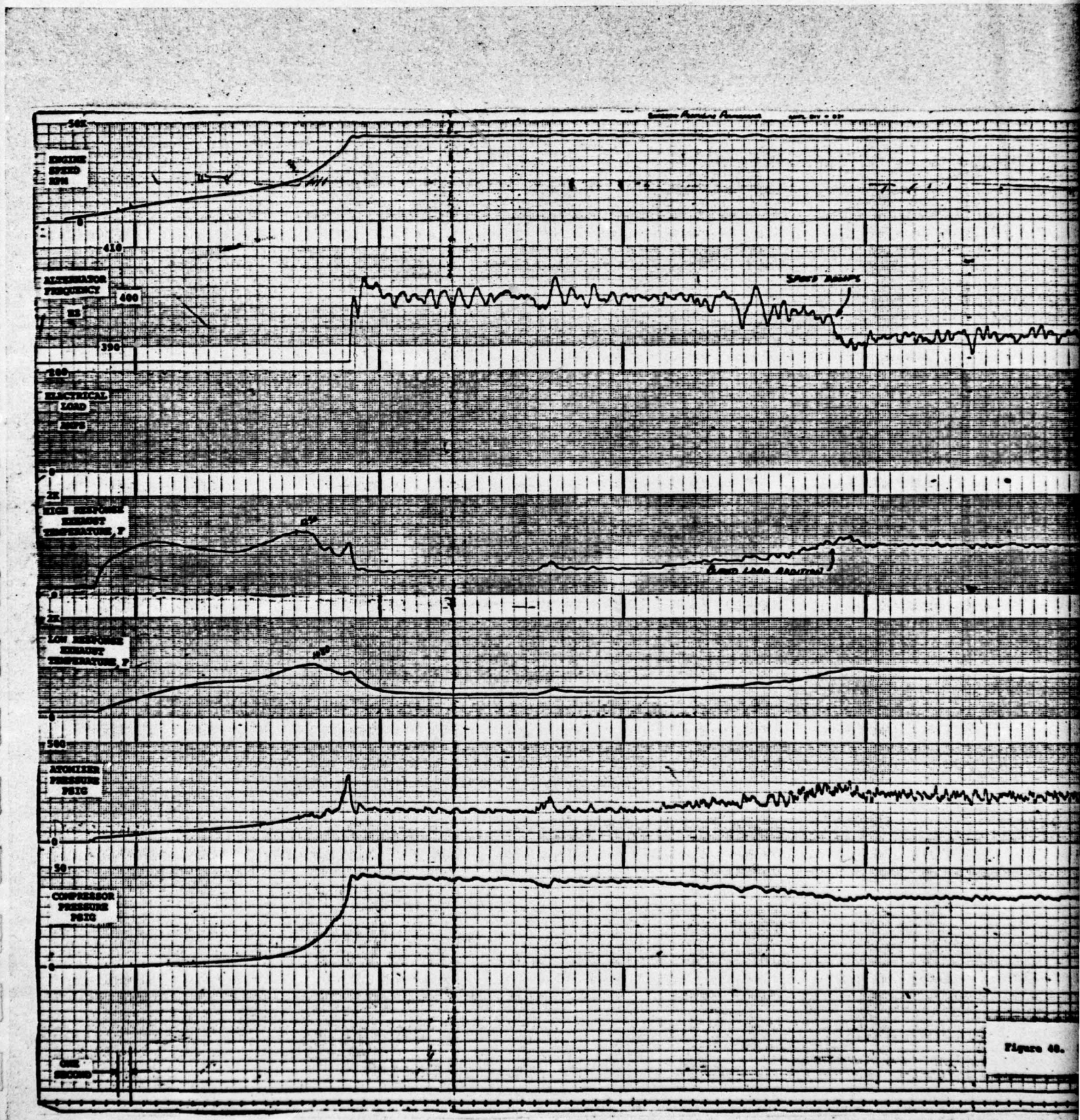
ENGINE SPEED RPM
5400
0
ALTERNATOR FREQUENCY
410
400
390
CPS
SPEED ADJUST
ELECTRICAL LOAD
AMPS
200
0
HIGH RESPONSE EXHAUST TEMPERATURE, F
1200
0
LOW RESPONSE EXHAUST TEMPERATURE, F
1200
0
ATOMIZER PRESSURE PSIG
500
0
COMPRESSOR PRESSURE PSIG
50
0
ONE SECOND

Figure 40.

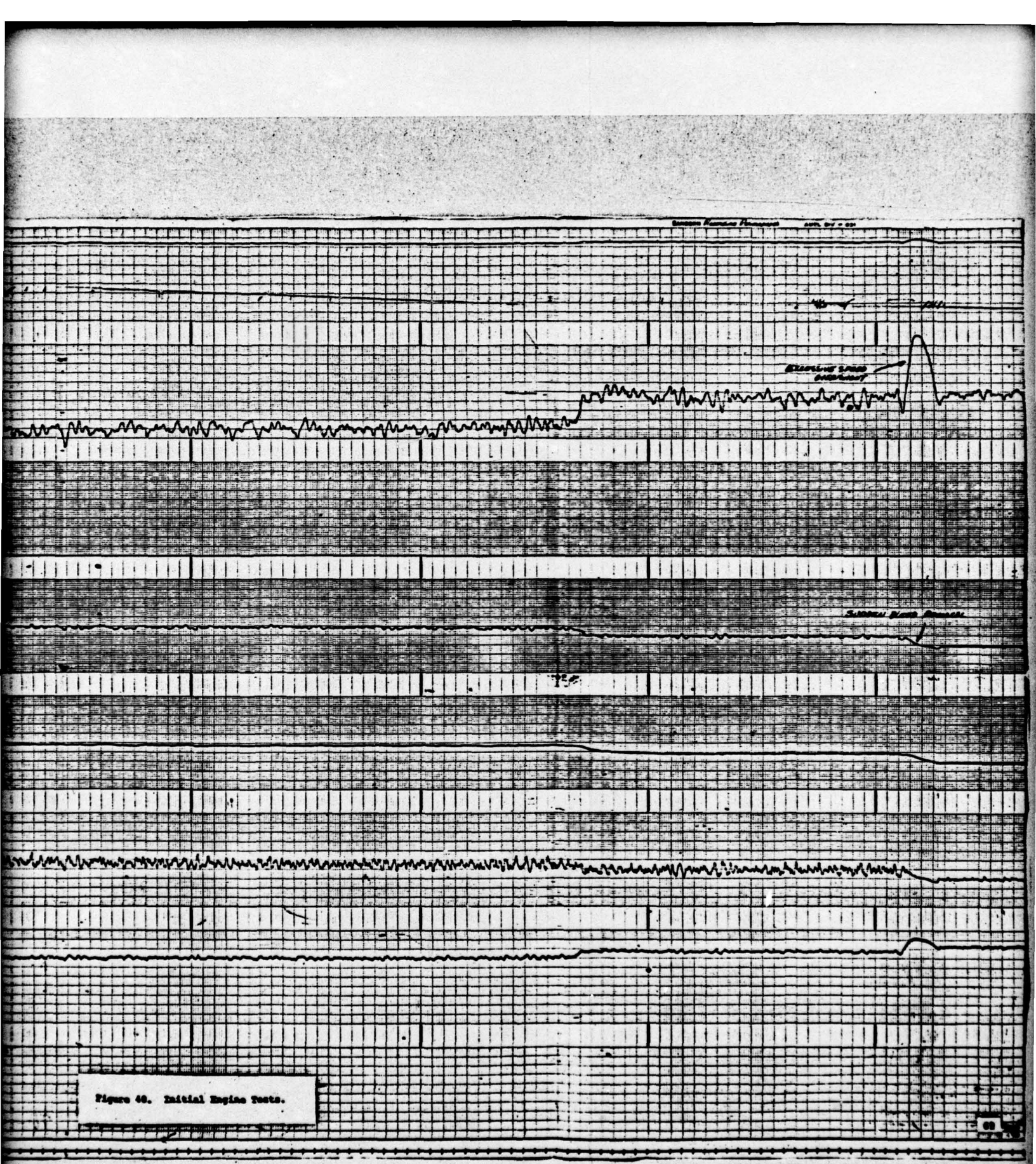

Figure 48. Initial Engine Tests.

3. Items 1 and 2 resulted in an underdamped system which would accept only a minimal amount of integral (fine-speed control) gain.

4. The minimum flow capability of the control was too high, allowing excessive speed overshoots during load removals.

Based upon these conclusions, the following corrective measures were taken.

1. An additional stage of amplification was added to the final gain cascade of the summation stack.

2. The aspect ratio of the final output fluidic amplifier was increased from three to four laminates.

3. The length of the metering valve push rod was decreased and the valve was readjusted to obtain lower minimum flows.

The control was retested on the fuel test bench with the resulting performance shown in Figure 41. When compared with Figure 36 of Section 2.3, it may be seen that the proportional gain was increased from 1.8 psi per rpm to 3.6 psi per rpm, and that the minimum atomizer pressure (and therefore fuel flow) was reduced from 125 psi to 100 psi. Increasing the gain of the fluidic output stages also helped to diminish the undesirable "rounding" of the curve at the lower end.

Engine testing of the control system with the modifications described above revealed that the former problems had been resolved. Figure 42 shows one run in which several combinations of maximum bleed load and electrical shaft load were applied to the engine. As shown, transient speed over and undershoots during step-load applications were maintained within the plus or minus two percent band as required by the model specification. Full electronic integral gain was applied to the system with no sign of instability observed. In addition, limiting of exhaust temperature through modulation of the load valve position was observed to be stable and accurate.

One problem still remained, however, relative to steady-state speed control accuracy. As shown in Figure 42, during any constant load condition, speed fluctuations greater than the allowable plus or minus 1/4 percent were observed. Several attemps to remedy this problem were made during the short time

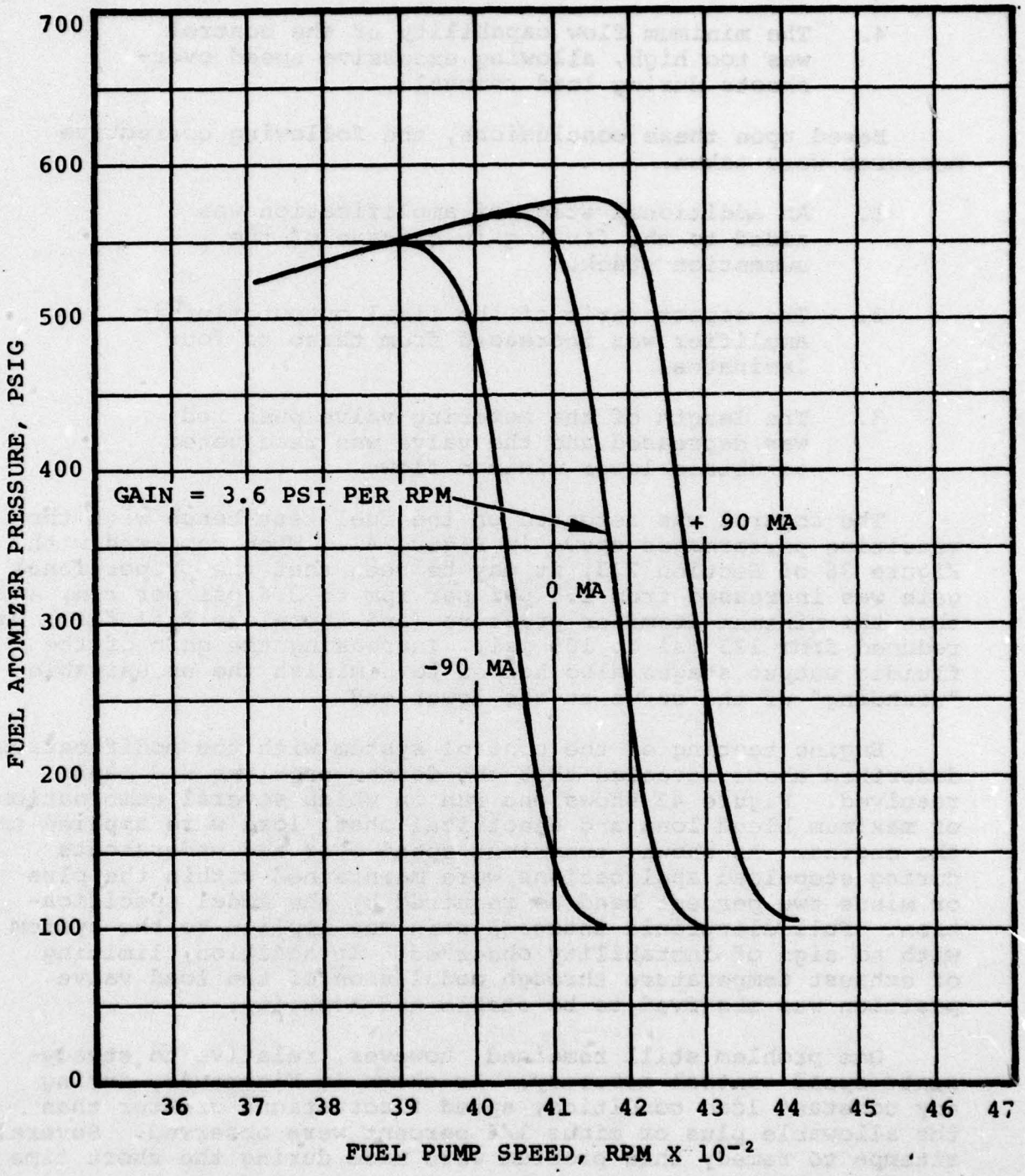


Figure 41. Speed Governing Function With Increased Gain.

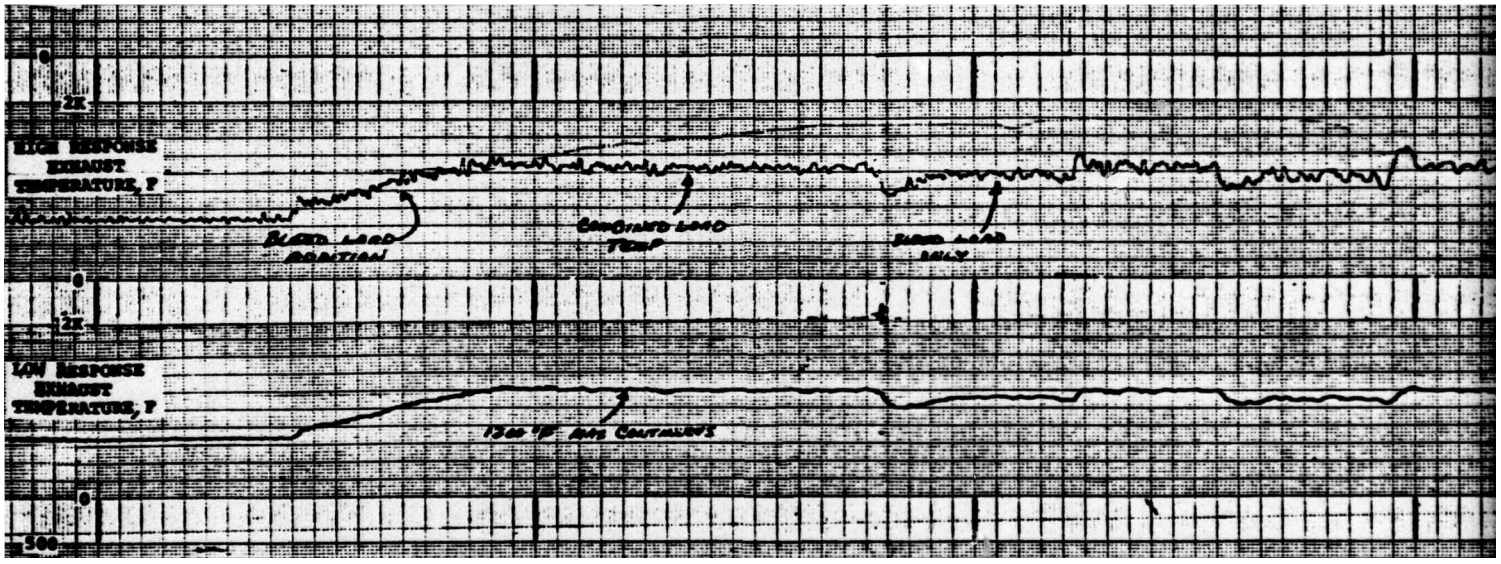
0
2X
HIGH RESPONSE
EXHAUST
TEMPERATURE, F
BLEED LOAD
REMOVED
CONSTANT LOAD
TEMP
BLEED LOAD
APPLY
0
2X
LOW RESPONSE
EXHAUST
TEMPERATURE, F
1200 °F EXH CONTINUITY
0
500

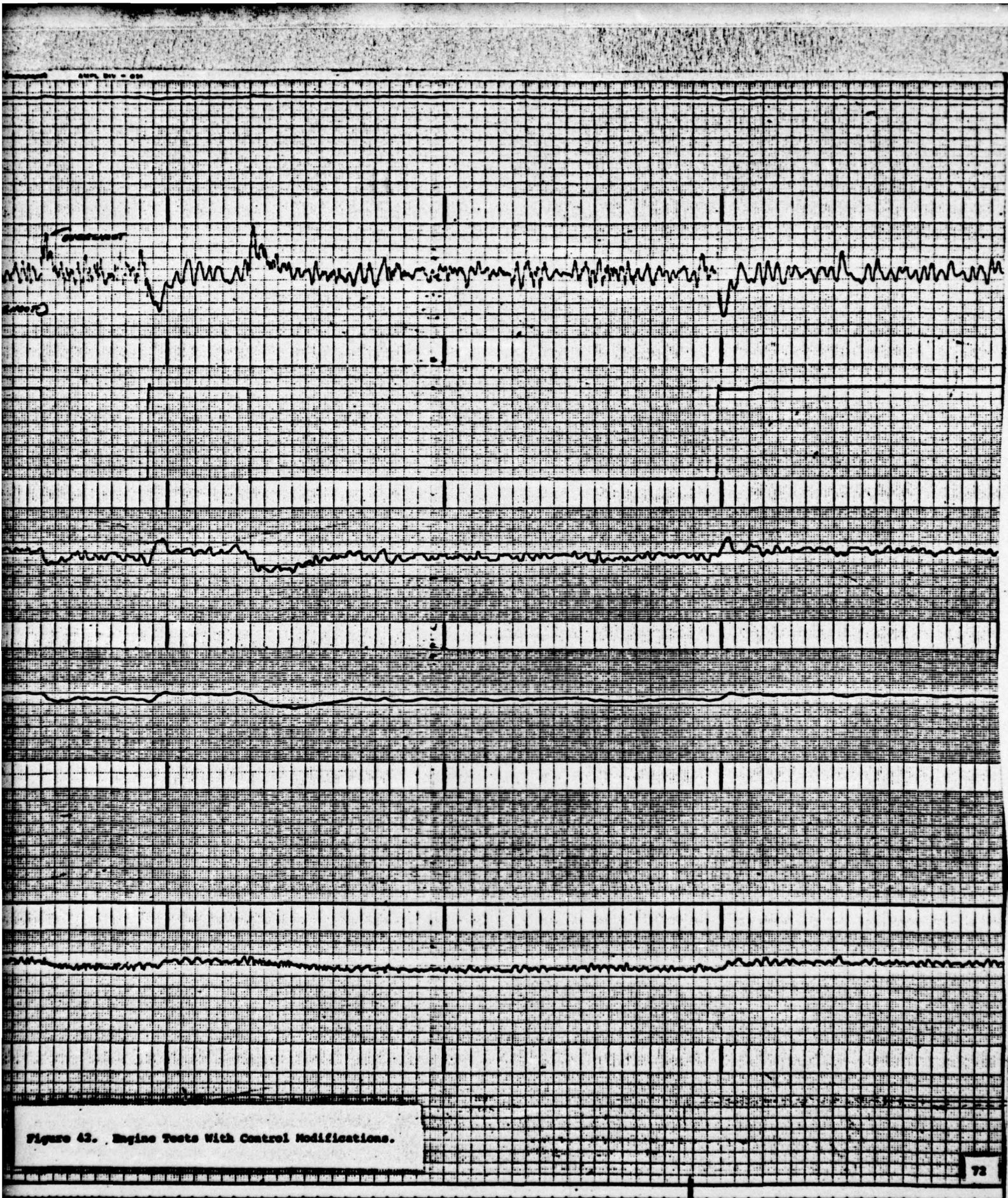

Figure 43. Engine Tests With Control Modifications.

available prior to demonstration of the system, but without success. Evaluation of the problem and plans for solution are presented in the following sections of the report.

## 2.5 POST-ENGINE RUN EVALUATION

As a result of the engine tests described in the previous section, it was concluded that the fluidic fuel and bleed load control system met all of the design goals with the exception of steady-state speed accuracy due to noise generated in the fluidic circuit.

Accordingly, a series of bench tests were conducted to determine the source of this noise within the fluidic circuit. In order to accomplish this, a new laboratory chopper drive system was fabricated which allows engine speed to be simulated and held constant within 0.1 percent. In addition, a miniature, transistor-type pressure transducer was fabricated. This unit was installed between elements in a fluidic stack, and was capable of responding to pressure pulsations in the frequency range of interest.

With these diagnostic tools, the fluidic frequency-to-analog speed circuit and summation circuit were evaluated and the following observations were made:

1. The overall signal-to-noise ratio from speed input to fluidic pressure output was only 3.0 to 1 (over the 200 rpm control band).

2. Signal-to-noise ratio of the F/A circuit was approximately 4.0 to 1.

3. All digital elements in the F/A circuit were switching properly.

4. The rectifier element in the F/A circuit exhibited high flow noise characteristics.

Based upon these observations, it was apparent that the fundamental source of noise was the F/A circuit and, in particular, the rectifier element.

It then was concluded that an order of magnitude improvement in signal-to-noise ratio must be made in the overall control performance in order to achieve the required steady-state control accuracy. Two simultaneous approaches to solving the noise problem were formulated. The first involves a modification of the F/A circuit to operate on a second order principle, as opposed to the linear approach used in the present circuit. With such a circuit, rectifier action will occur over a much

smaller speed range and produce an output of significantly higher gain. A circuit of this type has been designed and testing has been initiated. The second approach involves redesigning the rectifier element itself. Mr. Frank Manion, Harry Diamond Laboratories, reviewed the performance characteristics and design of the present rectifier following the engine demonstration runs and offered suggestions which are being incorporated into the design of a new rectifier.

## 3. CONCLUSIONS AND RECOMMENDATIONS

The development program, bench tests, and engine tests described in this report have shown that the fluidic fuel and air bleed load control system met the basic control requirements of the GTCP85-180 gas turbine engine. The specific design goals of engine starting, temperature limiting through load valve modulation, and electrical speed reset were met. One design goal was not achieved. Spurious noise generated in the fluidic frequency-to-analog speed circuit resulted in a steady-state engine speed error of plus-or-minus 1.0 percent which exceeds the plus-or-minus 0.25 percent limit established in the engine specification. Corrective measures have been formulated to improve the speed circuit signal-to-noise ratio. These will involve circuit modifications to increase gain in the operating speed range and redesign of the rectifier element to reduce flow-generated noise. Additional bench and engine tests are planned to confirm that the modifications result in the speed control accuracy required by the engine specification.

The successful completion of this phase of the program leads to the recommendation that the initial objectives of the total program be pursued, which is the field evaluation of a substantial number of systems.

## DISTRIBUTION LIST

| | |
|---|---|
| Defense Documentation Center<br>Cameron Station, Building 5<br>Alexandria, VA 22314 | 12 Copies |
| US Army Mobility Equipment Research<br>and Development Command<br>ATTN: DRXFB-EM (R. Ware)<br>Fort Belvoir, VA 22060 | 5 Copies |
| Harry Diamond Laboratories<br>ATTN: DRXDO-RCD (J. Goto)<br>2800 Powder Mill Road<br>Adelphia, MD 20783 | 2 Copies |
| Naval Air Systems Command<br>AIR 52022E (W. Langhrey)<br>Washington, DC 20360 | 1 Copy |
| Naval Ship Engineering Center<br>Philadelphia Division<br>ATTN: Code 6772 (D. Keyser)<br>Philadelphia, PA 19112 | 1 Copy |
| Naval Air Engineering Center<br>(96213) Ground Support Equipment Department<br>Lakehurst, NJ 08733 | 1 Copy |